THE OVARY, OOCYTE DEVELOPMENT, AND EGG VITELLINE ENVELOPE OF THE PIPEFISH, *SYNGNATHUS SCOVELLI*

By

PAUL CHRISTOPHER BEGOVAC

A DISSERTATION PRESENTED TO THE GRADUATE SCHOOL
OF THE UNIVERSITY OF FLORIDA IN
PARTIAL FULFILLMENT OF THE REQUIREMENTS
FOR THE DEGREE OF DOCTOR OF PHILOSOPHY

UNIVERSITY OF FLORIDA

1988

Copyright 1988

by

Paul Christopher Begovac

TO MY PARENTS

ACKNOWLEDGEMENTS

I would first like to express my gratitude to my mentor, Robin Wallace, for setting high professional standards and serving as an excellent role model for conducting scientific research. He provided unrestricted support and freedom to pursue problems of special interest to me. His lessons will serve me well throughout my career. A special thanks is due Dr. Kelly Selman, who taught me electron microscopy and allowed unlimited use of her laboratory on my frequent trips to Gainesville. Dr. Chris West was a constant source of critical thought and conversations with him were instrumental in the early phases of the vitelline envelope work. I also thank Dr. David Evans for serving as my outside committee member and for his review of the dissertation. The work presented in Chapter II is reproduced by permission of Alan R. Liss, Inc. (J. Morphol. 193:117-133).

I am indebted to Dr. Paul Linser and Margaret Perkins for teaching me the art of monoclonal antibody production. Mrs. Lynn Milstead helped simplify much of my research with her outstanding drawings. The use of the collecting facilities at Cedar Key were kindly provided by Dr. Frank Maturo of the Department of Zoology. Some of my most enjoyable days were spent collecting near Seahorse Key amidst the pelicans, ibises, ospreys, and frigate birds. I thank my peers, Deni Galileo and Steve Dworetzky, for our many discussions about each others experiments and science in general, but particularily the friendship we shared together in graduate school. Drs. Mark Greeley, Peter Lin, Teresa Lin-Petrino, and Sam Edwards were good friends and served as sounding boards for the interpretation of many experimental results. My family continually provided steadfast support and perspective throughout graduate school.

Finally, and most importantly, I'd like to thank my dear wife, Susan, for her enduring love and constant support throughout the ups and downs of the past five years. Her sacrifices, hard work, encouragement, and laughter always kept me optimistic about the future.

TABLE OF CONTENTS

Page

ACKNOWLEDGEMENTS iv

LIST OF FIGURES vii

ABBREVIATIONS xii

ABSTRACT xv

CHAPTERS

- I INTRODUCTION 1
  - Statement of Purpose 4
  - Terminology 7
- II THE OVARIAN ANATOMY 8
  - Introduction 8
  - Materials and Methods 9
  - Results 10
  - Discussion 35
- III STAGES OF OOCYTE DEVELOPMENT 47
  - Introduction 47
  - Materials and Methods 48
  - Results 52
  - Discussion 80
- IV EGG VITELLINE ENVELOPE CONSTITUENTS 93
  - Introduction 93
  - Materials and Methods 95
  - Results 101
  - Discussion 121
- V LOCALIZATION AND SYNTHESIS OF VITELLINE ENVELOPE PROTEINS IN THE PIPEFISH FOLLICLE 127
  - Introduction 127
  - Materials and Methods 129
  - Results 138
  - Discussion 163
- VI SUMMARY AND FUTURE DIRECTIONS 169

REFERENCES 176

BIOGRAPHICAL SKETCH 191

LIST OF FIGURES

Figure Page

1. Photomicrograph of fresh ovary spread............13

2. Transverse section of entire ovary depicting various stages of development.....................13

3. Transverse section of germinal ridge apposed to the ovarian wall.................................13

4. Region comparable to dashed area outlined in Figure 2..13

5. Extreme mature edge of ovarian sheet.............13

6. Postovulatory follicle near the mature edge......13

7. Electron micrograph of a transverse section of the ovarian wall................................18

8. Electron micrograph of luminal epithelium........18

9. Electron micrograph of luminal epithelial cell blebbing into ovary lumen.......................18

10. Transverse section showing a portion of the germinal ridge region of the ovary...............22

11. Intracellular filaments in prefollicle cell in the germinal ridge.............................22

12. Separation of contiguous cell borders of meiotic oocytes in germinal ridge by prefollicle cell....22

13. Follicle separation from the germinal ridge......24

14. Primordial follicle separating from the germinal ridge.....................................24

15. Photomicrograph of a portion of fresh ovary illustrating the relationship of the oocyte germinal vesicle to the ovarian lumen............28

16. Transverse section depicting mature edge luminal epithelium................................28

17. Unmyelinated nerve present at the mature edge....28

18. Connective tissue elements in stromata...........28

19. India ink preparations of fresh intact ovaries demonstrating extent of lymphatic network........32

Figure Page

20. Lymphatic space extending between the lateral borders of adjacent young oocytes................32

21. Triangular lymphatic space in basolateral region between adjacent early developing oocytes........32

22. Follicle relations to the luminal epithelium.....34

23. Oocyte relations to the ovarian wall.............34

24. Shared theca on lateral aspects of adjacent oocytes......................................34

25. Schematic summary of ovary and relations *in situ*.38

26. Electron micrograph of an oogonium...............55

27. Light micrograph of germinal ridge pulsed with ^{3}H-thymidine after 2 days in culture........55

28. Light micrograph of germinal ridge pulsed with ^{3}H-thymidine after 10 days in culture.......55

29. Electron micrograph of leptotene oocyte..........55

30. Electron micrograph of pachytene oocyte..........55

31. High magnification of germ cell-specific, dense-cored granules..............................55

32. Light micrograph of perinucleolar oocytes in the primary growth phase......................60

33. Light micrograph of dispersing Balbiani vitelline body in perinucleolar phase oocyte.....60

34. Electron micrograph of a portion of the Balbiani vitelline body..........................60

35. Higher magnification of multivesicular bodies associated with the Balbiani vitelline body......60

36. Electron micrograph of later stage perinucleolar oocyte...............................60

37. Photomicrograph of a portion of intact ovary stained with rhodamine 123.......................60

38. Photomicrograph of a portion of ovary stained with acridine orange.............................60

Figure Page

39. Light micrograph of cortical alveoli-stage oocyte....64

40. Electron micrograph of oocyte cortex in early cortical alveoli-stage oocyte....64

41. Electron micrograph of vitelline envelope....64

42. Electron micrograph of lipid in cortical alveoli stage-oocyte....64

43. Phase and fluorescence micrographs of oocytes stained with concanavalin A....64

44. Light micrograph of early vitellogenic oocyte....69

45. Light micrograph of midvitellogenic oocyte....69

46. Light micrograph of a late vitellogenic oocyte...69

47. Electron micrograph of early vitellogenic oocyte depicting yolk-sphere formation....69

48. Electron micrograph of early vitellogenic oocyte with transitional yolk spheres....69

49. Electron micrograph of mature yolk sphere....69

50. Electron micrograph of pinocytic vesicles in early vitellogenic oocyte....69

51. Photomicrograph of maturation-stage follicles....73

52. Photomicrograph of _in vitro_ matured follicles....73

53. Photomicrograph of _in vivo_ matured eggs....73

54. Maturation response of follicles treated with 17-alpha-hydroxy-20-beta-dihydroprogesterone....73

55. Protein content of individual follicles from 0.4-1.3 mm diameter....76

56. SDS-PAGE of proteins present in various sized follicles from <0.2-1.3 mm diameter....78

57. Schematic diagram of sequential stages of oocyte development as viewed in an optimal section....83

58. Model of oocyte progression through ovary during oocyte development....90

Figure Page

59. Light micrograph of vitelline envelope...........103

60. Light micrograph of developing follicles stained with PAS..................................103

61. Wheat germ agglutinin-staining of developing oocytes..103

62. Electron micrograph of vitelline envelope in early cortical alveoli-stage oocyte..............107

63. Electron micrograph of vitelline envelope in later cortical alveoli-stage oocyte..............107

64. Electron micrograph of vitelline envelope in a midvitellogenic stage oocyte...................107

65. Electron micrograph of vitelline envelope of mature egg..107

66. Photomicrograph of manually isolated vitelline envelopes..110

67. Electron micrograph of the vitelline envelope pellet obtained by the extraction protocol.......110

68. Higher magnification of the nonextractted vitelline envelope pellet..........................110

69. High magnification of insoluble residue..........110

70. SDS-PAGE of sequentially extracted vitelline envelope pellet proteins..........................114

71. SDS-PAGE of limited proteolytic digestion products of vitelline envelope proteins and egg proteins...118

72. SDS-PAGE of vitelline envelope proteins and egg proteins stained with Coomassie blue and PAS.....120

73. Immunoblot specificity of 5D6 antibody to pellet and supernatant extraction-protocol fractions....140

74. Immunoblot specificity of 5D6 antibody to plasma and liver proteins..............................142

75. Immunocytochemistry of 5D6 antibody to early developing follicles..............................145

76. Immunocytochemistry of 5D6 antibody to vitellogenic oocytes...............................145

Figure Page

77. Immunocytochemistry of 5D6 antibody to mature egg.....................................145

78. Control immunocytochemistry with 5A11 antibody to ovarian follicles...........................145

79. Immunocytochemistry of 5D6 antibody to liver.....145

80. Immunoelectron microscopy of 5D6 antibody to early vitellogenic stage oocyte..................147

81. Immunoelectron microscopy of 5D6 antibody to late vitellogenic stage oocyte........................147

82. Control immunoelectron microscopy of vitellogenic oocyte...............................149

83. Two-dimensional SDS-PAGE of extracted vitelline envelope proteins......................152

84. Immunoblot of two-dimensional SDS-PAGE of vitelline envelope proteins......................152

85. Autoradiogram of ^{35}S-methionine-labeled proteins within intact follicle..................155

86. Immunoblot of ^{35}S-methionine-labeled proteins within intact follicle............................155

87. Verification of cell dissociation procedures.....158

88. Higher resolution autoradiogram of ^{35}S-methionine-labeled proteins within intact follicle..................................160

89. Autoradiogram of ^{35}S-methionine-labeled proteins within denuded ooocyte..............................160

90. Autoradiogram of ^{35}S-methionine-labeled proteins within isolated follicle cell/theca complexes....160

91. Immunocytochemistry of 5D6 antibody to *Fundulus heteroclitus* follicle.............................162

92. Control immunocytochemistry of 5A11 antibody to *Fundulus heteroclitus* follicle................162

ABBREVIATIONS

BL	Basal lamina
C	Collagen
CA	Cortical alveoli
CAO	Cortical alveoli-stage oocyte
CE	Coelomic epithelium
CON A	Concanavalin A
CT	Connective tissue
D	Dorsal
DAB	Diaminobenzidine
E	Eggs
EC	Endothelial cells
EDTA	Ethylenediaminetetraacetic acid
F	Filaments (intracellular)
FC	Follicle cell
G	Golgi complexes
GR	Germinal ridge
GV	Germinal vesicle
GVBD	Germinal vesicle breakdown
^3H-	Tritiated
H&E	Hematoxylin and eosin
IEF	Isoelectric focussing
kDa	Kilodaltons
L	Ovarian lumen
LE	Luminal epithelium
LIV	Liver
LP	Lipid

LY	Lymphatic space
L-15	Leibovitz 15
mm	Millimeter
N	Unmyelinated nerve
NU	Oocyte nucleus
O	Oocyte
OG	Oogonia
OW	Ovarian wall
PAGE	Polyacrylamide gel electrophoresis
PAS	Periodic acid-Schiff's
PBS	Phosphate-buffered saline
PC	Peritoneal cavity
PF	Primordial follicle
PFC	Prefollicular cells
RCA	_Ricinus communis_ agglutinin
SDS	Sodium dodecyl sulfate
SEM	Standard error of the mean
SM	Smooth muscle
T	Thecal elements
TBS	Tris-buffered saline
ug	Microgram
ul	Microliter
um	Micrometer
V	Vein
VE	Vitelline envelope
VN	Ventral
VO	Vitellogenic oocyte

WGA	Wheat germ agglutinin
Y	Yolk sphere
YI	Primary yolk sphere
YII	Transitional yolk sphere
YIII	Mature yolk sphere
2D	Two-dimensional
17-alpha, 20-beta-DHP	17-alpha-hydroxy-20-beta-dihydroprogesterone

Abstract of Dissertation Presented to the Graduate School of the University of Florida in Partial Fulfillment of the Requirements for the Degree of Doctor of Philosophy

THE OVARY, OOCYTE DEVELOPMENT, AND EGG VITELLINE ENVELOPE OF THE PIPEFISH, *SYNGNATHUS SCOVELLI*

By

PAUL CHRISTOPHER BEGOVAC

April 1988

Chairman: Robin A. Wallace
Major Department: Anatomy and Cell Biology

The ovarian anatomy, stages of oocyte development, and biochemical properties of the vitelline envelope were documented for the pipefish, *Syngnathus scovelli*. This unusual vertebrate ovary possesses a sequential array of developing follicles originating from an outpocketed region of the luminal epithelium, the germinal ridge. Folliculogenesis occurs within the germinal ridge and newly formed follicles enter into a linear progression of developing follicles extending to the opposite mature edge where ovulation occurs. Later stage oocytes are polarized with respect to the luminal epithelium.

Six stages of oocyte development were identified as follows: I) Oogonia; II) Primary growth subdivided into a) chromatin-nucleolus and b) perinucleolar phases; III)

Cortical alveoli formation; IV) Vitellogenesis; V) Oocyte maturation; and VI) Mature egg. The ^{3}H-thymidine incorporation studies establish the germinal ridge as the proliferative segment of the ovary. Yolk sphere formation appears to involve a multivesicular body-like structure that may relate to multivesicular bodies observed in perinucleolar and cortical alveoli stage oocytes. Oocyte of 1.1 mm diameter have the capacity to undergo in vitro maturation in response to the steroid 17-alpha-hydroxy-20-beta-dihydroprogesterone.

The biochemical composition of the vitelline envelope was examined in further detail. Two major protein families of 109 and 98kDa were extracted from egg vitelline envelopes, with at least the 98kDa protein being a glycoprotein. Periodic acid-Schiff's staining of ovarian sections reveals an external layer that is strongly PAS-positive compared to the internal layer. Monoclonal antibodies prepared against the 109 and 98kDa vitelline envelope proteins were specific for the vitelline envelope by immunocytochemistry and immunoblot analyses. The vitelline envelope proteins were localized by immunoelectron microscopy to the internal layer of the vitelline envelope. Synthesis of at least the 98kDa family occurs within the ovarian follicle. The precise cellular origin of the vitelline envelope proteins, however, was not identified.

These studies have established the framework for future studies pertaining to oogenesis and oocyte development in the pipefish. The sequential pattern of follicle development in the pipefish ovary offers a potentially useful model system for study of especially early events in oogenesis and oocyte development.

CHAPTER I
INTRODUCTION

> That fish which is called Belone, at the season of reproduction, bursts asunder, and in this way the ova escape; for this fish has a division beneath the stomach and bowels like the serpents called typhlinae. When it has produced its ova it survives and the wound heals up again.
>
> Aristotle
> Book VI, Chapter 12
> 3rd Century B.C.

This passage, requoted from Gudger (1905, p. 449), is the earliest reference to reproduction in the pipefish. The peculiar brood pouch of the pipefish was, until the mid-19th century, the subject of considerable debate regarding which sex carried the developing embryos. Gudger's treatise recalls the history of this early confusion up until the late 19th century and provides a colorful survey of the Lophobranch literature until that time. The account by Gudger is the most complete writing dealing with the historical aspects of pipefish reproduction.

The Gulf pipefish, Syngnathus scovelli, is a teleost of the order Gasterosteiformes and a member of the family Syngnathidae (Fritzsche, 1984). This group of teleosts is widely distributed throughout the world, primarily in the tropical climates, but is also found in more temperate latitudes (Bohlke and Chaplin, 1970). Pipefish have been of general interest mainly as aquaria species because of the male brood pouch, where embryos develop in a manner similar to those of the closely related seahorse. Most of the documented reports pertaining to pipefish deal with phylogeny (Herald, 1942; Herald, 1959; Herald and Dawson, 1972; Dawson, 1977; Fritzsche, 1980), subtropical species distribution (Reid, 1954; McLane, 1955; Tagatz, 1968; Whatley, 1969; Dawson, 1970; Robins, 1971; Dawson, 1972; Herald and Randall, 1972; Dawson and Randall, 1975; Paxton, 1975; Dawson, 1977; Gilmore, 1977; Schooley, 1980; Dawson, 1981; Dawson, 1984), and temperate species distribution (Briggs, 1975; Bayer, 1980). Sexual dimorphism (Berglund et al., 1986) and properties of the male brood pouch (Quast and Howe, 1980; Haresign and Shumway, 1981) have also been examined. Field and life history studies specific to *Syngnathus scovelli* have appeared (Joseph, 1957; Whatley, 1969; Brown, 1972). In Florida, *Syngnathus scovelli* are abundant along the Gulf Coast (Reid, 1954; Joseph, 1957; Brown, 1972) as well as along the Atlantic Coast near the Indian River and Mosquito Lagoon (Gilmore, 1977; Schooley, 1980). Freshwater populations of *Syngnathus scovelli* are found in the St. John's River (McLane, 1955; Tagatz, 1968) and other Florida locations (summarized in Brown, 1972).

The reproductive processes in the pipefish, however, have received little study. The earliest depiction of the pipefish ovary was provided by Cunningham in 1898, but no subsequent studies by Cunningham followed up on the initial description of this remarkable ovary. Gudger (1905) examined the breeding habits and segmentation of the egg during early embryogenesis in the pipefish, *Syngnathus floridae*. Gudger was not concerned with the ovary itself, but rather postfertilization aspects. The uniqueness of the ovarian structure initially described by Cunningham (1898) was then generally lost until the 1960s when two reports appeared concerning vitelline envelope formation (Anderson, 1967) and cortical alveoli formation and vitellogenesis (Anderson, 1968). Subsequently, Wallace and Selman (1981) reaffirmed the unusual aspects of the pipefish ovary. In short, the processes of oogenesis and oocyte development in this rather unique vertebrate ovary have not been examined in sufficient detail.

The study of oogenesis and oocyte development has a long history and its significance is attested by the many volumes dealing with female gametogenesis (Wilson, 1928; Raven, 1961; Biggers and Schuetz, 1972; Jones, 1978; Metz and Monroy, 1985; Browder, 1985). There has been a broad interest in how eggs develop from a comparative standpoint between different classes of vertebrate and invertebrate species. There has also been an interest in specific questions such as germ cell proliferation (Tokarz, 1978), oocyte growth (Wallace, 1985), and oocyte maturation

(Masui, 1985) common to many different classes of organisms. Certain organisms lend themselves to the study of particular aspects of egg development because of the availability of large numbers of gametes (sea urchins), the ability to maintain animals in the laboratory (*Xenopus laevis*, mice), or the importance of the organism for commercial (salmon, cows, pigs) or clinical (human) applications. The study of specific aspects of gametogenesis among these many varied animals have contributed to the overall understanding of how eggs develop. One additional reason for studying female gametogenesis is the importance of events, which occur during oocyte development, for the storage of developmental information (Raven, 1961) and nutrients essential for embryogenesis.

The reasons for examining oogenesis and oocyte development in the pipefish stem primarily from the unique arrangement of follicle development that is distinct among vertebrate ovaries. The pipefish has no significant commercial value but is most appropriate for studying certain basic aspects of early oogenesis. There is also an interest from a comparative perspective for understanding female gametogenesis among teleosts in general.

Statement of Purpose

The first objective of this project is to establish the morphological foundation for the study of oogenesis and oocyte development in the pipefish, *Syngnathus scovelli*. The unusual organization of follicle development within the ovary offers promise in terms of expanding our understanding of the earliest events that occur during oogenesis and oocyte development. Previously, these aspects of oocyte development have not attracted the attention of investigators to the extent that other areas of oocyte development such as vitellogenesis (Wallace, 1985) and oocyte maturation (Masui, 1985) have received. The initial emphasis is placed on understanding the ovarian anatomy and the relationship of developing oocytes within this structure. These important cellular relationships should provide the framework for understanding how the pattern of developing follicles is elaborated and maintained. The second level of analysis will deal specifically with the germ cells: oogonia, oocytes and eggs. Central to the investigation of oocyte development in the pipefish is the establishment of a staging series that identifies the cellular characteristics of developing oocytes. This series will provide a framework for designing experiments and relating experimental observations to the developmental sequence in the ovary. A concurrent goal of these studies will be to identify potentially fruitful avenues for future experimentation.

The second objective of this project will be to begin examining in more detail one process initiated early during oocyte development, that of vitelline envelope formation. The morphological features of vitelline envelope formation have been addressed previously (Anderson, 1967), therefore, this will not to be the major emphasis of the present studies. The biochemical properties of the vitelline envelope and the relationship of the resident proteins to the structure of the vitelline envelope will be the focus of this section. The biochemistry of the vitelline envelope, particularly the protein constituents, have not been sufficiently analyzed in teleost fishes. Thus, these studies are intended to provide an understanding of the principal biochemical constituents of the vitelline envelope, a major structural element formed during oocyte development.

The overall objective of this research project is to establish the pipefish ovary as a useful model system for investigating oogenesis and oocyte development. The biochemical properties of the vitelline envelope are a specific area to be examined in further detail. Within the framework these studies provide, the spatial organization of developing oocytes should facilitate experimentation of the earliest events in oogenesis and oocyte development. These processes have previously been difficult to address due to the random organization typical of vertebrate ovaries in general.

Terminology

The terminology used throughout the dissertation will follow standard usage; however, at this point it will be useful to clarify a few specific terms. The term *oocyte* will be used to describe the female meiotic germ cell. The term *follicle* will describe the oocyte, its surrounding vitelline envelope, and investment of follicle cells and theca components. The term *theca* will apply to the connective tissue network surrounding the oocyte-follicle cell complex. The term *lymphatics* will be considered as distinct from the theca proper. *Maturational* will be used to describe the oocyte which is capable of but has not undergone germinal vesicle breakdown. Finally, the term *vitelline envelope* will be used to describe the extracellular matrix surrounding the developing oocyte and ovulated, mature egg. The term *chorion* will be applied only to the protective covering surrounding the embryo proper. The terminology of the teleost egg envelope covering has had a long and complicated history with many different designations being ascribed to this particular structure (Anderson, 1967; Dumont and Brummett, 1985). The usage as I have defined vitelline envelope reflects the biochemical and mechanical similarities of the vitelline envelope prior to fertilization and distinguish this structure from the postfertilization chorion.

CHAPTER II
THE OVARIAN ANATOMY

Introduction

In 1898, Cunningham described an ovary which was particularly well suited for use in the study of early events in oogenesis. He observed that the pipefish ovary consisted of "but one germinal lamina which extends along the ovarian tube lengthwise, and the germ cells are present only at the extreme edge of this lamina" (1898, p. 128). He also noted that oocytes were arranged in decreasing order of development towards the germinal lamina edge. Since Cunningham's early observations, the pipefish has not been widely utilized experimentally. Published reports concerning reproductive processes in the pipefish and/or the closely related seahorse include breeding and embryo segmentation (Gudger, 1905), vitelline envelope formation (Anderson, 1967), cortical alveoli and yolk formation (Anderson, 1968), and a short mention of the pipefish ovary in a review (Wallace and Selman, 1981). Outside of these reports, little is known about oogenesis in the pipefish.

The exceptional features of this ovary prompted me to begin reexploring oogenesis in the pipefish. General descriptions of teleost ovaries (Dodd, 1977) and a detailed analysis for the *Fundulus heteroclitus* ovary (Brummett et al., 1982) have appeared but no such study is available for the pipefish ovary. Light and electron microscopic analyses were utilized to provide an understanding of the pipefish ovarian anatomy. My initial emphasis was to provide a description of the general anatomical features of the pipefish ovary in relation to follicle development.

Materials and Methods

Female Gulf pipefish, *Syngnathus scovelli*, were collected in the vicinity of Seahorse Key near Cedar Key, FL using a beam trawl with one-quarter inch mesh netting. Fish were collected on a monthly basis from November 1984 to October 1985. After collection, fish were transported back to the Whitney Laboratory, equilibrated to room temperature, and transferred to aquaria for maintenance. Ovaries were processed for analyses within 72 hours of collection.

Ovaries were dissected from freshly killed fish and immediately fixed with 4% glutaraldehyde and 2% paraformaldehyde in 0.1 M sodium phosphate buffer, pH 7.4 (Karnovsky, 1965). After several minutes, ovaries were cut transversely into small segments and transferred into fresh fixative for two hours at 23° C. The ovary segments were washed with several changes of 0.1 M sodium phosphate buffer, pH 7.4, for two hours at 23° C, postfixed at 4° C for 90 minutes in 1% osmium tetroxide and 0.1 M sodium phosphate buffer, pH 7.4, dehydrated through graded alcohol series and flat-embedded in Epon 812. One-micron sections were cut for orientation purposes and stained with 0.1% toluidine blue containing 1% sodium borate. Silver and silver-gold thin sections were cut and stained with uranyl acetate and lead citrate (Reynolds, 1963). Sections were observed on a JEOL 100 transmission electron microscope at 60kV. Some tissue for light microscopy was processed as described above without osmication and embedded in JB-4 (Polysciences) resin. One-micron sections were cut and stained with Harris's hematoxylin and eosin (H&E), Masson's trichrome, periodic-acid Schiff (PAS) (Luna, 1968), and toluidine blue as described.

Demonstration of lymphatic spaces was accomplished by injection of India ink using an insulin syringe and 25-gauge needle (Perez-Clavier and Harrison, 1978). The needle was introduced parallel to and between the ovarian wall and underlying follicles of fresh ovaries. Injection pressure was controlled by hand. Images were photographed with a camera mounted on a stereomicroscope.

Results

General Morphology

The ovaries are paired structures that fuse caudally to give rise to a short oviduct that leads to the genital papilla. The teleost oviduct does not share embryological homology with the oviduct of other vertebrates. However, functionally, it does serve to transport eggs from the ovary to the genital papilla for transfer to the male brood pouch. Ovaries from adult females (mean length 121 mm) reach approximately two cm in length and contain up to approximately 200 eggs. They are supported from the dorsal body wall by a mesovarium through which the blood supply and nerves to the organ traverse. The ovary lies lengthwise in the peritoneal cavity and eggs are generally found along the entire length of the ovarian lumen. The ovary itself is a cylindrical tube whose outer layer is composed of a visceral coelomic epithelium overlying a multilaminar smooth muscle wall. The inner layer of the cylindrical tube consists of the ovarian luminal epithelium. Between the two epithelial layers, a tubular sheet of follicles and supporting stromata reside in a sandwichlike configuration.

The pipefish ovary represents an unusual vertebrate ovary due to the temporal and spatial relationship of oocyte development. As Figures 1 and 2 demonstrate, the germinal ridge is located along the entire length of one edge of the ovarian sheet. It is in this germinal ridge that proliferative germinal elements reside. There are two variations observed with respect to the germinal ridge. In one case, the germinal ridge and early developing follicles form a curl protruding into the ovarian lumen (Fig. 2). In the other variation, the germinal ridge and succeeding

Fig. 1. Photomicrograph of a portion of fresh ovary that has been opened lengthwise and spread out to demonstrate sequential array of developing follicles in the ovarian sheet. Germinal ridge (GR) is present at the upper edge of the spread with intermediate-stage follicles present at the lower portion of micrograph. x 40.

Fig. 2. Transverse section of an entire ovary depicting various stages of oocyte development. Note that the follicles are sandwiched between the outer ovarian wall and inner luminal epithelium. The germinal ridge (arrowhead) and young developing follicles have curled to protrude into the ovary lumen (L). The mature edge is indicated by the dotted line overlying the largest oocytes (O). Note also the region of the ovary lacking follicles between the ovarian wall and the luminal epithelium (arrow). General dorsal (D) and ventral (VN) relations are indicated. One um Epon, toluidine blue. x 100.

Fig. 3. Transverse section of germinal ridge apposed to the ovarian wall (OW). Germinal ridge (*) containing several meiotic oocytes (large nuclei) present in the outpocketed region of the luminal epithelium (arrowheads). Note the primordial follicle (white arrow) separating from the germinal ridge. JB-4 resin, H&E. x 440.

Fig. 4. Region comparable to dashed area outlined in Figure 2. Stromal tissue found associated with the regions between adjacent follicles near the mature edge. Note arterioles (arrows) interspersed among the connective tissue (CT). (OW) Ovarian wall. (O) Oocyte. JB-4 resin, H&E. x 270.

Fig. 5. Extreme mature edge of ovarian sheet with vein (V) among the connective tissue. Luminal epithelium (arrow) diverges from ovarian wall (OW) to overlie prematurational oocyte (O). Endothelial cells (arrowheads) can be observed lining a lymphatic space (LY). JB-4 resin, H&E. x 260.

Fig. 6. Postovulatory follicle (arrows) near the mature edge with hypertrophy of follicle remains. (L) Ovary lumen. One um Epon, toluidine blue. x 140.

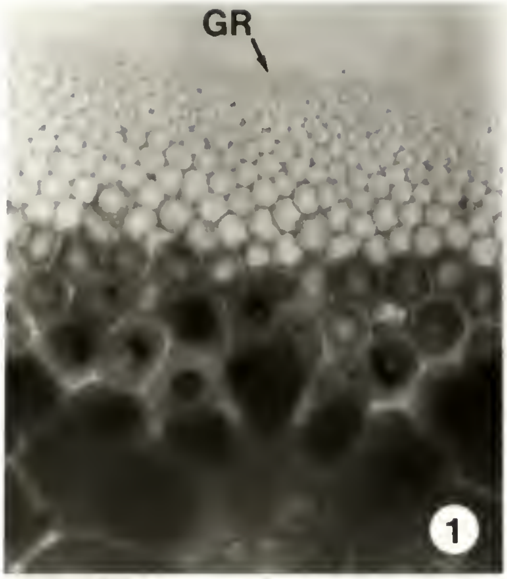
GR
1

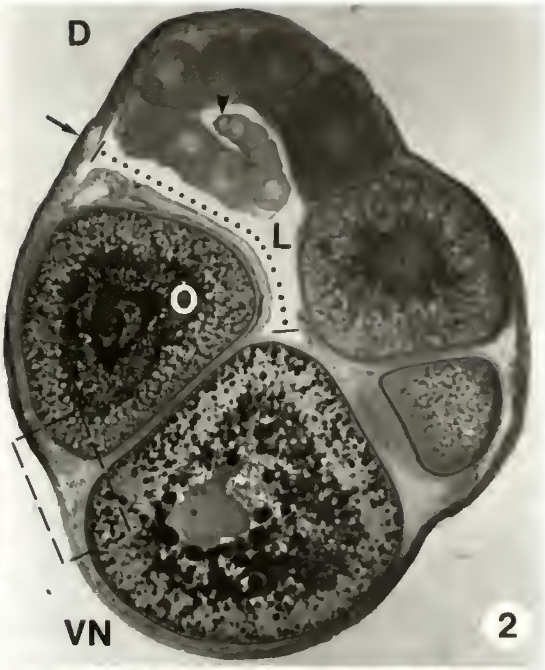
D
L
O
VN
2

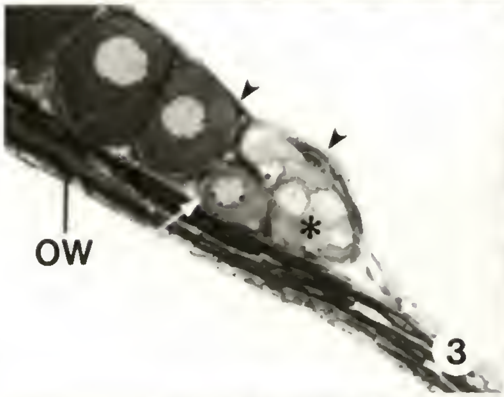
OW
*
3

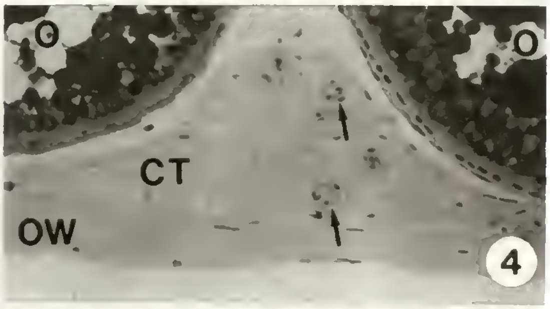
O
O
CT
OW
4

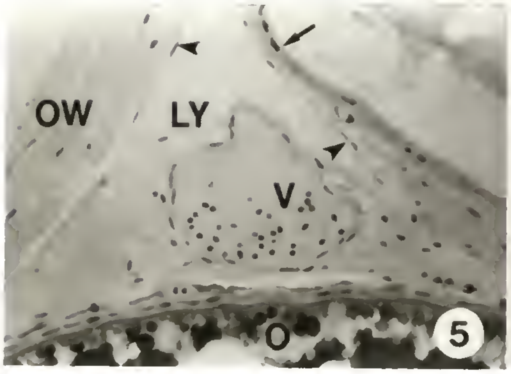
OW
LY
V
O
5

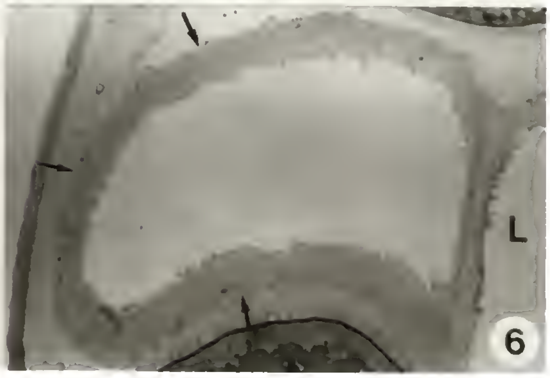
L
6

developing follicles are immediately apposed to the ovarian wall such that no curl protrudes into the lumen (Fig. 3). Regardless of which configuration exists, follicles always assume a sandwichlike configuration as follicle development progresses. At the opposite edge of the sheet, the mature edge (Figs. 2, 4, 5), oocytes undergo maturation and ovulate into the ovarian lumen. Postovulatory follicles are sometimes observed at the mature edge (Fig. 6). The interior cavity of these structures after ovulation is continuous with the ovarian lumen. Postovulatory follicles are distinct from atretic follicles, which also occur in the ovary. Atretic follicles typically contain cellular debris from the degenerating oocyte. Follicles between the germinal ridge and the mature edge form a sequential spiral with respect to oocyte development such that each follicle is followed by follicles of progressively increasing developmental age. The sequential array is consistent in the early follicles but becomes somewhat intermingled and less linear near the mature edge. This is most likely due to the pronounced expansion of oocytes during the vitellogenic growth period. Specific aspects of oocyte development will be dealt with in Chapter III. The sequential spiral lies in a transverse plane with respect to the lengthwise axis of the fish. In situ, the germinal ridge generally lies in relation to the dorsal body wall and the mature edge generally lies in relation to the ventral body wall (Fig. 2). These relationships are maintained throughout the entire length of the ovary.

Ovaries were examined during every month of the year and follicles of all developmental stages were present in adult fish. In addition, ovulated eggs were present within the ovarian lumen at all times of the year. There is no apparent regression of the ovarian structure or follicle development with respect to season. The availability of fish, however, does decrease during the winter months (December-February) but nonetheless, fish remain reproductively active. Pipefish can be maintained in laboratory aquaria if efforts are made to secure a constant source of live food such as brine shrimp and locally collected small crustaceans. Fish were maintained with such a feeding regime with the ovaries still having a normal appearance as indicated by the presence of all stages of developing oocytes.

Outer Ovarian Wall

The outer ovarian wall forms the outermost boundary of the ovarian cylindrical tube and encircles the ovary in a continuous fashion along its entire length. The ovarian wall has follicles associated with it along most of its circumference of the ovary but is devoid of underlying follicles along a region beyond the mature edge as the epithelium passes back towards the germinal ridge. This area (Fig. 2) allows for distension of the ovarian lumen to accommodate and store eggs after ovulation. The ovarian wall is covered externally by squamous visceral coelomic epithelium continuous with the epithelium of the peritoneal cavity. Internal to the coelomic epithelium is a smooth muscle layer which is several cell layers thick (Fig. 7). The smooth muscle cells are typical in structure and are predominantly arranged in a circumferential orientation perpendicular to the long axis of the ovary. Smooth muscle cells with a more longitudinal orientation were occasionally observed in the innermost and outermost region of the wall. A few fibroblasts are observed among the muscle cells. Arterioles are present among the smooth muscle cell layers at various levels of the lamina whereas venules are generally confined to the inner and outer portions of the wall boundaries. Internal to the ovarian wall, stromal elements supporting individual follicles are found. Unmyelinated nerves also reside between the smooth muscle cells at various levels of the ovarian wall lamina (Fig. 7). They appear to lie in a longitudinal orientation throughout the ovary. Myelinated nerves were not observed.

Inner Luminal Epithelium

The luminal epithelium forms the inner boundary of the cylindrical ovarian tube. It is a simple epithelium consisting of squamous-to-cuboidal cells resting on a basal lamina (Fig. 8). The apical cell surfaces possess microvilli that are found throughout the ovarian lumen.

Fig. 7. Electron micrograph of a transverse section of the ovarian wall. Coelomic epithelium (CE) of outer ovarian wall facing peritoneal cavity (PC) overlies several layers of smooth muscle (SM) cells. Note the orientation of the outermost longitudinal and inner circular muscle cells. Large bundles of unmyelinated nerves (N) present in the muscle layers among connective tissue elements. (*) Connective tissue cell. x 7,980.

Fig. 8. Luminal epithelium (LE) overlying a thin walled vein (V). Note tight junctions (arrows) and desmosomes on the apical and lateral borders, respectively, of the epithelial cells. Microvillar processes are seen extending into the ovarian lumen (L). The basal border of these epithelial cells rests on a basal lamina (arrowheads). x 3,240.

Fig. 9. Blebbing of luminal epithelial cell into ovary lumen (L). Highly secretory nature of these cells is apparent here and in Figure 8. Note the abundance of intracellular filaments (F). x 9,760.

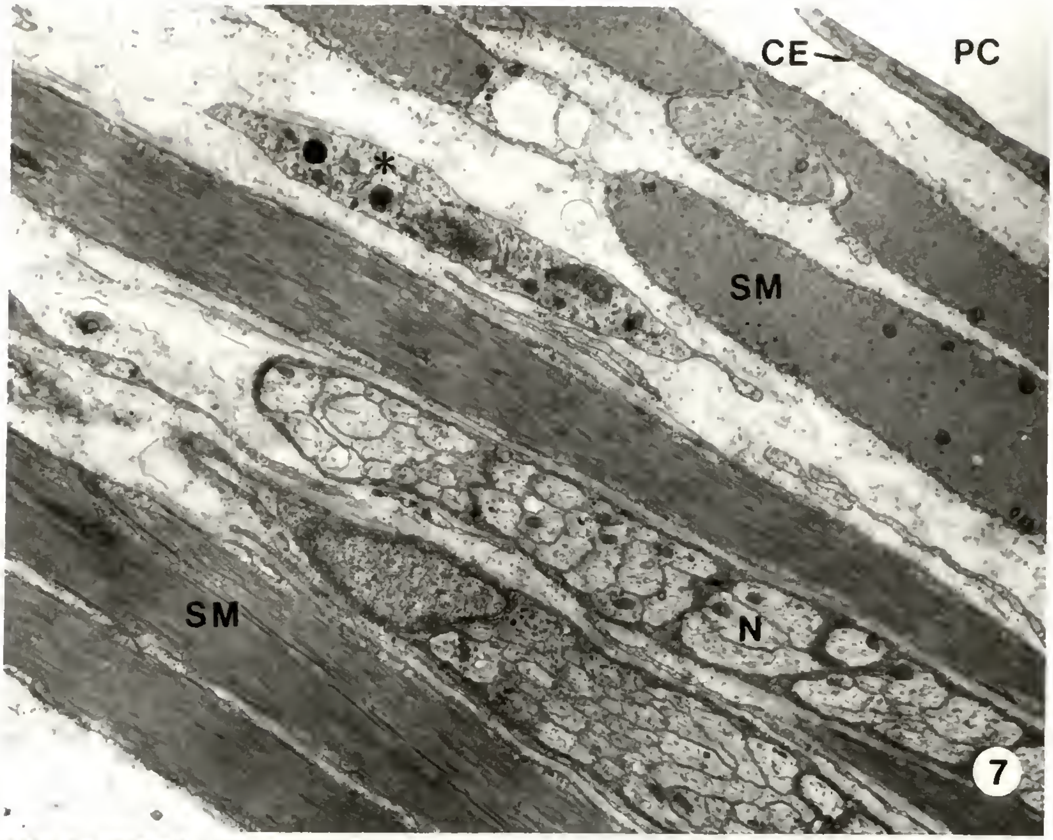

7

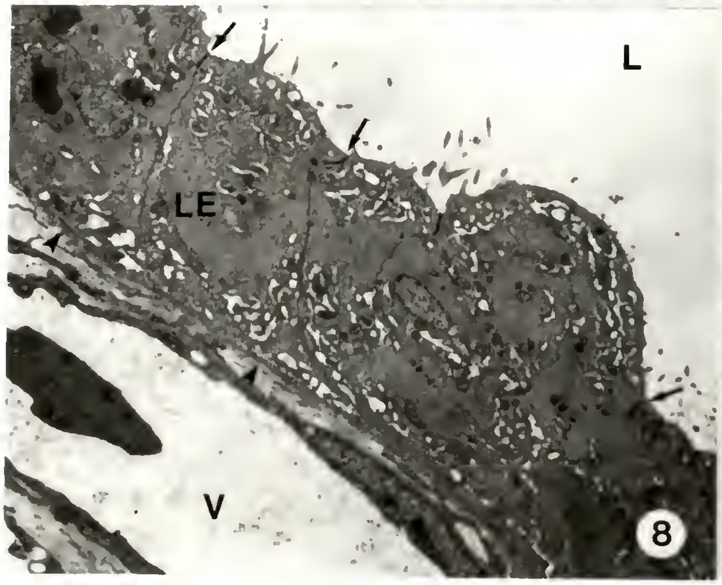

8

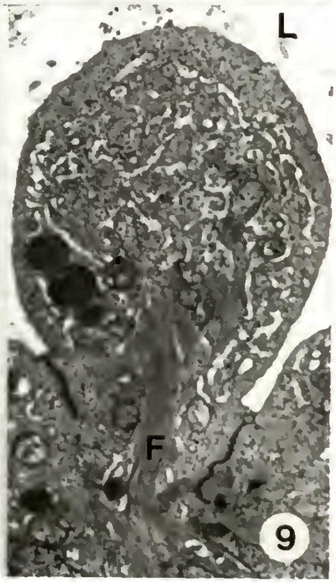

9

The epithelial cells in the germinal ridge regions of the ovarian sheet are typically more squamous than those of other regions. Epithelial cells overlying more developed follicles are generally more cuboidal. Certain epithelial cells possess a columnar shape and display blebs that protrude into the ovarian lumen (Fig. 9). The apical borders of the epithelial cells are joined by tight junctions. Desmosomes of variable size also occur on the lateral cell borders. Most of the luminal cells appear to be highly synthetic since they possess the organelles required for the synthesis of large amounts of protein (i.e., rough endoplasmic reticulum, Golgi, ribosomes) (Figs. 8, 9). A striking feature of the epithelial cells is the abundance of intracellular filaments (Fig. 9), which are present in cells throughout the ovarian lumen. Beneath the luminal epithelium, capillaries and venules are present at various positions along the follicle developmental spiral. Stromata consisting of connective tissue as well as lymphatics are also present in regions beneath the epithelium. Oogonia are associated with the luminal epithelium compartment near the germinal ridge (below).

Germinal Ridge

The germinal ridge region of the ovary lies along the entire length of one edge of the ovarian sheet (Figs. 1, 2, 3). The ridge is a consistent feature of all ovaries examined. The germinal ridge constitutes the proliferative stem-cell segment of the ovarian sheet from which oocytes are derived and follicles are formed. The germinal ridge is well defined and contains oogonia, early meiotic prophase I oocytes, somatic "prefollicular" cells, and occasional degenerating cells. The germinal ridge is distinguished as an outpocketing of the luminal epithelium as defined by its subjacent basal lamina (Fig. 10). External to the basal lamina enclosing the germinal ridge is a variable connective tissue layer. Meiotic germ cells in the germinal ridge initially lie in direct apposition with one another sharing cell borders to a variable degree (Figs. 10, 11). Intercellular bridges between germ cells have not been observed. The germ cells do not lie in direct contact with a basal lamina but are apposed to prefollicular (follicle-cell precursors) cells (Figs. 10, 11, 12). The prefollicular cells (Fig. 11) and follicle cells of a distinct primordial follicle (Figs. 13 a,b) contain a complement of filaments within their cytoplasm whereas early meiotic oocytes do not. These filaments are essentially the same as cytoplasmic filaments observed in luminal epithelial cells (Fig. 9). Follicle cells and their precursors also lie in direct contact with a basal lamina on one of their surfaces (Figs. 10, 11).

Follicle formation occurs within the germinal ridge. The prefollicular cells within the germinal ridge are observed extending cell processes between the contiguous

Fig. 10. Transverse section showing a portion of the germinal ridge region of the ovary. Note the continuity of the basal lamina (arrowheads) as it lies beneath the luminal epithelium (LE) and how it diverges from the luminal epithelium cells to envelop the germinal ridge to completely surround it. Groups of oocyte (O) germ cells and prefollicle cells (PFC) can be seen in the germinal ridge. Note the contiguous borders (arrows) of adjacent oocytes. x 5,720.

Fig. 11. Intracellular filaments (arrows) in prefollicle cell (PFC) of the germinal ridge. Basal lamina surrounding germinal ridge contacts one surface of the prefollicle cell. Meiotic oocytes (O) with shared cell borders are indicated. x 13,380.

Fig. 12. Separation of contiguous cell borders of meiotic oocytes (O) in germinal ridge by prefollicle cell (PFC) process (arrows) extending between germ cells. Note the desmosomal contact (arrowhead) with adjacent prefollicle cell. x 16,200.

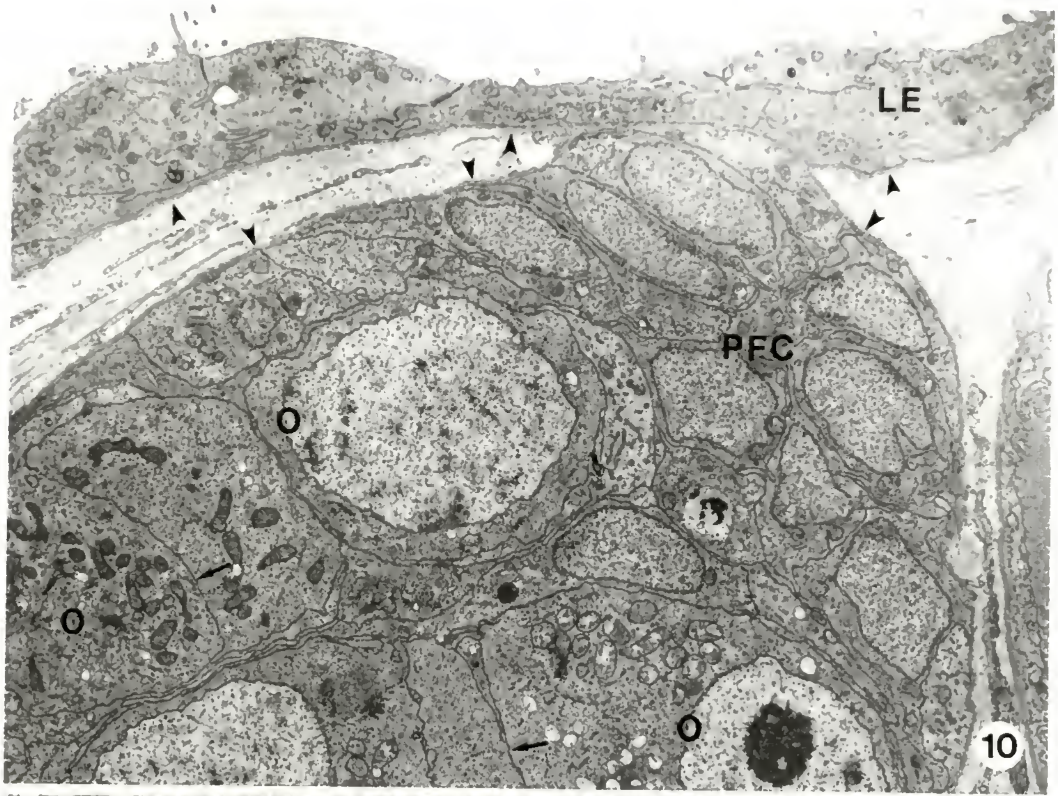
10

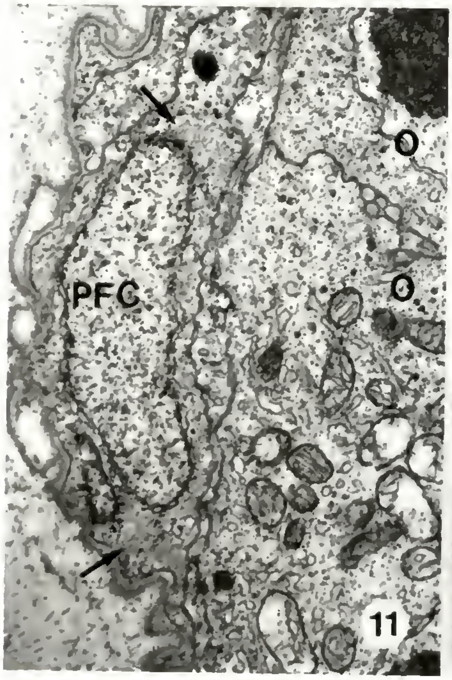
11

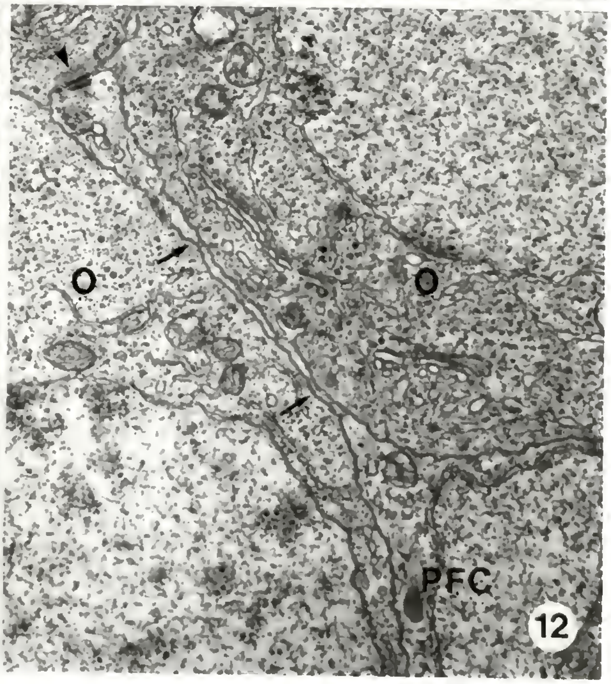
12

Fig. 13. a) Follicle separation from the germinal ridge (GR). Definitive follicle cells (*) surround the primordial follicle (PF) as it "pinches" (arrows) away from the ridge. Note the thin connective tissue layer and lymphatic space (LY) surrounding the germinal ridge and primordial follicle. The basal lamina (arrowheads) can be followed and noted to enclose the entire germinal ridge and primordial follicle. Oocyte (O) in definitive follicle of early follicle progression is indicated. (LE) Luminal epithelium. x 3,660. b) Higher magnification of boxed area in Figure 13a demonstrating definitive follicle cell containing abundant intracellular filaments (arrows). These filaments compare to those seen in Figure 11. x 18,500.

Fig. 14. a) Primordial follicle (PF) as it separates from the germinal ridge (GR). Note the basal lamina (arrows) as it surrounds germinal ridge and primordial follicle. (FC) Follicle cell. x 6,120. b) Higher magnification of separation site of primordial follicle from germinal ridge depicted in Figure 14a. The basal lamina almost completely separates the primordial follicle from the germinal ridge (arrows). Note the maintenance of distinct compartments as this separation occurs. x 14,200.

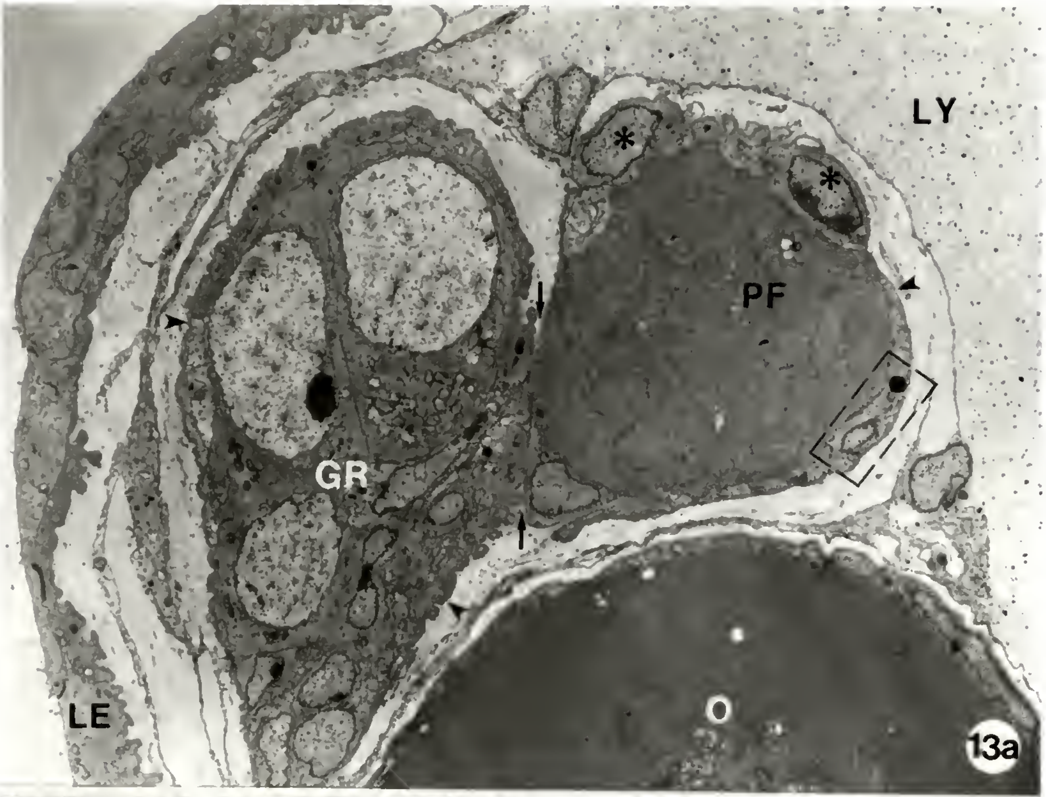

13a

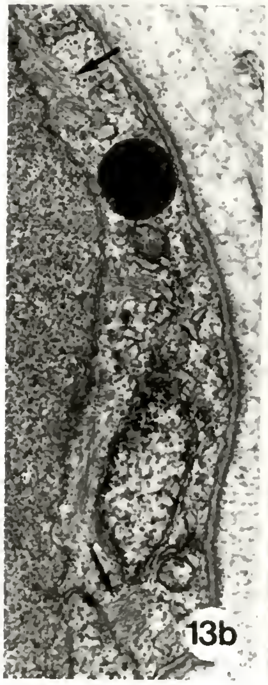

13b

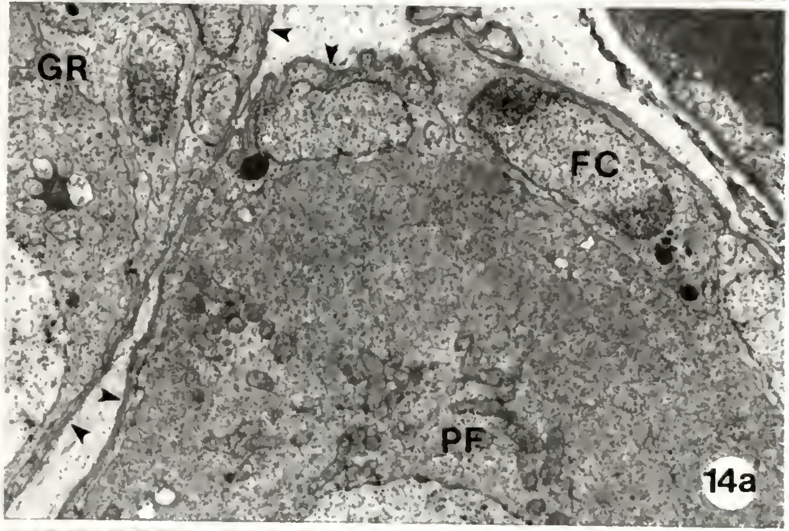

14a

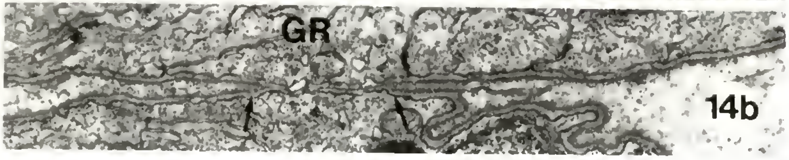

14b

meiotic oocytes, thereby completely separating the oocyte from other germ cells (Fig. 12). Meiotic oocytes undergo some primary growth while still within the germinal ridge. Primordial follicles, still associated with the germinal ridge, are observed at various stages of separation from the ridge (Figs. 13 a,b). This separation appears to occur as the primordial follicle "pinches" off of the germinal ridge to become a definitive follicle unit surrounded by its own basal lamina (Figs. 14 a,b). This basal lamina surrounding the newly-formed follicle, therefore, is derived originally in part from that which is overlying the germinal ridge. The newly formed follicles in the progression have a thin theca and often have lymphatic spaces around their borders. The young follicles then enter into the sequential follicle developmental spiral. As the oocytes progress through different stages, they assume their complement of thecal cells which appear to be derived from mesenchymal tissue. Thus, oocytes and associated follicle cells are originally derived from the luminal epithelial compartment of the ovary, whereas the cells of the theca are not.

Mature Edge

The mature edge of the ovarian sheet is defined by the position of the largest follicles that are ready for maturation and ovulation (Figs. 2, 5). Prematurational oocytes are present along this edge of the ovary in one or two longitudinal rows. The oocyte animal pole (defined by position of the nucleus) is oriented towards the luminal epithelium as indicated by the oocyte germinal vesicle that can be visualized through the luminal epithelium (Fig. 15). The germinal vesicle is generally within approximately a 20-30 degree radius whose axis runs through the oocyte from the luminal epithelium to the ovarian wall. This organization indicates that the oocytes possess a polarity in relation to the general ovarian anatomy. Large veins and venules are present beneath the luminal epithelium in this region of the ovary, with arterioles generally absent (Fig. 5). Stromal and lymphatic components, present to variable degree, are found on the lateral aspects of the follicles. Bundles of smooth muscle whose fibers are oriented parallel to the long axis of the ovary are also present (Fig. 16). The muscle cells appear beneath the luminal epithelium as it moves away from the ovary wall to lie over the large follicles. Unmyelinated nerves can also be found among the longitudinal smooth muscle cells (Fig. 17).

The luminal epithelial cells at the mature edge appear to undergo changes including vacuolation that may precede ovulation. This degeneration is confined only to the region of the luminal epithelium that apposes the follicle. Subsequent to ovulation, a postovulatory follicle remains and the follicle cells undergo marked

Fig. 15. Photomicrograph of a portion of fresh ovary illustrating the relationship of the late-stage oocyte germinal vesicle to the ovarian lumen. This view is looking directly down onto the luminal epithelial surface of an ovary that has been opened up lengthwise. Oocyte germinal vesicles (arrows) are clearly visible just beneath and oriented towards the luminal epithelium. Note also the intermingling of intermediate-size follicles in this region of the ovary. x 20.

Fig. 16. Transverse section depicting mature edge luminal epithelium (LE) with bundles of smooth muscle (SM) cells having a longitudinal orientation. x 6,300.

Fig. 17. Unmyelinated nerve (N) present amongst the longitudinally oriented smooth muscle (SM) cells at the mature edge. x 6,900.

Fig. 18. Connective tissue consisting of collagen (C) and connective tissue cells (*). x 8,960.

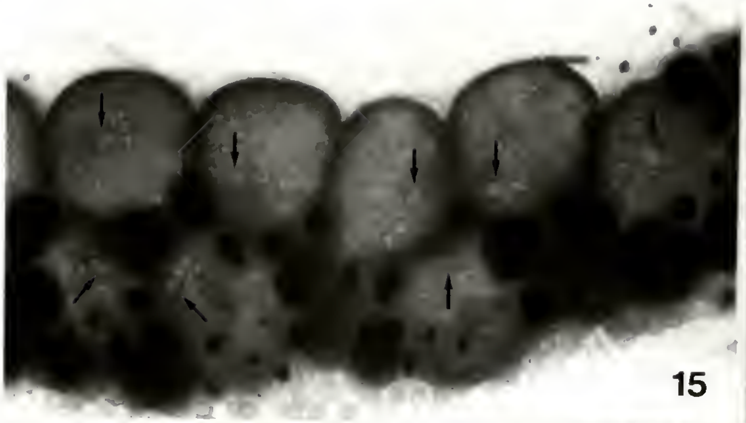

15

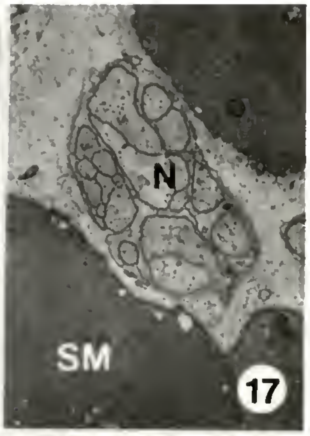

17

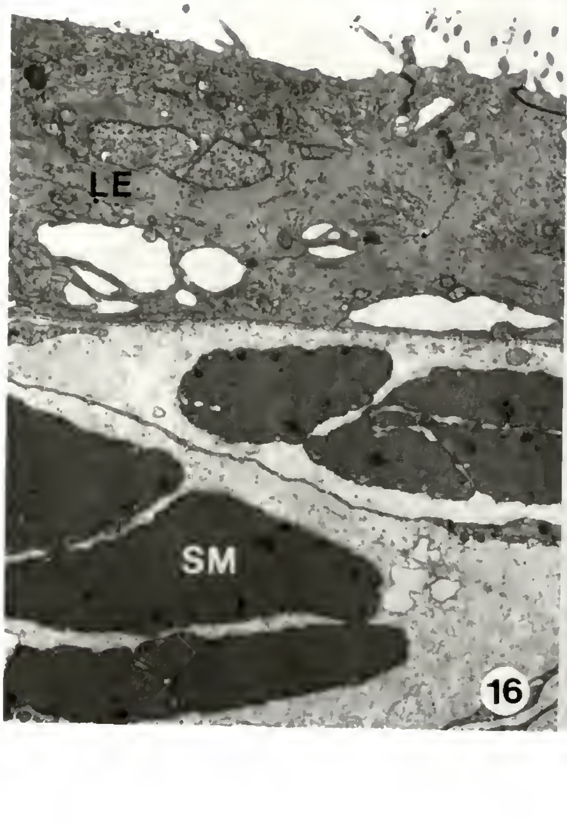

16

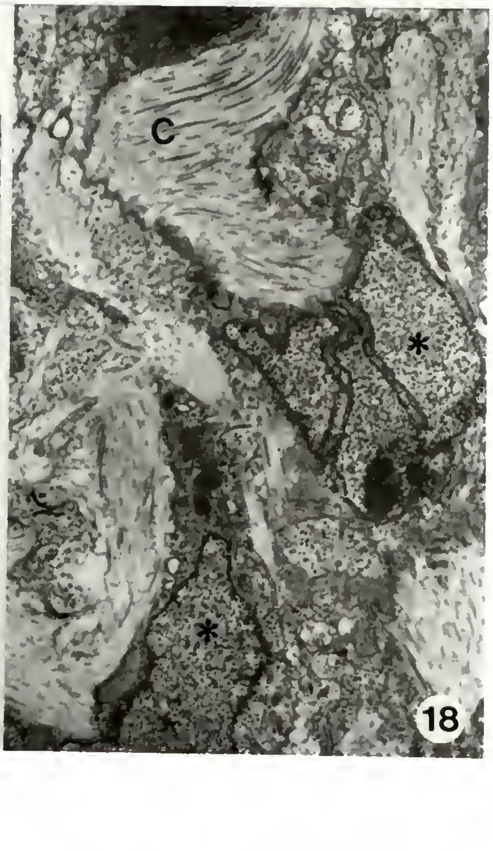

18

hypertrophy (Fig. 6). The follicular hypertrophy includes the presence of rough endoplasmic reticulum and Golgi elements in the now-columnar follicle cells.

Stromal and Lymphatic Compartments

The stromal elements of the ovarian sandwich consist of fibroblasts, connective tissue fibers, and blood vessels in addition to a substantial lymphatic compartment. The sandwichlike nature of the ovary gives rise to triangular spaces in the apicolateral (associated with the ovarian lumen) or basolateral (associated with the ovarian wall) portions between follicles. Stromal elements are present in these spaces (Fig. 4). Collagen fibers are multidirectionally oriented throughout the stromal network. They are interposed by stromata consisting of fibroblasts and blood vessels that form the connective tissue (Figs. 4, 18). The connective tissue is found in the thecal region of each follicle as well as in the bordering spaces between adjacent follicles, and is particularly pronounced between the largest prematurational follicles of the mature edge. The vascular supply can also be found amongst the stromal elements interior to the ovarian wall (Fig. 4). Additionally, capillaries are abundant beneath the luminal epithelium at all levels of the follicle developmental spiral. At the mature edge, venules and collecting veins are localized just beneath the luminal epithelium and can occasionally be seen to be continuous with small vessels overlying the largest prematurational follicles.

A significant portion of the stromal network contains a well developed lymphatic compartment that is lined by attenuated endothelial cells. Spaces between adjacent endothelial-cell processes can be observed as well as desmosomal contacts between the cells. India ink injections were used to demonstrate the extent of the lymphatic compartment (Fig. 19). Upon introduction of the syringe needle between the ovarian wall and the underlying follicles, ink is observed flowing between follicles within several seconds. With a slight positive pressure, the ink disperses to fill much of the interstitial space among follicles throughout the ovary within minutes. Thus, the lymphatic network is extensive throughout the ovary. In the early spiral portion of the follicle progression, the lymphatic space occupies much of the space between follicles (Fig. 20). The lymphatics can sometimes be seen to extend from the inner aspect of the ovarian wall all the way to the luminal epithelium between adjacent follicles. The lymphatics, however, are most frequently observed in the apico- and basolateral regions between adjacent follicles (Fig. 21). Large follicles tend to have greater amounts of connective tissue in addition to variable lymphatic regions on their lateral borders.

Fig. 19. India ink preparations of fresh intact ovaries demonstrating extent of lymphatic network in basolateral spaces between follicles. Note that the lymphatics end abruptly at the extreme mature edge (arrows) as eggs (E) are visible in ovarian lumen. The ovary on the right demonstrates extent of lymphatics in the early follicle progression. x 27.

Fig. 20. Lymphatic space (LY) extending between the lateral borders of adjacent young oocytes (O). x 3,300.

Fig. 21. Triangular lymphatic space (LY) in basolateral region between adjacent early developing oocytes (O) in relation to the ovarian wall (OW). Distinct endothelial cell (EC) lines the lymphatic space. x 7,850.

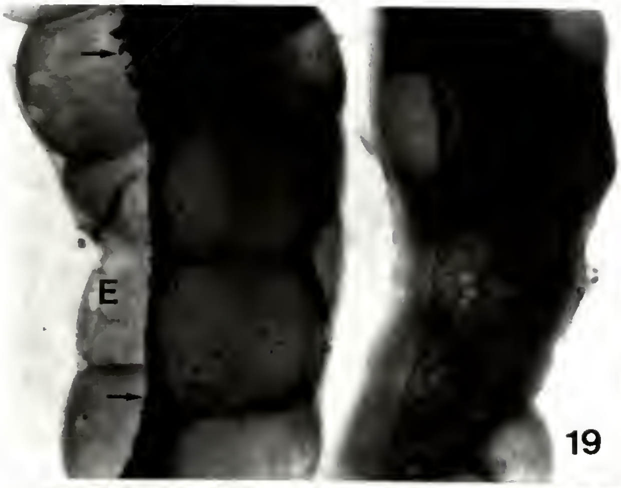
19

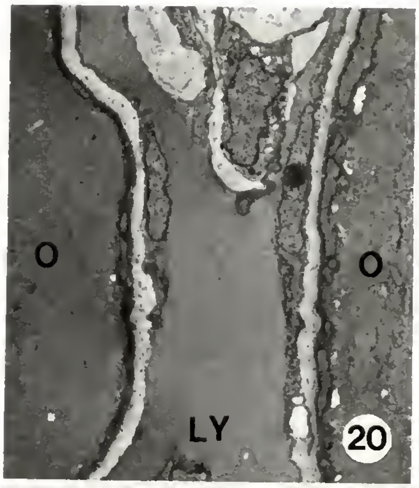
20

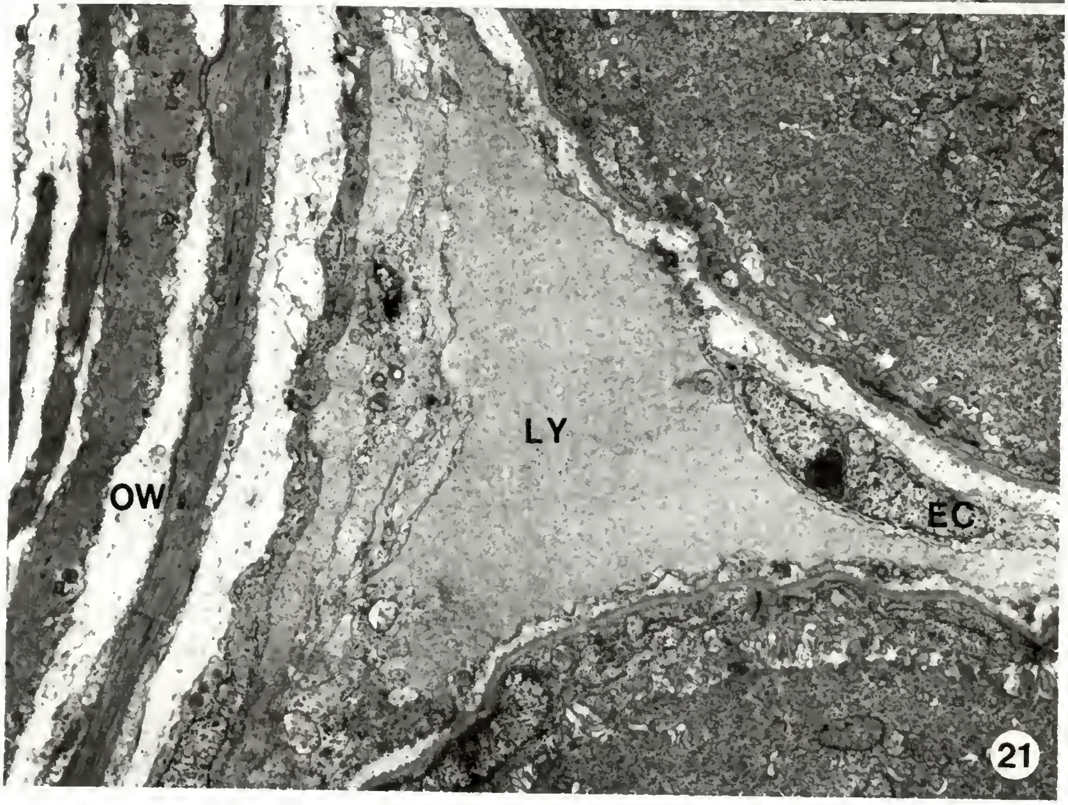
21

Fig. 22. Follicle relations to the luminal epithelium (LE). Note the somewhat cuboidal follicle cells (FC) with thick basal lamina (arrows) enclosing the oocyte (O) and follicle cells. Note that the thecal elements (T) are becoming more well developed. x 7,650.

Fig. 23. Oocyte (O) relations to the ovarian wall (OW). Note the presence of a lymphatic space (LY) between the theca (T) and the ovarian wall. x 3,450.

Fig. 24. Shared theca (T) on lateral aspects of adjacent oocytes (O). The theca contains primarily connective tissue elements, and note that individual follicles are not enclosed by a distinct epithelial cell layer. x 5,550.

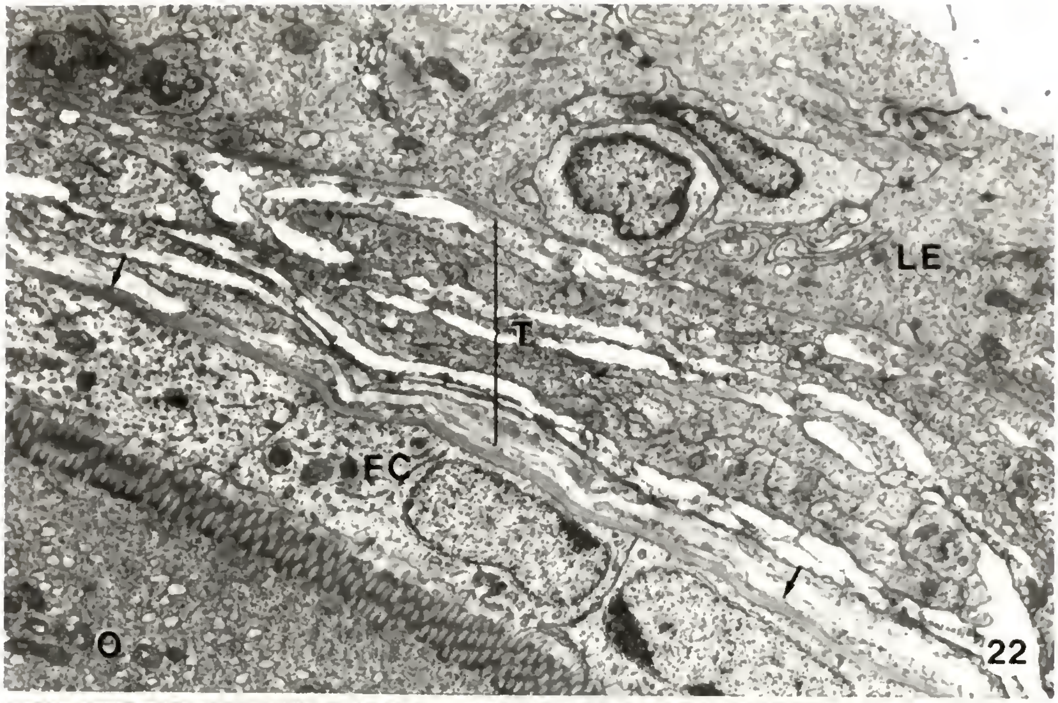
LE
T
FC
O
22

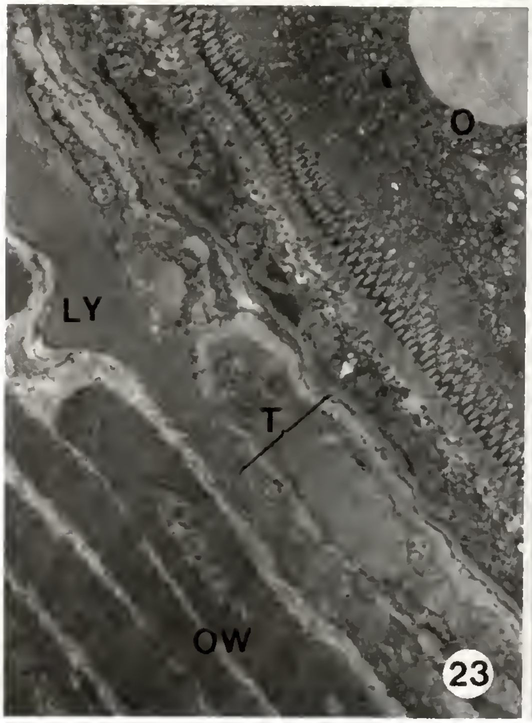
O
LY
T
OW
23

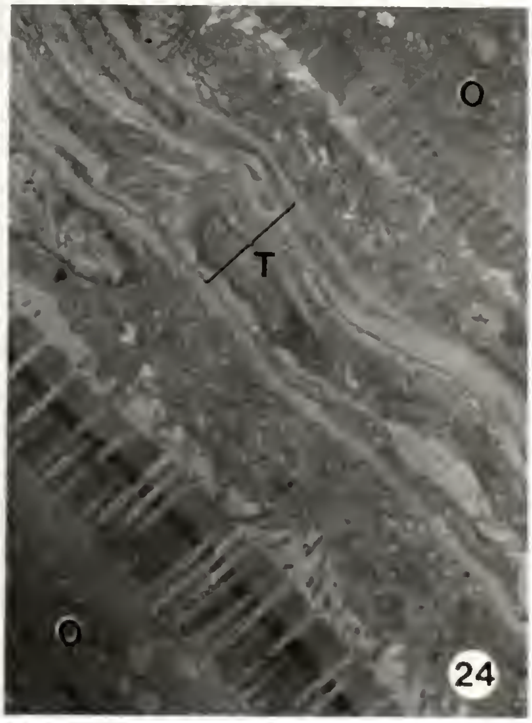
O
T
O
24

The sandwichlike arrangement of follicles between the luminal epithelium and ovarian wall results in a connective tissue sheath which does not just circumscribe individual follicles. The arrangement of connective tissue is such that follicles in fact have shared rather than individual thecal elements on their lateral aspects. On the apical aspect of the follicles, the theca is situated just beneath the luminal epithelium (Fig. 22), while on the basal aspect, the theca is apposed to the ovarian wall (Fig. 23). On the lateral portion of the follicles, the theca is shared with adjacent follicles (Fig. 24). Lymphatics may lie outside the theca all along the follicle spiral but are not considered part of the theca proper. The theca is initially sparse near newly formed follicles but becomes better developed as oocyte development progresses. Thus, the combination of connective tissue elements and lymphatic network form the supporting structure for developing follicles.

Discussion

According to Dodd (1977), the pipefish ovary would be classified developmentally as a cystovarian type and thus bears similarity to those of many other bony fishes in having a coelom-derived ovarian lumen continuous with the oviduct. The pipefish ovary has also been classified as an asynchronous type (Wallace and Selman, 1981), possessing a heterogeneous population of follicles of all developmental stages. The pipefish is reproductively active throughout the year instead of cycling annually as is the case for many other fishes (Matthews, 1938; Barr, 1963; Braekevelt and McMillan, 1967; Moser, 1967). The yearlong reproductivity of the pipefish is corroborated by observations that males carrying embryos can be found during all seasons (Brown, 1972). Unlike other teleost ovaries, the pipefish ovary lacks ovigerous lamellae common to fish such as _F. heteroclitus_ (Brummett et al., 1982) and _Sebastodes paucispinis_ (Moser, 1967). Rather, there exists a cylindrical tubular structure in which the follicles are sandwiched between an outer ovarian wall and an inner luminal epithelium. The follicles are arranged in a spiral of sequential development originating from the germinal ridge and extending to the mature edge. The processes of oocyte growth and development in this ovary parallel those in many other fishes. A schematic drawing (Fig. 25) summarizes the distinguishing features of the pipefish ovary and follicle relationships in relation to the environment _in situ_. It emphasizes follicle progressions, germinal ridge and lumen epithelium, lymphatics, and shared thecal components.

The arrangement of predominantly circular smooth muscle cells and longitudinal nerve fibers in the ovarian wall is probably important in egg release from the ovary. In the pipefish, egg laying occurs as the male and female

Fig. 25. Schematic summary of ovary and relations *in situ*. The upper diagram indicates the paired ovaries which join to give rise to the oviduct. Note that the ovaries have a bilateral symmetry with respect to the early follicle progressions that lie on the lateral aspect of each ovary. The dashed line indicates a segment of the ovary that is enlarged in the lower diagram maintaining *in situ* relations. The middle section has been unfurled to allow visualization of the follicles and ovarian lumen. Note that a strip of luminal epithelium has been removed except near the germinal ridge along with the underlying connective tissue elements to visualize the follicle progression in the ovarian sheet. The association of the luminal epithelium with the germinal ridge is indicated. The germinal ridge in the reflected segment of the luminal epithelium depicts primordial follicles in various stages of separation. The sandwichlike nature of the ovary is apparent in the unfurled region with follicles lying between the ovarian wall and the luminal epithelium. Arterioles, veins, and lymphatic spaces are indicated in typical locations. Smooth muscle bundles near the mature edge and smooth muscle fibers in the ovarian wall are apparent. A theca encloses each follicle and can be seen to be shared on lateral borders. This schematic is prepared to highlight features of the ovary and is not drawn fully to scale.

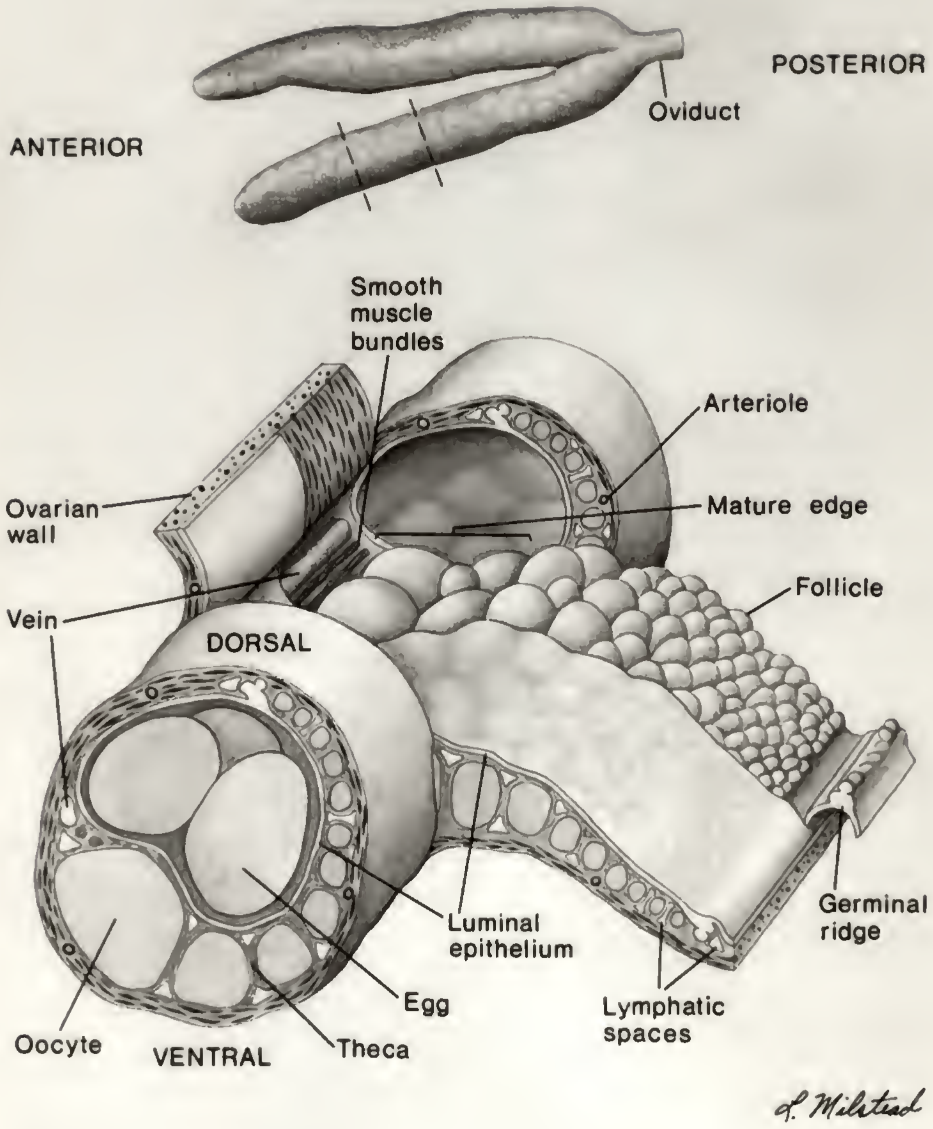
POSTERIOR
Oviduct
ANTERIOR
Smooth muscle bundles
Arteriole
Ovarian wall
Mature edge
Follicle
Vein
DORSAL
Luminal epithelium
Germinal ridge
Egg
Lymphatic spaces
Oocyte
VENTRAL
Theca
L. Milstead

swim in unison during which time the female deposits eggs into the male brood pouch (Gudger, 1905). Therefore, the expulsion of eggs from the female into the brood pouch requires a precisely coordinated timing of egg release from the ovary so that egg transfer can be effected. Consequently, it is probable that the spawning response is controlled in part by neural input. Therefore, I suggest that egg release may be controlled with a contraction wave of the ovarian wall beginning cranially and proceeding in a caudal direction, in effect squeezing the eggs out of the ovarian lumen. The eggs would then be transferred through the oviduct and deposited in the male brood pouch.

The presence of longitudinally oriented smooth muscle cells beneath the luminal epithelium at the mature edge is a bit perplexing. In this region of the ovary, a transition from circular to longitudinal fibers is noted where the inner luminal epithelium dissociates from the ovarian wall to overlie the prematurational and preovulatory follicles. I intend here primarily to note this observation. Contractile mechanisms involving microfilaments or contractile cells have been implicated as participating in ovulation, but the evidence is not conclusive (reviewed by Goetz, 1983). Spontaneous contractions of the *F. heteroclitus* ovary have also been reported (Winner and Taylor, 1985). It is clear that no specific conclusion can be drawn from the current study.

However, the pipefish ovary may provide an opportunity to address the question of contractile involvement in ovulation in a more detailed manner because the position of preovulatory follicles is precisely arranged.

The germinal ridge, which runs the entire length of the ovary, serves as a continuing source of primordial follicles for future egg production. The distinguishing feature of this germinal ridge is its existence as an outpocketing of the luminal epithelium, demonstrating that the germinal ridge and luminal epithelium are co-occupants in the same compartment of the ovary. This observation represents the first clear evidence in teleosts with respect to the association of the luminal epithelium with folliculogenesis. There is a report for the guinea pig that indicates that germ cells and prefollicular cells are compartmentalized in the surface epithelium (Jeppesen, 1975). In teleosts, however, there has been much speculation about the compartment in which the oogonia and early oocytes reside and from which source the follicle cells are derived. Suggestions include oocytes being derived from the luminal epithelium (Bullough, 1942; Lehri, 1968) as well as being formed from amongst the stromata beneath the lumen epithelium (Brummett et al., 1982). Also, follicle cells have been described as having a mesenchymal (Mendoza, 1943; Braekevelt and McMillan, 1967) or an epithelial origin (Bullough, 1942; Moser, 1967).

Observations on the viviparous cyprinodont, Neatoca bilineata, indicate that many of the gonial nests are derived from invaginations of the ovigerous fold epithelium (Mendoza, 1943). In this report, the suggestion was made that the gonial nests pinch off as a complete unit from the epithelium and, therefore, arise from the ovarian epithelium. Mendoza (1943, p. 90) described follicle cells as being "modified fibrocytes of subepithelial connective tissue." The data presented here provide additional understanding of these observations and clarify the process of folliculogenesis.

My observations on the pipefish ovary indicate that both the germ cells and the prefollicle cells originally reside within the ovarian luminal epithelial compartment. This study has also defined a mechanism by which the primordial follicle becomes enclosed by a basal lamina sac, a process which has not been addressed previously. My interpretation of folliculogenesis from static images is as follows: Follicle formation occurs within the germinal ridge. An early event in the process is the formation by oogonial division of primary oocytes that are in the early stages of meiosis prophase I. These early oocytes initially share cell borders but subsequently become completely separated from one another as prefollicle cells extend processes between the contiguous meiotic oocytes, thereby completely separating a newly formed oocyte from other meiotic germ cells. The enclosed oocyte then undergoes some initial growth while still within the ridge. Ultimately, the primordial follicle becomes distinct from the germinal ridge as it "pinches" off to become a newly formed definitive follicle surrounded by its own basal lamina and thin connective tissue sheath. The basal lamina of the follicle thus originates from that of the germinal ridge. The germinal ridge remains contiguous with the luminal epithelial compartment, with the continuity of the basal lamina surrounding the germinal ridge being maintained. The new follicle then enters into the sequential follicle developmental spiral. Subsequently, as follicle growth proceeds, mesenchymally derived cells come into association with the definitive follicle to form the theca of the developing follicle. The theca becomes increasingly well developed as oocyte growth proceeds. The process repeats itself as each primordial follicle leaves the germinal ridge to enter into the follicle progression.

A fundamental conclusion is that both the early germ cells and the prefollicle cells originate from within the luminal epithelial compartment. This is indicated by the outpocketing of the luminal epithelium to form the germinal ridge. The oocytes in the germinal ridge are a product of oogonial division, which also occurs in the germinal ridge of the luminal epithelium. Filaments in pipefish follicle cells were first noted by Anderson (1967). The demonstration in this study of cytoplasmic filaments in the prefollicle cells and early definitive follicle cells provides a convenient cytoplasmic marker and suggests that follicle cells may be derived from a source similar to the luminal epithelial cells, which also possess a substantial number of filaments in their cytoplasm.

The orientation of the oocyte germinal vesicle relative to the luminal epithelium indicates an organized polarity of the late-stage oocytes with respect to the ovarian anatomy. In the frog, _Xenopus laevis_, the orientation of the oocyte to the ovarian structure has been determined to be random (Van Gansen and Weber, 1972). However, there does not seem to be any documentation of these relationships for teleost ovaries. In the pipefish, oocyte polarity in relation to the ovary is not apparent in early oocytes but instead becomes notable in the later stages of oocyte development. Although the orientation of the oocyte to the luminal epithelium is not precise, the germinal vesicle is observable quite readily within approximately a 20-30 degree radius with respect to a perpendicular axis between the luminal epithelium to the ovarian wall passing through the oocyte. The establishment of this relationship during follicle development remains an interesting problem.

The shared theca, particularly between adjacent oocytes, is different from the situation in other fish in which a theca and surface epithelium appears to enclose individual developing follicles. The developing follicles of the pipefish thus share to a large extent the same general external environment. Therefore, recruitment of oocytes into the various stages may well be a result of not only external cues but internal regulation as well. Specialized thecal cells (Nagahama, 1983) have not been observed in the theca but cannot be excluded. Thus, the theca appears to form a general supportive network within the ovary and coexists with the extensive lymphatic portions to form the complete ovarian stromata.

The pipefish ovary possesses an extensive lymphatic network in the interstitial regions between follicles. This, in effect, forms a "sea" in which the developing follicles reside bounded by the luminal epithelium apically and the ovarian wall basally. Relevant to the lymphatic compartment is the vascular supply to the ovary. The distribution of arterioles near the ovarian wall and capillaries and veins near the luminal epithelium suggests a directional vascular flow from the ovarian wall towards the luminal epithelium. Such a flow would bathe the follicles with blood nutrients and plasma proteins, most notably vitellogenin, the yolk protein precursor (Wallace, 1985). Plasma protein bathing would be expected due to the high capillary permeability of vessels in the ovary, as indicated by several studies using exogenous tracers

(Dumont, 1978; Ellinwood et al., 1978; Abraham et al., 1982; Selman and Wallace, 1982, 1983). The exact function of the lymphatics in the ovary remains unclear. It has been suggested that the lymphatic compartment helps to regulate plasma flow and interstitial fluid volume (Ellinwood et al., 1978). It may also serve to transport ovarian secretions such as hormones back into the systemic circulation. The lymphatic compartment in the pipefish ovary is thought to have a dynamic structure in order to accommodate changes in follicle size during oocyte growth. Compliance of the lymphatic network would allow follicle growth to proceed in a stable fashion within the ovary.

The unusual features of the sequential follicle development and germinal ridge make the pipefish ovary suited for experimental analyses of particularly early events in oogenesis. In addition to sharing many general features and processes with other teleost ovaries, the pipefish ovary possesses several intriguing variations. The sequential pattern of follicle development, germinal ridge participation in folliculogenesis, shared theca and lymphatics among follicles, and the apparent polarization of later stage oocytes with respect to the luminal epithelium distinguish the pipefish ovary from other vertebrate ovaries. With the exception of the closely related seahorse (Anderson, 1967), the sequential arrangement of follicles has not been described for other vertebrate ovaries. This sequential arrangement is found, however, in a variety of insects (Gutzeit and Sander, 1985).

CHAPTER III
STAGES OF OOCYTE DEVELOPMENT

Introduction

Oocyte development is spatially and temporally arranged in the ovary of the pipefish. The unusual pattern of oocyte development in the pipefish was first described by Cunningham in 1898. More recent studies have dealt specifically with vitelline envelope formation (Anderson, 1967), cortical alveoli formation and vitellogenesis (Anderson 1968), and ovarian anatomy (Begovac and Wallace, 1987). However, an adequate staging series for oogenesis and oocyte development has not been established for this experimentally useful animal.

Several staging series for teleost oogenesis have been described (Wourms, 1976; Shackley and King, 1977; Selman and Wallace, 1986). These staging series are helpful for understanding cellular events during oogenesis and serving as the basis for experimentation and comparison to other species. In two previous reports dealing with pipefish oogenesis (Anderson, 1967, 1968), oocyte stages were defined by convenience according to size. Together, these studies examined three different species of fish and consequently are confusing because of inconsistencies in the use of various stage designations and the application of these stages to different fish in the same study. The current investigations concerning pipefish oogenesis have indicated the need for a well defined staging series for oocyte development. Therefore, this report provides such a series for the pipefish, Syngnathus scovelli. The stages of oogenesis and oocyte development described are identified according to the cytological characteristics and physiological parameters of the developing oocytes.

Materials and Methods

Animals

Adult female Syngnathus scovelli, the Gulf pipefish, were collected near Cedar Key, FL, transported back to the Whitney Laboratory, and maintained in sea water aquaria. Tissues were processed for microscopy within 72 hours of collection. Ovaries were dissected from freshly killed fish, rinsed briefly in solution FO (Wallace and Selman, 1978), and immediately fixed with 4% glutaraldehyde and 2% paraformaldehyde in 0.1 M sodium phosphate buffer, pH 7.4 (Karnovsky, 1965), for 2 hours at 23° C. Individual follicles of various sizes were also dissected from ovaries using watchmaker forceps, measured with an ocular micrometer, and fixed as described. Tissues were washed in 0.1 M sodium phosphate buffer, postfixed with 1% osmium tetroxide, and embedded in Epon 812 as detailed previously (Begovac and Wallace, 1987). Tissues were also prepared as described above for light microscopy, with and without osmication, and embedded in JB-4 resin (Polysciences) or Historesin (LKB). Thick (1-3 um) sections were cut and stained with Harris's hematoxylin and eosin, Masson's trichrome, periodic acid-Schiff's reagent (PAS), alcian blue, pH 2.5 (Luna, 1968), and 0.1% toluidine blue in 1% sodium borate. For electron microscopy, silver and silver-gold thin sections were cut and stained with uranyl acetate and lead citrate (Reynolds, 1963). Sections were observed with a JEOL 100 transmission electron microscope operated at 60 kV.

Lectin binding was observed on tissues fixed with 4% paraformaldeyde in 0.1 M sodium phosphate, pH 7.4, and embedded in Historesin. Sections were incubated with phosphate-buffered saline containing hemoglobin (2 mg/ml) to block nonspecific staining. Slides were then incubated with fluorescein-conjugated concanavalin A (5 mg/ml; 1:50 dilution), washed, and viewed with an epifluorescence microscope.

Tissue Culture

Ovaries and follicles were cultured in a medium consisting of 85% Leibovitz L-15 (Sigma) containing 1 mM freshly prepared glutamine and 10 mM HEPES buffer, pH 7.6, at 20° C (hereafter referred to as 85% L-15). This culture media was empirically determined to be optimal with respect to cell viability over extended culture periods.

Tritiated-thymidine incorporation was examined in isolated longitudinal ovary segments containing the germinal ridge. These ovary segments were cultured in 85% L-15 medium and incubated at 20° C for periods up to 14 days. The incubation media was replaced every 2-3 days with fresh media. On days 0, 2, 5, 7, 10, the ovary fragments were pulsed with 20 uCi/ml methyl-^{3}H-thymidine (ICN; specific activity 6.7= Ci/mmol) for 24 hours and then processed as described above for light microscopy. Thick sections of these ovaries were cut and the slides coated with NTB-2 autoradiographic emulsion (Kodak). Slides were exposed for various times at 4° C and the emulsion developed for 90 seconds at 68° C with 1 part Dektol (Kodak) and 2 parts water. Sections were lightly stained with toluidine blue after development.

The fluorescent dyes rhodamine 123 (Johnson et al., 1980) and acridine orange (Allison and Young, 1969; Albertini, 1984) were used to assess the intracellular localizations of mitochondria and lysosomes, respectively. Intact ovary segments were incubated in 85% L-15 containing either rhodamine 123 (10 ug/ml) or acridine orange (1-10 ug/ml). Ovaries were incubated for 30-60 minutes at 20° C and then rinsed three times for 10 minutes each in media lacking the dye. The ovaries were pinned out on a microscope slide having silicon borders to allow visualization of the entire ovarian sheet. These preparations were observed with phase optics and epifluorescence microscopy. Rhodamine 123 was visualized using a rhodamine bypass filter. Acridine orange localization was determined with fluorescein and rhodamine bypass filters in combination to discriminate between ribonucleoprotein- and lysosome-specific staining. [The rhodamine bypass filter eliminates the background green fluorescence that is due to the ribonucleoprotein and allows visualization of the lysosomal network (Albertini, 1984)].

Oocyte competence to undergo oocyte maturation *in vitro* was determined after culture media optimization. In preliminary experiments, various steroids were tested for the ability to stimulate oocyte maturation *in vitro*. The steroid 17-alpha-hydroxy-20-beta-dihydroprogesterone (17-alpha,20-beta-DHP) was found to be the most effective and therefore was utilized for further experiments. Individual follicles were dissected free of ovarian stroma in solution FO using watchmaker forceps. Oocytes were separated into various size groups (0.7, 0.8, 0.9, 1.0, 1.1 mm diameter) and checked for the presence of a germinal vesicle (oocyte nucleus). Follicles from several animals were pooled for each experiment. For each size group, follicles were placed in 10x35 mm petri dishes containing 3 ml of 85% L-15 media. Experimental treatment groups received 17-alpha,20-beta-DHP (1 ug/ml final concentration) in 10 ul ethanol carrier. Control treatment groups received 10 ul of ethanol alone added to the media. Follicles were incubated at 20° C and scored for germinal vesicle breakdown after 40 hours of incubation using a dissecting microscope. Follicles that underwent atresia during the culture period were discounted from the results.

Protein content for various size follicles was determined according to the Pederson modification of the Lowry method (Pederson, 1977). Follicles were dissected free of stromal tissue and homogenized in 100 ul of solution F0. Follicles larger than 0.9 mm diameter were homogenized as described and the sample divided into two aliquots with the sum of these aliquots giving the total protein content per follicle value. Homogenates were then processed exactly as per the Peterson procedure. Bovine serum albumin was used to generate the protein standard curve.

Results

Stage I: Oogonia (approximately 10 um diameter)

The oogonia constitute the stem cells of the germ cell lineage. Oogonia are found in the luminal epithelium near the germinal ridge and within the germinal ridge itself. The germinal ridge is an outpocketed region of the ovarian luminal epithelium (Begovac and Wallace, 1987). Oogonia are oval to somewhat spherical in shape and are conspicuous by their smaller size and large nuclear-to-cytoplasmic ratio (Fig. 26). Oogonial nuclei are oval in shape and contain one to three nucleoli. Dense-cored granules of unknown composition are also observed within the nucleus (Fig. 26). These dense-cored granules are specific to nuclei of the germ cell lineage and are also present in larger oocytes. The oogonial chromatin is somewhat electron dense compared to the more electron lucent nature of chromatin found in other meiotic oocytes. The oogonial cytoplasm contains mitochondria, ribosomes, and scant endoplasmic reticulum, but appears to lack Golgi complexes. Aggregates of nuage material are frequently associated with the mitochondria. Nuage provides a good, reliable marker for germ cells (Eddy, 1975). Oogonia are contiguous with other germ cells and somatic cells but are not in immediate contact with the basal lamina of the luminal epithelium or that surrounding the germinal ridge.

To identify proliferating germ cells, ovary segments were pulsed with ^{3}H-thymidine. These studies demonstrated that only germ cells within the germinal ridge incorporated thymidine (Figs. 27, 28); oocyte nuclei at later stages in the follicle progression did not incorporate ^{3}-thymidine. Germ cells were observed to incorporate ^{3}H-thymidine even after being cultured in vitro for 2, 5, 7, and 10 days (Fig. 28). Somatic cells, including follicle cells and

Fig. 26. Electron micrograph of an oogonium (OG) present within the germinal ridge. Note the oval shape of the nucleus and the single nucleolus. Mitochondria, nuage material (arrows), and endoplasmic reticulum are present within the cytoplasm. Some dense-cored granules are seen above the nucleolus (arrowhead). x 14,000.

Fig. 27. Light micrograph of germinal ridge region of ovary that had been pulsed with ^{3}H-thymidine after 2 days in culture. Note the heavy concentration of silver grains (arrows) that completely cover the nuclei of germ cells. Note the unlabeled germ cell nucleus (arrowhead) in the germinal ridge and the larger oocyte (O) with an unlabeled nucleus. JB-4 resin, toluidine blue. x 470.

Fig. 28. Light micrograph of germinal ridge segment of ovary pulsed with ^{3}H-thymidine after 10 days in culture. Germ-cell labeling (arrows) still occurs after this culture period. JB-4 resin, toluidine blue. x 510.

Fig. 29. Electron micrograph of leptotene chromatin-nucleolus oocyte (O). Cellular organelles are located in a juxtanuclear position around the centrioles (arrow). Note that Golgi complexes (arrowheads) have appeared. The nucleus is spherical and the chromatin remains electron dense. x 12,640.

Fig. 30. Electron micrograph of chromatin-nucleolus stage oocyte (O) in pachytene. Long synaptonemal complexes (arrows) and micronucleolar fragments are present in the nucleus. Note that the nucleus is more electron lucent than those shown in Figures 26 and 29. Dense-cored granules (arrowhead) can also be observed in the nucleus. x 8,080.

Fig. 31. Higher magnification electron micrograph of dense-cored granules specific for germ cell nuclei. x 65,200.

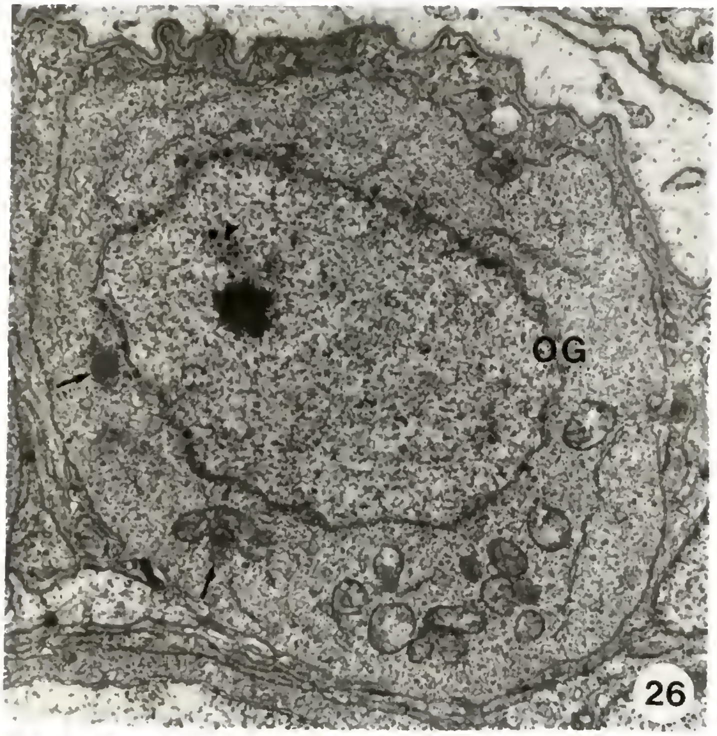

26

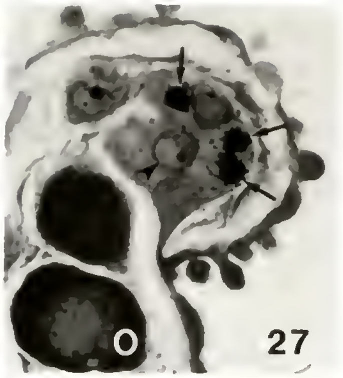

27

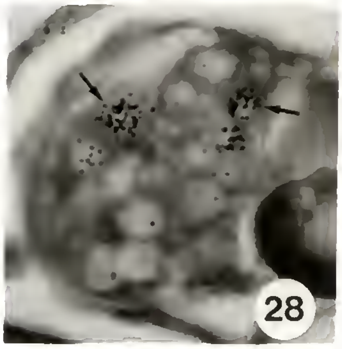
28

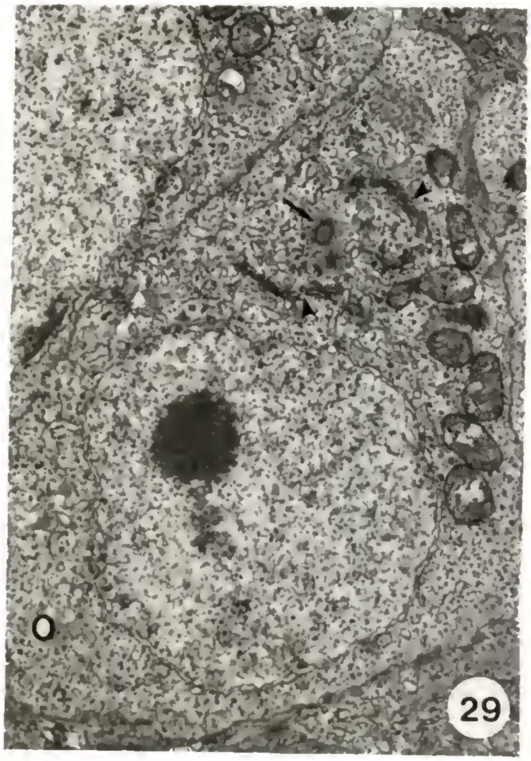

29

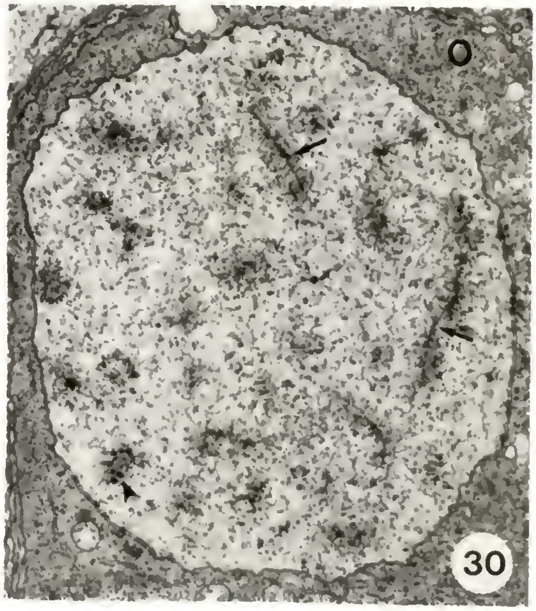

30

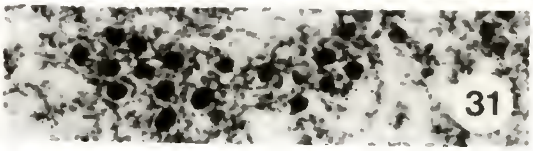
31

connective tissue cells, incorporated thymidine during these time periods as well.

Stage IIa: Primary Growth, Chromatin-Nucleolus Phase (approximately 10-20 um diameter)

The primary growth stage is initiated by true oogenesis, or oocyte formation. It is the period of follicle formation and an increase in the amount of cytoplasm and cellular organelles within the oocyte.

Chromatin-nucleolus oocytes are found within the germinal ridge and have not yet become incorporated into definitive follicles. They are formed by the transformation of oogonial daughter cells into prophase I meiotic oocytes. It is unclear as to how this process occurs and whether the oogonial division that produces the oocytes is symmetric or asymmetric. It is difficult to positively identify leptotene oocytes from the transforming oogonia, but loss of the perinuclear ring of mitochondria and the appearance of Golgi elements (Fig. 29) appear to be noticeable changes that distinguish an early oocyte from an oogonium. The organelles are localized in a polarized juxtanuclear aggregation that seems to form around the centrioles (Fig. 29). The nucleus of leptotene oocytes become more spherical in shape as compared to oogonial nuclei. The nucleus of leptotene oocytes also contains dense-cored granules and the chromatin remains somewhat electron dense. Oocytes in zygotene and pachytene can more easily be distinguished by the appearance of synaptonemal complexes within the nucleus (Fig. 30). During zygotene, the synaptonemal complexes are short, as initial chromosomal pairing occurs, and nucleoli can still be observed in the nucleus. By pachytene, the synaptonemal complexes are long and the nucleoli have become more dispersed and fragmented (Fig. 30). Zygotene and pachytene nuclei also become noticeably less electron-dense when compared to oogonia and leptotene nuclei (Figs. 26, 29, 30). The nuclei of later chromatin-nucleolus oocytes also contain dense-cored granules (Figs. 30, 31). Oocytes in zygotene and pachytene grow slightly, with an increase in cell organelles including mitochondria, Golgi complexes, ribosomes, and endoplasmic reticulum. These organelles are typically located in a juxtanuclear aggregate within the oocyte. Nuage continues to be present in the cytoplasm, often associated with mitochondria. Leptotene, zygotene, and pachytene oocytes generally share at least part of their cell borders with contiguous oocytes, and the remaining cell surfaces are in contact with prefollicular cells within the germinal ridge.

The later chromatin-nucleolus oocytes become arrested in early diplotene of meiotic prophase I as synaptonemal complexes dissociate within the oocyte nucleus. During this phase, the ooplasmic matrix increases along with the numbers of cell organelles. The organelles tend to remain polarized in a juxtanuclear location. Nucleoli of typical structure reappear adjacent to the inner layer of the nuclear envelope. The appearance of multiple nucleoli seems to coincide with the formation of the definitive follicle as it separates from the germinal ridge. Final follicle formation occurs with these diplotene-arrested oocytes. The definitive follicle now consists of an oocyte surrounded by a monolayer of flattened follicle cells with the entire complex enclosed by a basal lamina. Sparse thecal elements associate with the follicle external to the basal lamina at this stage. The details of folliculogenesis have been presented elsewhere (Begovac and Wallace, 1987).

Stage IIb: Primary Growth, Perinucleolar Phase (20-140 um diameter)

This phase of primary growth typically begins as the definitive follicle separates from the germinal ridge. In the light microscope, the perinucleolar oocytes are transparent with the nucleus clearly visible. The nucleus is generally spherical and contains multiple nucleoli in a perinuclear position adjacent to the inner layer of the nuclear envelope (Figs. 32, 33, 34). Dense-cored granules can still be observed in oocyte nuclei. During this stage, the nucleus increases in size and the nucleoli increase in number.

Perinucleolar oocytes also increase in size due to the continued elaboration of cytoplasm, mitochondria, Golgi, ribosomes, endoplasmic reticulum, and multivesicular

Fig. 32. Light micrograph of perinucleolar oocytes in the primary growth phase. Note the multiple nucleoli in a perinuclear position within the germinal vesicle (GV). The Balbiani vitelline body is also clearly visible in two of the oocytes, first as a juxtanuclear aggregate (arrow) and later assuming a crescentlike shape (arrowheads). JB-4 resin, H&E. x 330.

Fig. 33. Light micrograph of perinucleolar phase oocyte illustrating perinuclear ring organization of the Balbiani vitelline body (arrows). (GV) Germinal vesicle. JB-4 resin, H&E. x 310.

Fig. 34. Electron micrograph of a perinucleolar oocyte with the Balbiani vitelline body containing mitochondria and an aggregate of multivesicular bodies (arrows). Oocyte nucleus (NU) contains perinuclear nucleoli (arrowhead). (BL) Basal lamina. x 7,500.

Fig. 35. Higher magnification of multivesicular bodies [one of which is labeled with an (*)] associated with the Balbiani vitelline body. x 27,300.

Fig. 36. Later stage perinucleolar oocyte (O) with mitochondria and Golgi complexes (G) in the peripheral ooplasm. A basal lamina (arrowhead) overlies the squamous follicle cells (FC). Note that the oocyte has started to elaborate numerous microvillar processes (arrow). x 7,800.

Fig. 37. Photomicrograph of a portion of intact ovary that has been stained with rhodamine 123 to follow movements of mitochondria in developing oocytes. Note the regions of juxtanuclear fluorescence in the smallest oocytes (arrow). As oocytes increase in size, the staining becomes perinuclear and finally disperses throughout the oocyte (arrowhead). x 85.

Fig. 38. Photomicrograph illustrating the lysosomal localizations in developing oocytes using acridine orange staining. Note that the staining pattern is similar to that of rhodamine 123 (Fig. 37). Initially a juxtanuclear staining (arrow) is observed, followed by a crescent-shaped staining (arrowhead), becoming perinuclear, and finally dispersing throughout the oocyte (*). x 82.

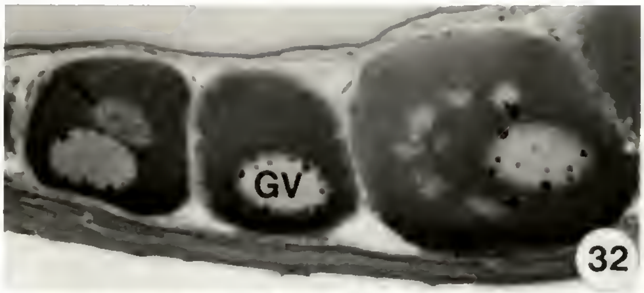

32

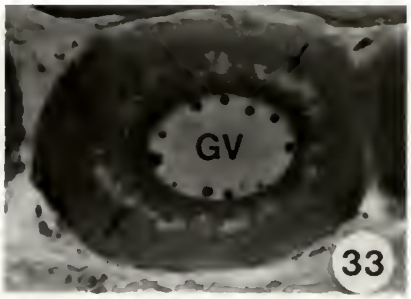

33

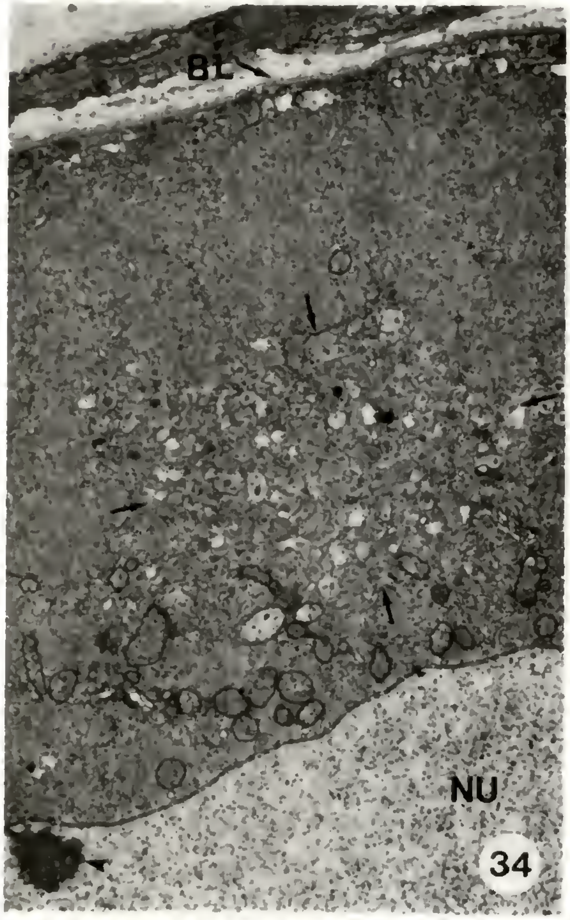

34

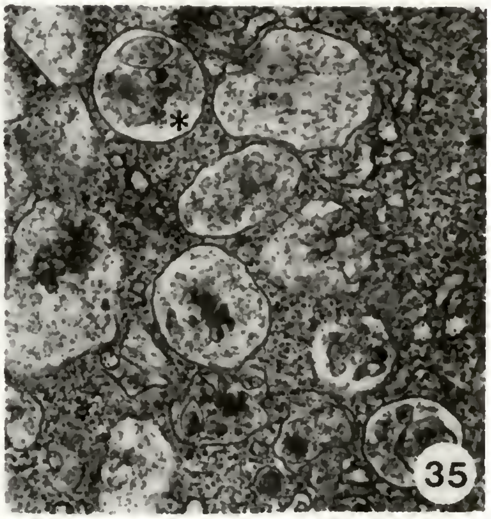

35

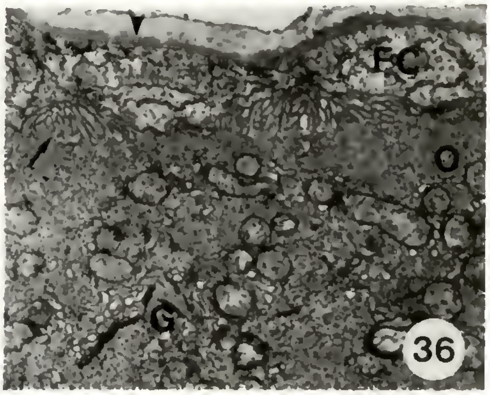

36

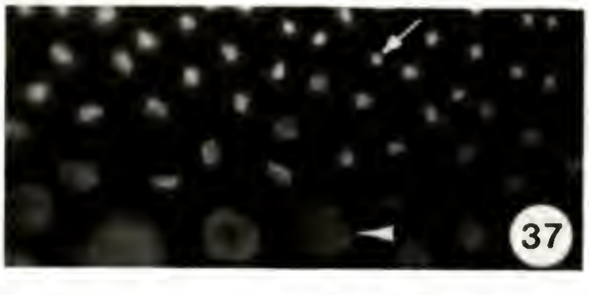

37

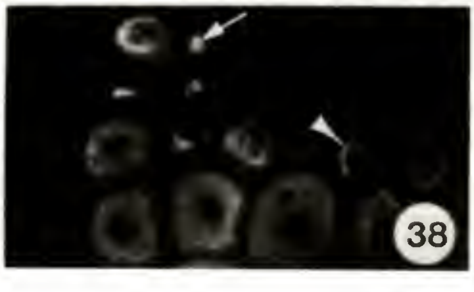

38

bodies (Figs. 34, 35, 36). In early perinucleolar oocytes, most of these cellular organelles are typically present as a juxtanuclear mass (Fig. 32, 34) commonly known as the Balbiani vitelline body (Guraya, 1979) or mitochondrial cloud (Heasman et al., 1984). Mitochondria and multivesicular bodies comprise the major components of the Balbiani vitelline body (Fig. 34). Multivesicular bodies initially appear during the middle of the perinucleolar stage, are heterogeneous with respect to size, shape, and contents (Fig. 35), and remain into early vitellogenesis. As stage IIb progresses, the juxtanuclear Balbiani vitelline body changes to form first a crescent shape (Fig. 32), then progresses to a perinuclear ring (Fig. 33) that finally disperses throughout the oocyte by late perinucleolar growth. This progression can be also visualized in living oocytes using the vital dyes rhodamine 123 for mitochondria (Fig. 37) or acridine orange for acidic, lysosomal elements (Fig. 38).

In the early perinucleolar phase, the peripheral ooplasm contains cytoplasmic matrix, ribosomes, and smooth endoplasmic reticulum, while the oocyte surface is typically smooth. After the Balbiani vitelline body disperses in late perinucleolar growth, mitochondria and multivesicular bodies are found throughout the oocyte cytoplasm, whereas the abundant Golgi complexes become mostly confined to the peripheral cytoplasm (Fig. 36). The oocyte has also begun to elaborate numerous microvillar processes towards the overlying follicle cells (Fig. 36).

The follicle cells also extend microvilli, but do so later than the oocyte. Follicular investments surrounding perinucleolar oocytes include squamous follicle cells, connective tissue elements, and blood vessels. The follicle cells possess a large nucleus and primarily mitochondria and rough endoplasmic reticulum in the cytoplasm, with only scant Golgi complexes.

Stage III: Cortical Alveoli Formation (140-260 um diameter)

This stage is characterized by the initial appearance of three components: 1) cortical alveoli; 2) vitelline envelope; and 3) lipid (Fig. 39). The cortical alveoli and vitelline envelope initially appear at approximately the same time (Fig. 40a). Cortical alveoli, indicated by PAS-positive reactivity, are first observed in the light microscope throughout the peripheral cytoplasm of oocytes. This is confirmed by ultrastructural observations indicating that the cortical alveoli are membrane-limited structures having a homogeneous appearance (Fig. 40a). The smaller cortical alveoli sometimes contain a denser inclusion that is not membrane bound (Fig. 40b). As oocytes increase in size, the cortical alveoli increase in number and become heterogeneous in size as they fill much of the oocyte cytoplasm. The larger cortical alveoli stain less intensely with PAS, while in the electron microscope,

Fig. 39. Light micrograph of cortical alveoli-stage oocyte with much of the oocyte filled with larger sized cortical alveoli (CA). The vitelline envelope (VE) is present between the oocyte and overlying follicle cells. Lipid (LP) is present in a perinuclear position. Multiple nucleoli are still present in the germinal vesicle (*). JB-4 resin, H&E. x 140.

Fig. 40. a) Electron micrograph of the cortex in an early cortical alveoli-stage oocyte. The vitelline envelope (VE) has appeared between the microvillar processes and cortical alveoli (CA) are present. Note the Golgi complexes (G) intermingled with the mitochondria. (FC) Follicle cell. x 10,700. b) Cortical alveolus with electron dense inclusion (arrow). x 19,200.

Fig. 41. Vitelline envelope (VE) of later cortical alveoli-stage oocyte (O) now having trilaminar appearance due to continued formation. (FC) Follicle cell. x 12,240.

Fig. 42. Electron micrograph of lipid (LP) in cortical alveoli-stage oocyte. The void in the center of the lipid spheres represents an artifact caused by partial extraction of the lipid during fixation and processing. x 13,920.

Fig. 43. a) Phase micrograph of cortical alveoli-stage oocyte (CAO) and vitellogenic oocyte (VO). x 325. b) Fluorescence photomicrograph of same section treated with the fluorescent lectin, Con A. Note the positive staining of the different size cortical alveoli populations (arrows). The smaller cortical alveoli generally react most intensely. Note also that the vitelline envelope stains (arrowheads) with this lectin. x 325. c) Control micrograph containing sequentially cut section of same block treated with 0.5 M glucose and the fluorescent lectin. No reactivity is observed. x 325.

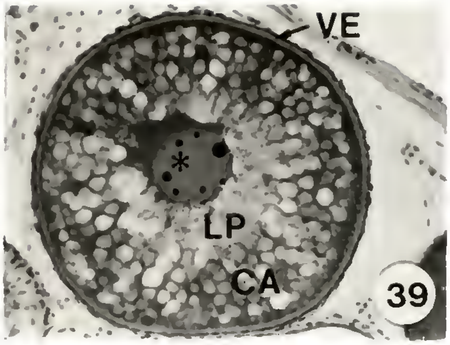
VE
*
LP
CA
39

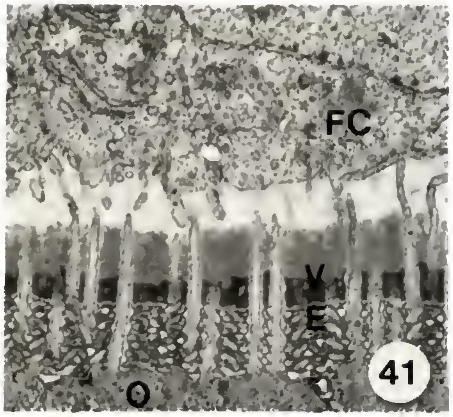
FC
V
E
O
41

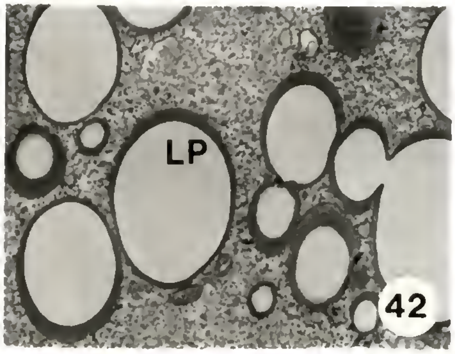
LP
42

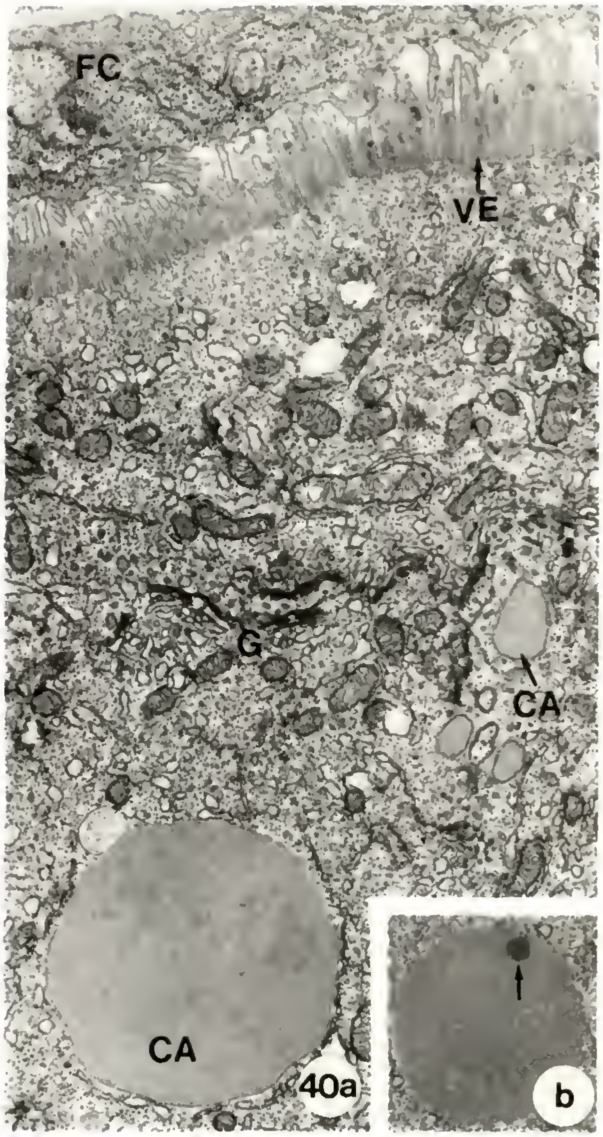
FC
VE
G
CA
CA
40a
b

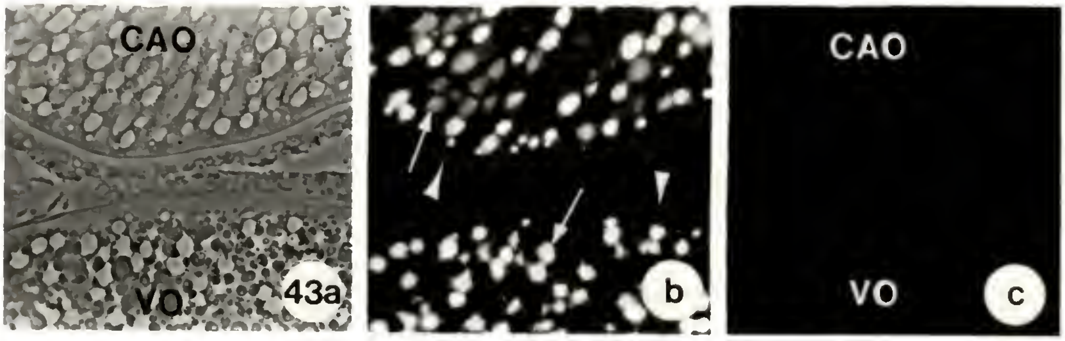
CAO
VO
43a
b
CAO
VO
c

they are more electron lucent and appear to contain a filamentous network. Additional details regarding cortical alveoli may be found in Anderson (1968).

The vitelline envelope appears coincident with cortical alveoli in follicles of approximately 140 um diameter. The formation of this structure has been previously described (Anderson, 1967). In the light microscope, the vitelline envelope is first observed as a thin band between the oocyte and overlying follicle cells (Fig. 39); it also stains positively with PAS. Ultrastructurally, the vitelline envelope first becomes apparent with the appearance of a homogeneous material between the microvillar processes of the oocyte (Fig. 40a). As the follicle reaches approximately 200 um diameter, a trilaminar appearance of the vitelline envelope is attained (Fig. 41), with architecturally complex Z1, Z2, and Z3 layers (terminology of Anderson, 1967). In the later cortical alveoli-stage oocytes, the Z3 layer becomes thickened relative to Z1 and Z2.

A third process that occurs in cortical alveoli-stage oocytes is the formation and accumulation of lipid droplets. Lipid accumulation is first apparent in follicles approximately 200 um in diameter. The lipid droplets at this size are small and aggregated in perinuclear positions (Figs. 39, 42). The lipid mass continues to enlarge in a perinuclear position in later cortical alveoli-stage oocytes. In freshly isolated oocytes, the lipid has a dark appearance while later on during oocyte development, the lipid droplets increase in size and appear brilliant orange in the living oocyte. The processes of lipogenesis and lipid accumulation during oocyte development are poorly understood.

During the cortical alveoli stage, the oocyte surface begins to display pinocytic vesicles at the base of the microvillar processes. Microvilli continue to lengthen as the vitelline envelope thickens. The follicle cells also elaborate microvilli that begin to interdigitate with the oocyte processes. Follicle cells remain somewhat squamous in shape and contain mitochondria and rough endoplasmic reticulum, while Golgi complexes become more abundant. The specialized micropylar cell also appears during this stage and is involved in the formation of the micropyle.

Concanavalin A treatment of oocytes demonstrated that the cortical alveoli and the vitelline envelope bind this lectin (Figs. 43a, b). Staining is abolished in the presence of 0.5 M glucose (Fig. 43c) and/or mannose. Cortical alveoli bind concanavalin A throughout oocyte growth although the intensity of staining is lower in the larger cortical alveoli, presumably due to a loss of vesicular contents during tissue preparation. The vitelline envelope binds this lectin stains throughout oocyte growth as well.

Stage IV: Vitellogenesis (260-1,100 um diameter)

Vitellogenesis involves the accumulation of exogenously derived yolk protein precursors into the oocyte and is responsible for the majority of oocyte growth (Wallace, 1985). Oocytes in early vitellogenesis are characterized in the light microscope by the appearance of small yolk spheres in the oocyte periphery and interior (Fig. 44). As oocyte growth proceeds, the interior yolk spheres become heterogeneous in size (Fig. 45), while smaller yolk spheres still are present in the peripheral ooplasm. The accumulation of yolk spheres in the oocyte interior results in the progressive displacement of cortical alveoli and lipid to the peripheral cytoplasm. The larger yolk spheres apparently form by fusion of the smaller yolk spheres. In late vitellogenic oocytes, most of the individual yolk spheres disappear and a large central fluid yolk mass is formed (Fig. 46). The cytoplasm containing small yolk spheres, cortical alveoli and lipid is displaced to a thin rim at the oocyte periphery.

At the ultrastructural level, yolk spheres are somewhat electron-dense, membrane-limited structures (Figs. 47-49). They also contain highly electron-dense inclusions (Figs. 47-49). The ultrastructural appearance of this inclusion remains unchanged in osmicated and nonosmicated tissues, but the inclusion occasionally has a fine granular appearance. Although, the biochemical nature of the dense

Fig. 44. Light micrograph of early vitellogenic oocyte containing numerous small yolk spheres (Y) within its interior. Note the displacement of cortical alveoli (CA) to the oocyte periphery. Lipid (LP) is still present internally near the germinal vesicle and amongst the yolk spheres. x 120.

Fig. 45. Light micrograph of midvitellogenic oocyte in which the yolk spheres (Y) are becoming larger in size. Cortical alveoli (CA) and lipid become more progressively displaced to the peripheral ooplasm. x 255.

Fig. 46. Light micrograph of a late vitellogenic stage oocyte in which most of the yolk spheres (Y) have coalesced to form a large central fluid yolk mass. Lipid droplets (*) remain in the peripheral part of the yolk mass along with cortical alveoli (CA). Vitelline envelope (arrowhead). x 150.

Fig. 47. Transmission electron micrograph depicting early vitellogenic oocyte with yolk spheres in the process of being formed. The primary yolk spheres (YI) containing condensing yolk and vesicular structures are illustrated. Fully formed yolk spheres (YIII) containing the highly electron dense, yolk-specific inclusions (arrow) are also present. x 17,400.

Fig. 48. Electron micrograph of early vitellogenic oocyte with transitional yolk-spheres (YII). Note the condensing yolk material and the presence of vesicular structures in these transitional yolk spheres. Note in particular the transitional yolk sphere (YII) containing the electron-dense, yolk-specific marker (arrow) in addition to vesicular elements. (LP) Lipid. x 20,300.

Fig. 49. Large mature yolk sphere (YIII) of midvitellogenic oocyte containing a heterogeneous population of the yolk-specific inclusions (arrowheads). Note that the yplk spheres are membrane bound (arrows). Other smaller yolk spheres are also present. x 12,800.

Fig. 50. Electron micrograph of oocyte periphery illustrating the pinocytic nature of vitellogenic oocytes. Note that these pinocytic vesicles are clathrin-coated (arrows). (VE) Vitelline envelope. x 36,600.

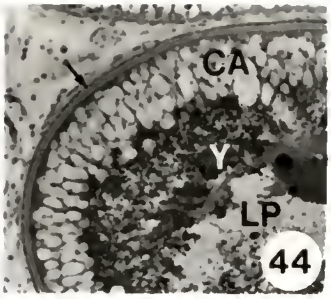
44

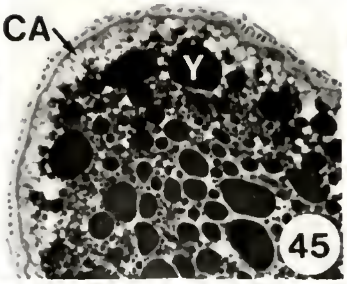
45

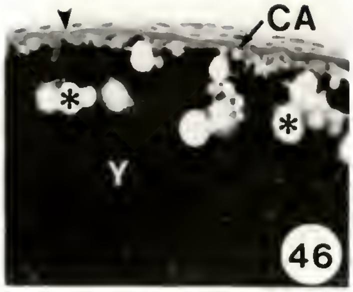
46

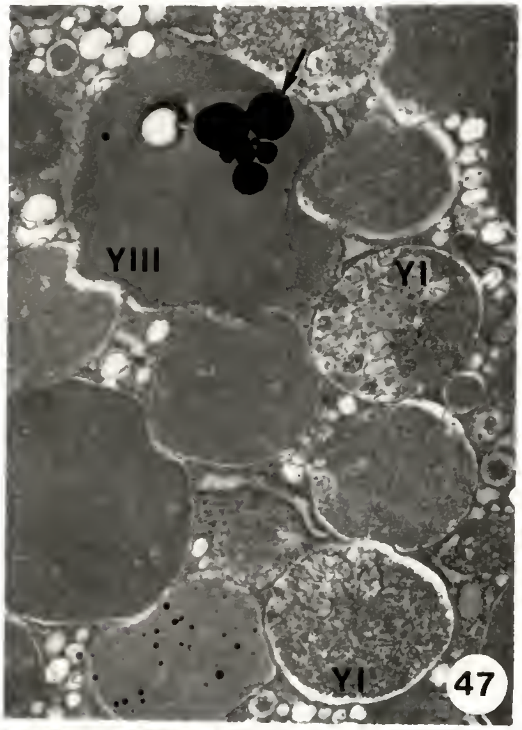
47

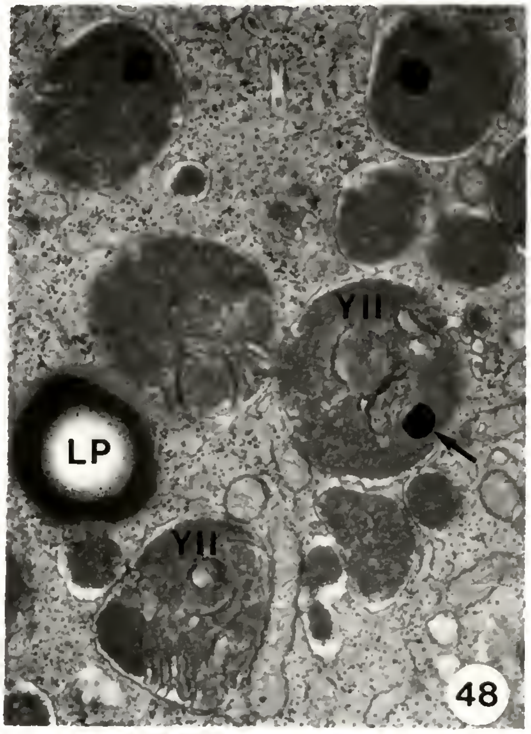
48

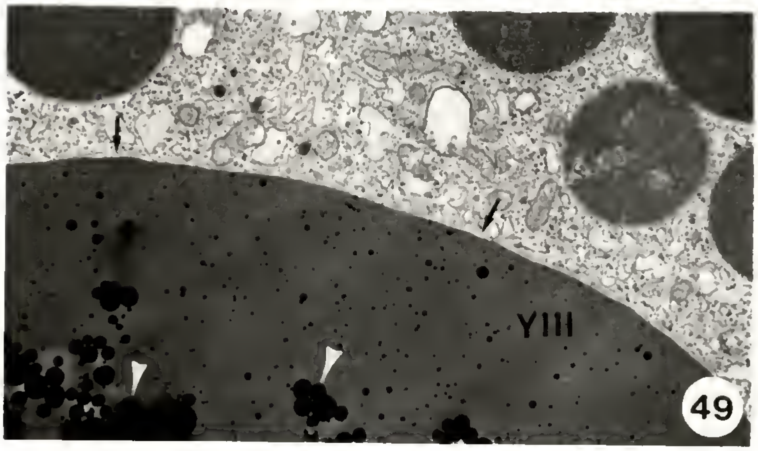
49

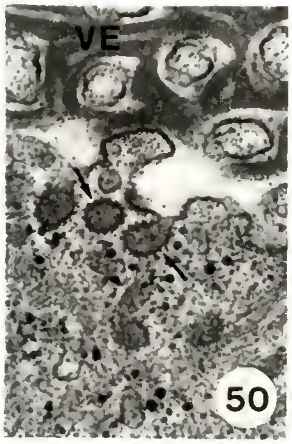
50

inclusion is unclear, it does provide a specific, reliable marker for following yolk formation.

Early vitellogenic oocytes possess many small, somewhat electron-dense structures at the oocyte periphery and interior among the cortical alveoli (Fig. 47). There are several populations of these membrane-bound structures including primary, transitional and mature yolk spheres. The primary spheres appear to contain proteinaceous material interspersed among multivesicular elements (Fig. 47). The intermediate, transitional spheres contain proteinaceous material, variable vesicular elements, and the yolk-specific, electron-dense inclusion (Fig. 48). The mature spheres contain homogeneous condensed yolk and a heterogeneous size and distribution of the yolk-specific marker (Fig. 49). Yolk sphere formation is first apparent in the oocyte periphery, with accumulation occurring in the internal regions of the oocyte as the mature yolk spheres fuse with one another. Oocytes continue to display pinocytic vesicles during vitellogensis (Fig. 50). These vesicles are clathrin-coated and most likely are involved in the sequestration of yolk protein precursors as has been documented in other animals (Wallace, 1985).

Several other events occur during the vitellogenic stage. By midvitellogenesis, the vitelline envelope has lost its trilaminar appearance and has undergone condensation, particularly of the Z2 and Z3 layers. Lipid droplets continue to accumulate and increase in size. The lipid becomes brilliantly colored and consequently contributes the major coloration of later stage oocytes. Cortical alveoli probably continue to be formed during vitellogenesis as well (Selman et al., 1986).

Follicle cells surrounding vitellogenic oocytes become somewhat cuboidal in shape. The follicle cells possess abundant rough endoplasmic reticulum, mitochondria, and Golgi complexes. Follicle-cell microvillar processes extend deep into the vitelline envelope pore canals approaching the oocyte surface. Both follicle-cell and oocyte microvillar processes are present within a single pore canal.

Stage V: Oocyte Maturation (1,100-1,300 um diameter)

When oocytes reach this stage, they become capable of resuming first meiotic division by undergoing germinal vesicle breakdown. Structurally, the postvitellogenic oocyte contains a large central fluid yolk mass and has at its periphery a thin rim of cytoplasm containing mostly cortical alveoli and lipid (Fig. 46). The vitelline envelope is highly compacted and possesses pore canals prior to maturation. However, at some undefined point during maturation and prior to ovulation, the pore canals disappear as the oocyte and follicle-cell microvillar processes are retracted or lost.

Figs. 51-53. Photomicrographs of maturation-stage follicles and mature eggs demonstrating both the animal pole (left) and vegetal pole (right) in each pair.

Fig. 51. Prematuration follicles with disperse lipid droplets throughout the oocyte and the germinal vesicle (arrow) clearly visible beneath the animal pole.

Fig. 52. Postmaturation follicles that have been matured *in vitro* by treatment with the steroid 17-alpha,20-beta-DHP. Note the loss of the germinal vesicle over the animal pole (left follicle). x 18.

Fig 53. Normal appearance of *in vivo* matured eggs. Note the loss of the germinal vesicle (arrow) and the lipid redistribution towards the animal pole. x 18.

Fig. 54. Maturation response of various size follicles to treatment with the steroid 17-alpha,20-beta-DHP. Values represent the means and SEM of the percentage of follicles within each size pool that underwent germinal vesicle breakdown (GVBD). Experimental and control values are indicated and represent three separate experiments. Follicles (10-40) were incubated in each follicle size pool. There in an increase in competence to undergo *in vitro* maturation with respect to follicle diameter. Follicles that are 1.1 mm in diameter are fully competent to undergo 100% germinal vesicle breakdown. Control groups receiving ethanol vehicle (EtOH) showed no response except for a single case in the 1.1 mm diameter group.

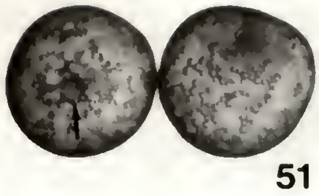

51

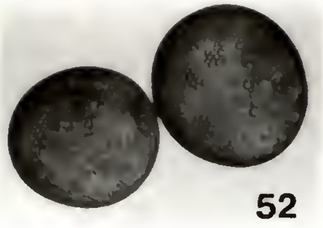

52

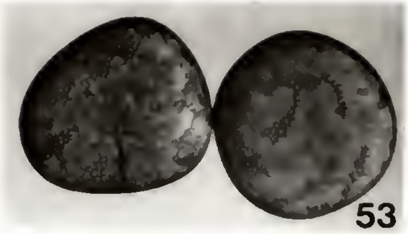

53

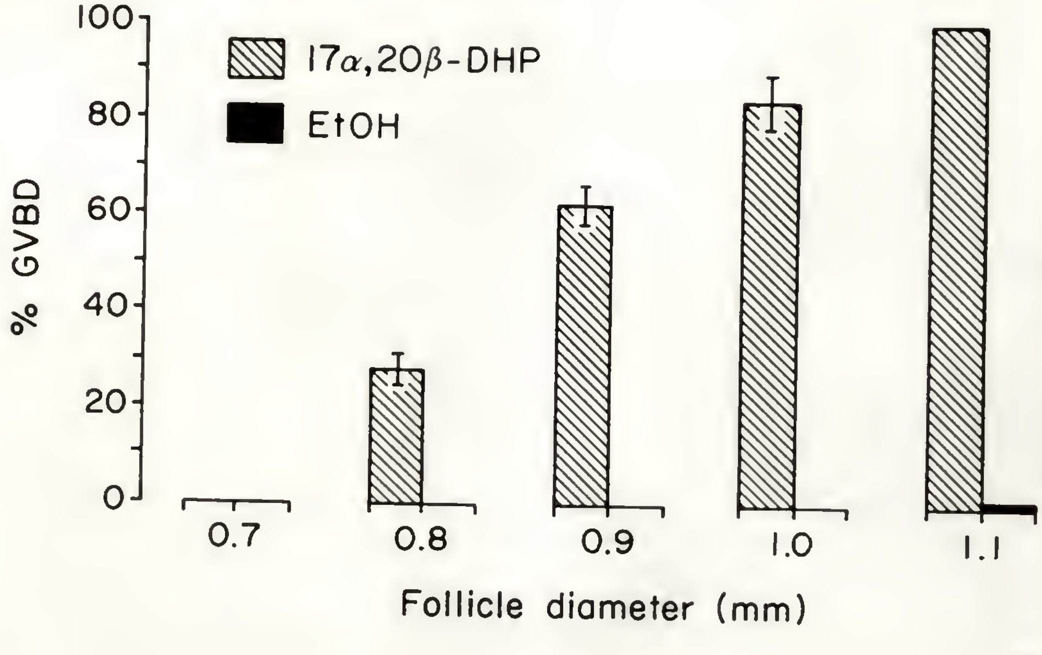
▨ 17α,20β-DHP
■ EtOH
% GVBD
100
80
60
40
20
0
0.7
0.8
0.9
1.0
1.1
Follicle diameter (mm)

54

The germinal vesicle is located near the animal pole just beneath the oocyte surface (Fig. 51). The identification of the maturational stage has been established by examining fresh ovaries and using *in vitro* follicle culture to define the size at which oocytes become fully competent to respond to steroid stimulation by undergoing germinal vesicle breakdown. The results of the culture experiments (Fig. 54) indicate that follicles of 1.1 mm diameter undergo 100% germinal vesicle breakdown in response to 17-alpha,20-beta-DHP. Oocytes matured *in vitro* have a similar appearance to *in vivo* matured oocytes (Figs. 52, 53) except for being smaller in size. Lipid droplets in prematurational oocytes are generally distributed around the entire oocyte periphery prior to maturation. After maturation, *in vivo* or *in vitro*, most lipid droplets aggregate towards the animal pole region where the oocyte nucleus was previously located. The vegetal pole therefore becomes cleared with only scattered lipid droplets still remaining. There is an increased intensity of the orange coloration of the oocyte that is a result of the clearing process. After germinal vesicle breakdown, the oocytes ovulate into the ovarian lumen and become mature eggs.

A determination of protein content in different sized follicles indicated that a slight change in the rate of protein accumulation occurs as oocytes reach the maturational stage and become eggs (Fig. 55). No change in

Fig. 55. Protein content of individual follicles from 0.4-1.3 mm diameter. Values indicate means and SEM for each follicle size. Closed circles indicate oocytes within their follicles. The open circle indicates mature eggs. The major contribution to total protein content occurs during the vitellogenic period of oocyte growth. The rate of protein increase appears linear for follicles between 0.4-1.1 mm diameter (solid line). A slower rate of increase appears to occur for follicles between 1.1 and 1.3 mm (dashed line). The lines were constructed by least squares fit for data points between 0.4-1.1 mm diameters and 1.1-1.3 mm diameters, respectively.

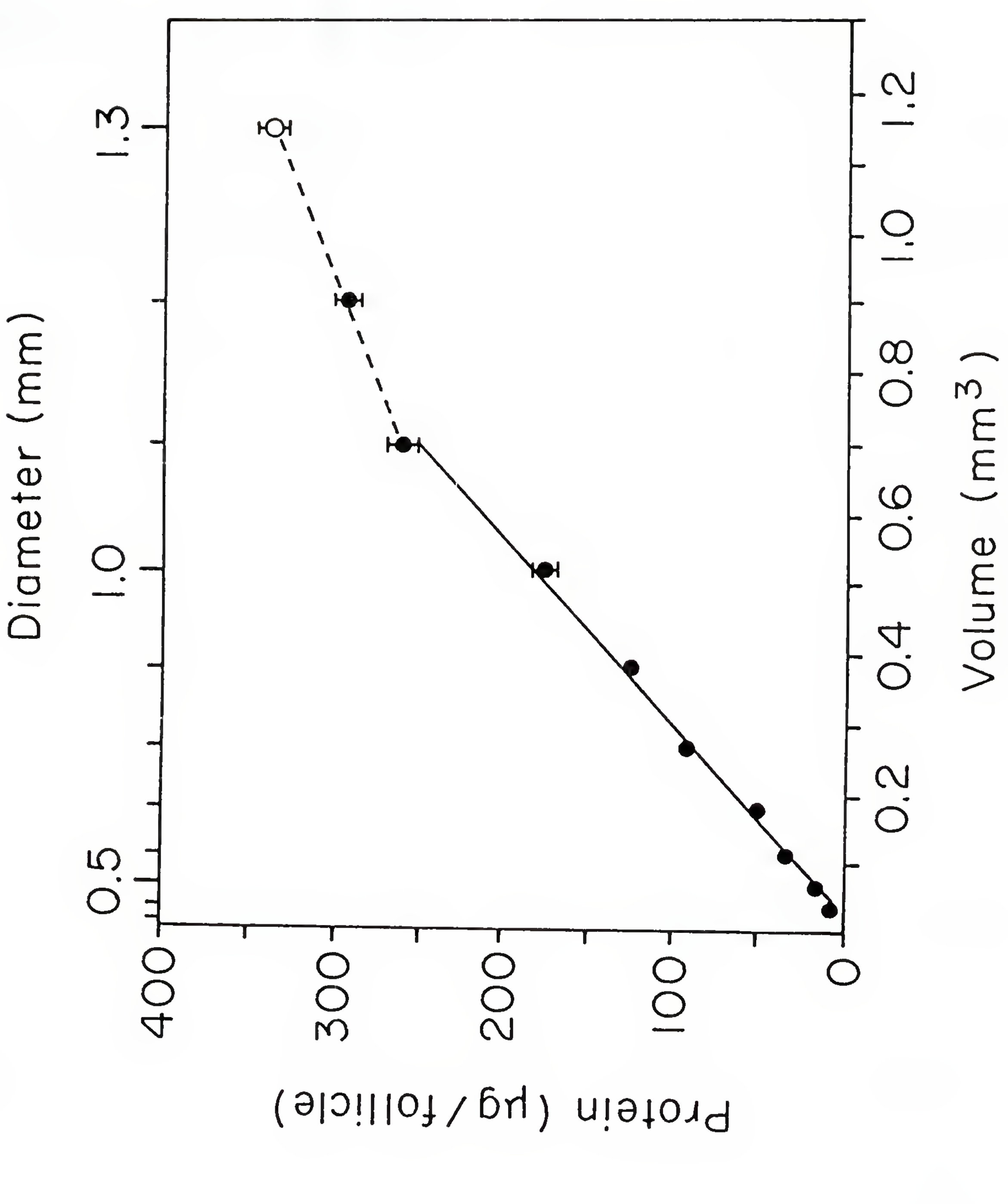
Diameter (mm)
0.5
1.0
1.3
Volume (mm³)
0.2
0.4
0.6
0.8
1.0
1.2
Protein (µg / follicle)
0
100
200
300
400

Fig. 56. SDS-PAGE profiles of predominant proteins in follicles and eggs <0.2-1.3 mm diameter. Follicle diameters are listed above their respective lanes. Molecular weight standards are listed to the left of the gel. Note that no change in protein patterns occurs as oocytes undergo maturation (1.1-1.2 mm diameter) and become mature egg (1.3 mm diameter). Note also that the major protein constituents of all follicles above 0.4 mm diameter are the various yolk proteins, which are distinct from the the cytoplasmic proteins indicated for the smallest (yolk-free) oocytes. Approximate protein content of samples are: < 0.2 mm, no value; 0.3 mm, no value; 0.4 mm, 7.9 ug; 0.5 mm, 16.0 ug; 0.6 mm, 27.1 ug; 0.7 mm, 20.5 ug, 0.8 mm, 27.8 ug, 0.9 mm, 25.1 ug; 1.0 mm, 35.0 ug; 1.1 mm, 39.3 ug; 1.2 mm, 44.1 ug; 1.3 mm, 50.8 ug.

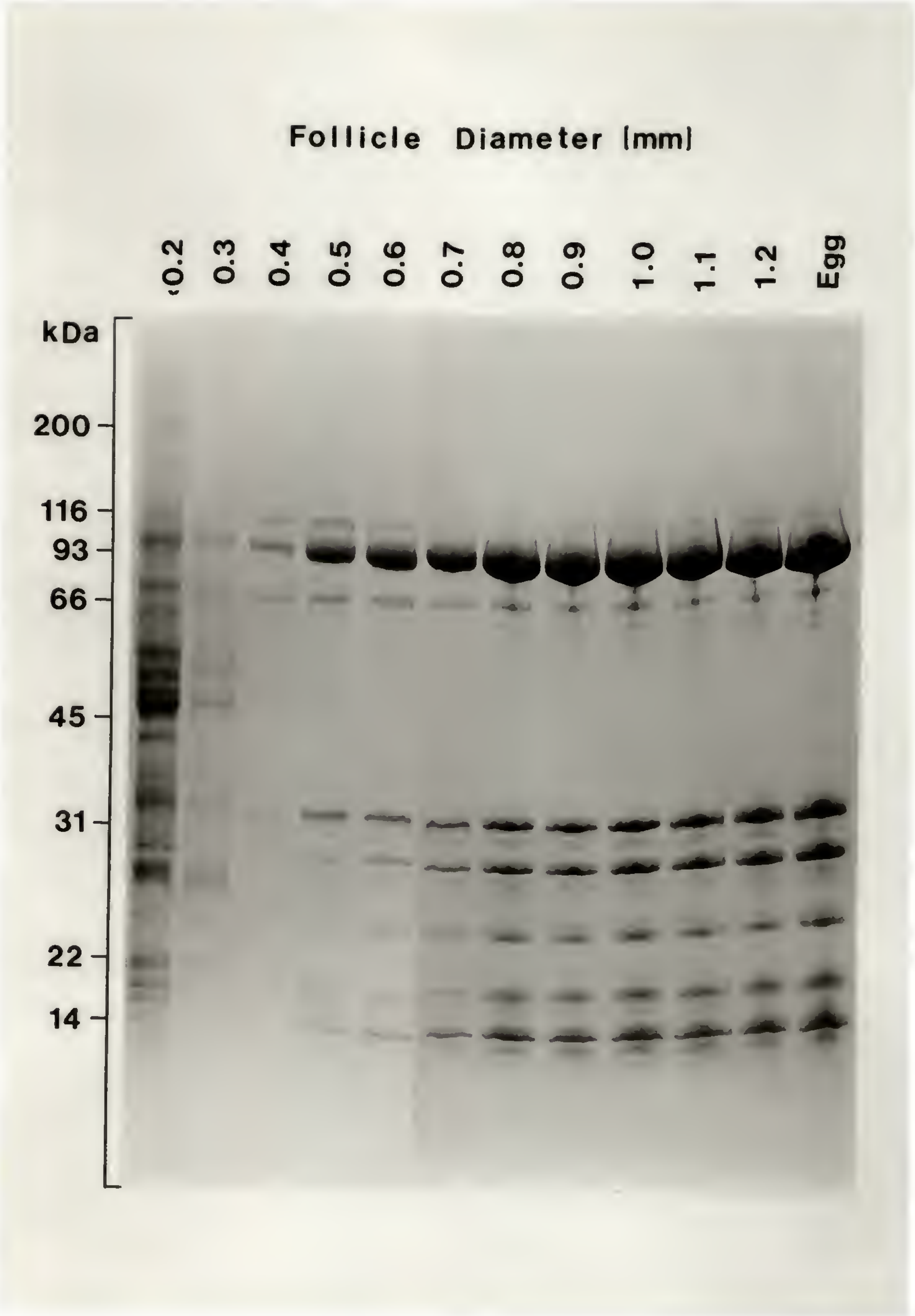
Follicle Diameter (mm)
<0.2
0.3
0.4
0.5
0.6
0.7
0.8
0.9
1.0
1.1
1.2
Egg
kDa
200
116
93
66
45
31
22
14

the major yolk proteins takes place during maturation (Fig. 56), unlike the situation recently found for the oocytes of several other teleosts (Greeley et al., 1986b).

Stage VI: Mature egg (approximately 1,300 um)

This stage is the culmination of oocyte development and represents a cell capable of being fertilized. Macroscopically, the egg is oval to pear-shaped and brilliantly colored orange because of the lipid droplets. The nucleus has undergone dissolution as a result of final maturation and the egg and the animal pole has an opaque appearance (Fig. 53). The mature egg retains the large central fluid yolk mass. Cortical alveoli are uniformly distributed around the oocyte periphery beneath the oolemma. The lipid droplets, however, become more aggregated towards the animal pole while the vegetal pole has fewer lipid droplets and is more clear (Fig. 53). The vitelline envelope consists of a thin Z1 layer and highly compacted Z2, Z3 layers and lacks the pore canals seen in the envelope surrounding oocytes. The micropyle is visible on the outer egg surface since there are no cellular investments surrounding the egg. Eggs are stored within the ovarian lumen until the time of fertilization and are somewhat fragile. After fertilization, they become turgid when the vitelline envelope elevates to form the chorion.

Discussion

Oocyte development in the pipefish is considered to be asynchronous (Wallace and Selman, 1981), with a heterogeneous population of different-stage oocytes. Many of the cellular processes that occur during oocyte development in the pipefish parallel those found in other nonmammalian vertebrates. These include oogonial proliferation (Tokarz, 1978), formation and dispersal of the Balbiani vitelline body (Guraya, 1979; Heasman et al., 1984), formation of cortical alveoli and a vitelline envelope (Anderson, 1967, 1968; Selman et al., 1986), vitellogenesis (Anderson, 1968; Selman and Wallace, 1983; Wallace, 1985) and oocyte maturation (Masui, 1985; Greeley et al., 1986a). The unique features of oogenesis in the pipefish, however, relate to the ovarian anatomy whereby oocytes are sequentially arranged according to developmental age (Begovac and Wallace, 1987). This arrangement is particularly useful when examining specific cellular events such as oogonial dynamics, vitelline envelope formation, and vitellogenesis. One is able to study such processes with respect to a developmental time frame on a single cross section of the ovary in which all oocyte stages have been treated in the same manner. Additionally, the very earliest events of oogonial proliferation and early follicle formation, because of their specific location within the ovary, become accessible to experimental manipulation. Experiments of this nature are much more difficult in other vertebrate ovaries because of the random organization of developing oocytes. Therefore, many of the advantageous features for studying oogenesis in the pipefish stem from this temporal and spatial pattern of oocyte development. The schematic diagram shown in Figure 57 highlights oocyte development in the pipefish and summarizes the cytological and physiological changes seen during specific stages.

The initial phase of oocyte development involves the true genesis of an oocyte as a result of oogonial proliferation and differentiation. The dynamics of cellular divisions that result in this transformation are unclear. The period of oogonial proliferation varies from species to species and may be continuous or cyclical in teleosts (reviewed by Tokarz, 1978). In the pipefish, oogonial proliferation is probably continuous because fully developed ovaries are present throughout the year (Begovac and Wallace, 1987). The present ^{3}H-thymidine experiments indicate the qualitative labeling of proliferating germ cells. Complete nuclear labeling with ^{3}H-thymidine will occur in mitotically active cells and preleptotene meiotic germ cells, whereas localized labeling will be observed over nucleoli in the amplification state (Coggins and Gall, 1972; Coggins, 1973). Consequently, proliferating oogonia and preleptotene oocytes are the two populations of germ

Fig. 57. Schematic diagram illustrating sequential stages of oocyte development as viewed in an optimal section. This schematic, in conjunction with a schematic of the ovarian anatomy (Chapter II, Figure 25) provides a reconstruction of oocyte development within the ovarian structure. The orientation of this drawing reflects the general relationships that oocytes possess *in vivo*. Stage designations are indicated as Roman numerals on the inner layer. The positions of the oocytes up through the first vitellogenic oocyte accurately reflect the approximate position of these stages in the developmental spiral. Later vitellogenic stages are drawn in for completeness of stages observed. Nuclei are depicted in most of the oocytes. The vitelline envelope and follicular investments have not been illustrated. The label (VI) is positioned over the animal pole of the mature egg. This schematic was prepared to highlight the reorganization of the major cytological features within the oocytes as they progress through the oocyte developmental spiral. It is not fully drawn to scale.

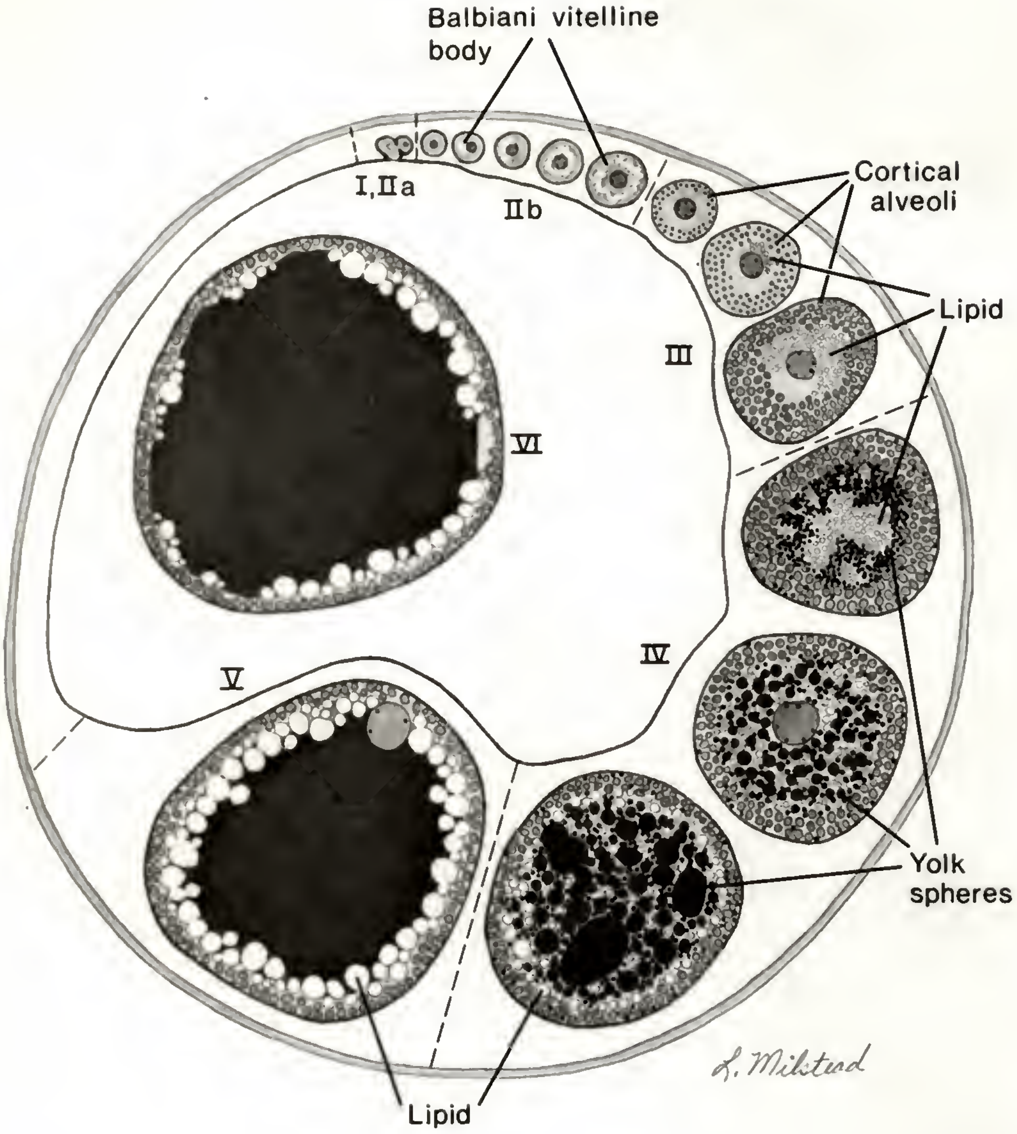

I. Oogonia

II. Primary Growth
   a. Chromatin-Nucleolus Phase
   b. Perinucleolar Phase

III. Cortical Alveoli Formation

IV. Vitellogenesis

V. Oocyte Maturation

VI. Mature Egg

cells that can be identified with this technique. The present studies do not allow a distinction between these two cell types in the light microscope. These experiments do demonstrate, however, that only germ cells within the germinal ridge exhibit nuclear labeling indicative of chromosomal duplication. Therefore, the germinal ridge region of the ovary is the proliferative germinal segment that serves as the source of all newly formed oocytes.

The observation that germ cells incorporate ^{3}H-thymidine over the entire nucleus even after being in culture for a period of 10 days was also interesting. The control mechanisms that regulate oogonial proliferation remain uncertain (reviewed by Tokarz, 1978). Gonadotropins (Dadzie and Hyder, 1976) and estrogen (Bullough, 1942) have been implicated in controlling oogonial proliferation. On the other hand, Remacle et al. (1976) suggested that hormonal stimulation was not necessary for oogonial proliferation *in vitro*. The present results demonstrate that complete nuclear labeling with ^{3}H-thymidine occurs even in germ cells cultured for 10 days in the absence of external hormones. During this culture period the media was replaced every 2-3 days, therefore, after the 10 day culture period one would expect any systemic control mechanisms to be severely diminished if not absent. Local control mechanisms within the ovary segments, however, cannot be excluded in these experiments. Nonetheless, these results would be consistent with the notion that oogonial proliferation and/or transformation to oocytes are gonadotropin-independent processes. Further experimentation should allow better definition of these observations and provide additional insight regarding an endogenous or exogenous control of oogonial proliferation and oogenesis.

Following this proliferative phase, the oogonial cells must undergo a phenotypic change as they transform to oocytes. In the pipefish, the earliest changes seen in newly formed oocytes are an increased size, with greater amounts of cellular organelles that redistribute to a juxtanuclear aggregate. This type of redistribution has also been noted in *Xenopus laevis* leptotene oocytes (Al-Mukhtar and Webb, 1971). Once the oocyte has been formed, the nuclear features with respect to synaptonemal complex formation, nucleoli fragmentation, and arrest in diplotene of prophase I are similar to those seen in the goldfish (Yamamoto and Onozato, 1965), mullet (Brusle and Brusle, 1978; Brusle, 1980), medaka (Satoh, 1974), and the amphibian *Xenopus laevis* (Al-Mukhtar and Webb, 1971; Coggins, 1973).

The Balbiani vitelline body within young oocytes of many organisms has been described (reviewed by Guraya, 1979). The Balbiani vitelline body is the predominant cytoplasmic structure within the perinucleolar stage pipefish oocyte. It disperses throughout the oocyte prior to cortical alveoli formation. As with other organisms, mitochondria (Guraya, 1979; Heasman et al., 1984) and multivesicular bodies (Shackley and King, 1977; Guraya, 1979) are present in the Balbiani vitelline body and, in fact, comprise a significant portion of this structure in the pipefish. The vital dye experiments using rhodamine 123 and acridine orange allow us to folllow the movements of the Balbiani vitelline body in live perinucleolar oocytes and corroborate the ultrastructural observations. The correlation observed between the localization of multivesicular bodies, as seen by electron microscopy and acridine orange staining, which is indicative of lysosomal structures (Albertini, 1984), also suggests that the multivesicular bodies represent a lysosomal compartment in pipefish perinucleolar oocytes.

A multivesicular body or lysosomal involvement in vitellogenesis has been previously suggested (Pasteels, 1973; Wallace, 1985). Recently, multivesicular bodies have been demonstrated to be involved in vitellogenin processing in the trout (Busson-Mabillot, 1984) as well as *Xenopus laevis* (Wall and Meleka, 1985; Wall and Patel, 1987). My own morphological observations using the highly electron-dense, yolk-specific marker of the pipefish to follow the early stages of yolk sphere formation is consistent with these studies. In examining many sections, it appears that the multivesicular bodies may represent a precursor compartment for yolk sphere formation. This is suggested by the changing appearance that multivesicular bodies undergo during the transition into vitellogenesis. Initially, multivesicular body-like structures, apparently containing proteinaceous material and abundant vesicular elements, are observed (Fig. 47). In other multivesicular body-like structures, the condensing yolk material takes on a greater degree of homogeneity with fewer vesicular elements, and acquire the highly electron-dense, yolk-specific inclusions (Fig. 48). Subsequently, the yolk spheres condense to mature yolk spheres that lack internal vesicular elements but retain the highly electron-dense inclusions (Fig. 49). In the pipefish, multivesicular bodies seem to disappear as vitellogenesis progresses, as has been noted in other species (Shackley and King, 1977; Selman and Wallace, 1986).

Although I have not provided direct evidence for the involvement of multivesicular bodies in yolk sphere formation, there exists definite transitional yolk sphere structures containing multiple vesicles that appear to be intermediates in the formation of mature yolk spheres. Alternatively, the multivesicular bodies could play a role in cortical alveoli formation. This possibility seems unlikely though, because the electron-dense, yolk-specific marker is only seen in mature yolk spheres and in transitional structures (Fig. 48) and not in cortical alveoli. Thus, taken together, these observations are consistent with the notion that the multivesicular bodies represent a modified lysosomal compartment involved in yolk-sphere formation during vitellogenesis in the pipefish.

The steroid 17-alpha,20-beta-DHP has been shown to be the most effective stimulator of maturation in a variety of fish (Nagahama and Adachi, 1985; Greeley et al., 1986a). Pipefish follicles 1.1 mm in diameter are also fully competent to undergo 100% germinal vesicle breakdown in response to this steroid. These data are consistent with the disposition of the oocytes within the ovary as oocytes larger than 1.1 mm and still possessing a germinal vesicle are typically not observed. The mature egg has a diameter of approximately 1.3 mm and a volume of 1.15 mm^3. Thus, there is a volume change of approximately 60% that occurs during maturation in vivo. The protein content increases by 23% during maturation (Fig. 55), presumably by continued vitellogenesis (Wallace and Selman, 1985). However, the rate of protein increase per unit oocyte volume appears to be somewhat less during maturation than during vitellogenesis (Fig. 55), indicating that other processes may also be responsible for the volume increase. In certain other teleosts, hydration coupled to yolk protein proteolysis has been found to be a prominent feature of

Fig. 58. Schematic model of follicle progression through the ovarian stroma. Dorsal and ventral relations are indicated diagram a. This orientation is maintained in all diagrams. Each succeeding diagram (a-f) represents a later time during follicle development. The germinal ridge remains stationary in a dorsal position. The movement of follicles in this "conveyer belt mechanism" can be followed by observing the movement of individually numbered follicles. Note how each follicle becomes more ventrally located as this process occurs until the oocytes finally ovulate as mature eggs into the ovary lumen.

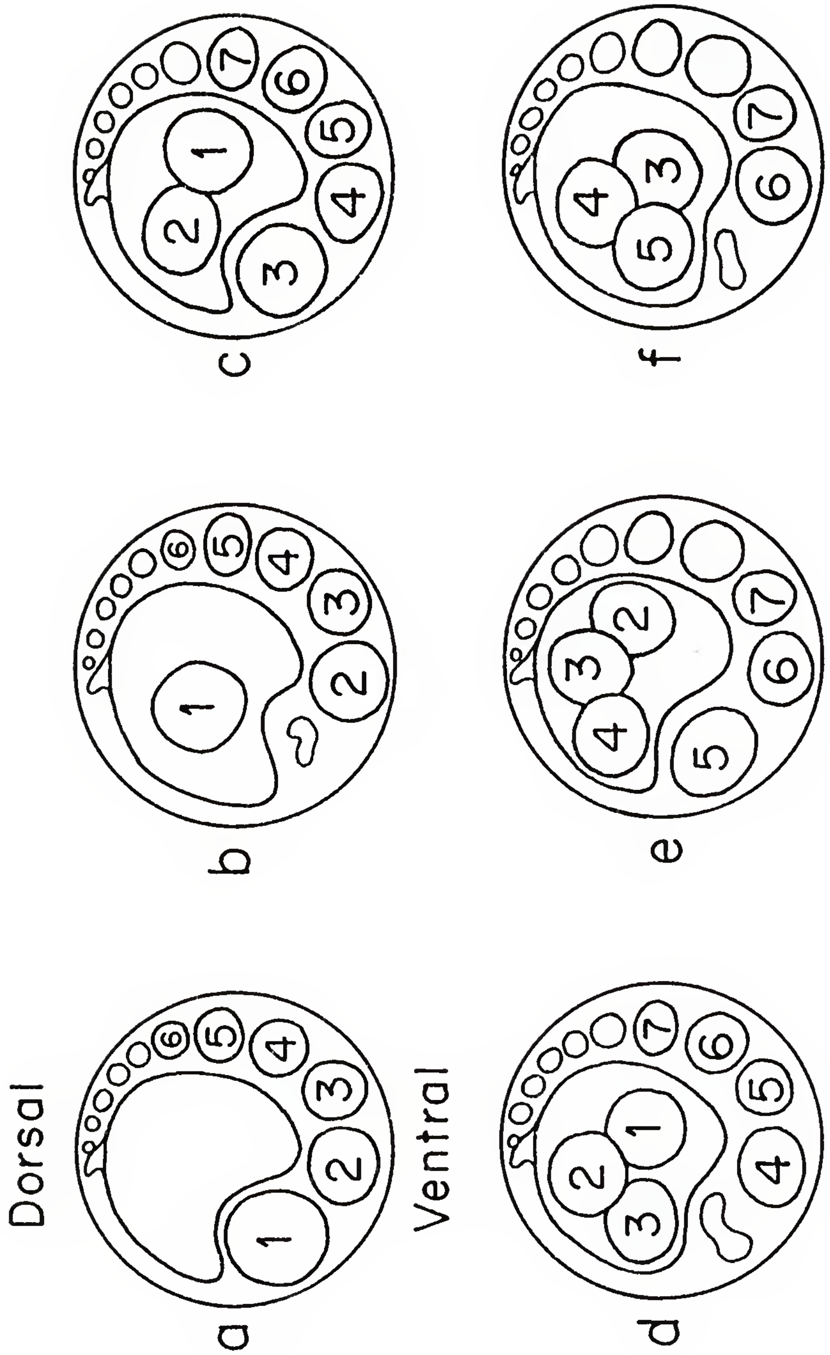
Dorsal
Ventral
a
b
c
d
e
f

maturation (Greeley et al., 1986b). In contrast to other species (Wallace and Selman, 1978, 1981; Greeley et al., 1986a, 1986b), however, the pipefish oocyte undergoes very little if any detectable size increase when induced to undergo maturation in a vitellogenin-free medium *in vitro*, and no changes occur in the yolk proteins during maturation *in vivo* (Fig. 56). Thus, it still remains unclear to what extent these various processes contribute to the overall size increase that naturally occurs during maturation.

The dynamics of the oocyte developmental pattern indicate that there is physical movement of follicles during oocyte development. If one considers the position of oocytes at a given time and postulates their position at a later time, the model presented in Figure 58 illustrates the changing relationships. This "conveyor belt model" accounts for the apparently fixed position of the germinal ridge in a dorsal position within the ovary. Movement of the developing follicles occurs in a ventro-lateral direction from the germinal ridge toward the mature edge. Continued follicle formation from the germinal ridge would replenish the later stage oocytes as they mature and ovulate.

The spatial and temporal relationships of oocyte development in the pipefish offer a useful model system for exploring many cellular events during oogenesis. I have here provided a staging series of oocyte development and have begun to address some of the physiological processes occurring during oogenesis and oocyte development in the pipefish. Many questions relating to the dynamics of oogonial proliferation, function of the Balbiani vitelline body, cortical alveoli and vitelline envelope formation, lipogenesis, vitellogenesis, and maturation may be explored in the pipefish, particularly with respect to the correlation of these developmental processes in time and space. This study helps lay the foundation and provides guidance for future studies of these phenomena during oocyte development in this unique teleost.

CHAPTER IV
EGG VITELLINE ENVELOPE CONSTITUENTS

Introduction

The vitelline envelope is a complex extracellular matrix that circumscribes the developing oocyte and mature egg; it becomes the chorion of the developing embryo. This extracellular matrix is layed down during oocyte development and undergoes structural and mechanical changes as a result of fertilization (Kudo, 1982). During ooctye development, the vitelline envelope is porous due to the presence of pore canals that allow plasma proteins access to the oocyte (Selman and Wallace, 1982; Abraham et al., 1982, 1984). The teleost vitelline envelope presumably plays a role during fertilization as a barrier to polyspermy but its main functions occur postfertilization when the chorion serves as a protective covering and permeability barrier during embryogenesis (Dumont and Brummett, 1985). The chorion is retained until the time of hatching when the prehatching fry produces a hatching enzyme, chorionase, that digests the chorion from inside out and allows the fry to escape (Yamagami, 1981).

The egg vitelline envelope has been extensively studied in a host of organisms (reviewed by Dumont and

Brummett, 1985). In teleosts, the vitelline envelope has been examined morphologically in many species (Hurley and Fisher, 1966; Anderson, 1967; Flugel, 1967a,b; Lonning, 1972; Busson-Mabillot, 1973; Hagenmaier, 1973; Azevedo, 1974; Wourms, 1976; Flegler, 1977; Tesoriero, 1977a; Stehr and Hawkes, 1979, 1983; Dumont and Brummett, 1980; Laale, 1980; Kudo, 1982). Histochemical or biochemical analyses of the teleost vitelline envelope have also been published (Busson-Mabillot, 1973; Hagenmaier, 1973; Tesoriero, 1977b; Kudo, 1982). These latter studies indicated general constituents of the vitelline envelope, but the identification of specific molecules associated with the teleost vitelline envlope was lacking. Studies on the biochemical compostion of other vertebrate (Wolf et al., 1976; Bleil and Wasserman, 1980a; Dunbar et al., 1980; Back et al., 1982; Hedrick and Wardrip, 1987) and invertebrate (Glabe and Vacquier, 1977; Fargnoli and Waring, 1982; Niman et al., 1984) vitelline envelopes have been reported. However, only recently has preliminary work identifying proteins associated with the pipefish (Begovac and Wallace, 1986), the medaka, Oryzias latipes (Hamazaki et al., 1987b) and goldfish (Cotelli et al., 1986) vitelline envelopes been published. The lack of previous information on teleosts was probably a consequence of the apparently insoluble nature of teleost vitelline envelopes in particular.

The initial morphological studies of the pipefish vitelline envelope were reported by Anderson (1967). Based on static images of vesicular elements in continuity with the forming vitelline envelope, he suggested that the vitelline envelope was a primary envelope derived from the oocyte, although no biochemical data was provided to support this conclusion. Recently, Hamazaki et al., (1985, 87a, 87b) has indicated that the origin of vitelline envelope proteins in the medaka is the liver, rather than the oocyte. Thus, in order to resolve this discrepency, we needed to understand more fully the macromolecular constituents of the pipefish vitelline envelope. This chapter provides such an analysis.

Materials and Methods

Light Microscopy

Ovarian tissue and dissected follicles were placed into a fixative containing 4% paraformaldehyde in 0.1 M sodium phosphate buffer, pH 7.4 for two hours at 23° C. Tissues were washed in 0.1 M sodium phosphate for two hours at 23° C, dehydrated in graded ethanol series and embedded in Historesin (LKB). Tissue sections were stained with Harris's hematoxylin and eosin, periodic acid-Schiff's reagent (Luna, 1968), and lectins (below).

Lectin binding studies were carried out using a panel of fluorescein-conjugated lectins (Vector Laboratories) including: concanavalin A (Con A), specific for D-mannose and D-glucose; *Dolichos biflorus* agglutnin, specific for N-acetyl-D-galactosamine; peanut agglutinin, specific for terminal-B-galactosamine; *Ricinus communis* (RCA), specific for D-galactose; soy bean agglutinin, specific for -B-N-acetyl-D-galactosamine; *Ulex europaeus* agglutinin, specific for L-fucose; and wheat germ agglutinin (WGA), specific for N-acetyl-glucosamine and sialic acid (McCoy, 1986). Preliminary experiments identified which lectins bound the vitelline envelope. Reactive lectins were tested for sugar specificity on control sections by coincubating lectins with 0.5 M D-mannose and/or 0.5 M D-glucose for Con A, 1 M N-acetylglucosamine or 10 mM chitotriose for WGA, and 0.5 M D-galactose for RCA. Experiments were performed at 23° C by rehydrating sections in phosphate-buffered saline (PBS; 137 mM NaCl, 1.5 mM KH_2HPO_4, 8.1 mM Na_2HPO_4, 2.7 mM KCl, pH 7.4) for 30 minutes. Sections were incubated in PBS containing hemoglobin (2mg/ml) for 15 minutes to block nonspecific adsorption. Slides were then incubated for 45 minutes in specific lectins (5 mg/ml; 1:50 dilution) in PBS. Slides were washed in PBS containing 2% hemoglobin for 15 minutes and rinsed twice in PBS for 10 minutes each. Slides were coverslipped with 50% glycerol in water or PBS containing freshly prepared paraphenylenediamine (0.3-0.5%) to retard fluorescence quenching (Valnes and Brandtzaeg, 1985). Sections were analyzed with a Leitz-Dialux fluorescense microscope equipped with a fluorescein bypass filter. Images were photographed with Kodak (400 ASA) Tri-X or Ektachrome film.

Electron Microscopy

Eggs were removed from the ovary lumen, placed in solution FO (Wallace and Selman, 1978) and processed according to the vitelline envelope extraction protocol (below). Samples were prepared with and without sodium dodecyl sulfate (SDS)-sample buffer extraction. The SDS-sample buffer extracted pellets were not mechanically homogenized to prevent structural artifacts. The pellets were fixed and processed for electron microscopy as described in Chapter II.

Vitelline Envelope Protein Extraction

Freshly collected eggs or frozen egg stocks were placed in solution FO and homogenized with a loose-fitting Dounce homogenizer. (No difference in protein patterns was observed between fresh and frozen egg preparations.) Vitelline envelopes were pelleted for 5 minutes at 180xg and the supernatant discarded or saved as a protein sample. The pellet was washed in 3 changes of H_2O, centrifuged for 5 minutes at 400xg after each wash, and supernatants saved or discarded. The pellets were then washed 3 times in 1.0 M NaCl, with sonication (level 2-3 for 10-15 seconds) during the first two washes, and centrifuged 5 min at 1000xg after each wash. Following one final wash in H_2O to remove residual salt, the pellet (purified vitelline envelope fraction) was extracted with SDS-sample buffer [40 mM dithiothreitol, 10 mM ethylenediaminetetraacetic acid (EDTA), 0.0025% bromophenol blue, 1.25% SDS, 62.5 mM Tris-Cl, pH 6.8, and 12.5% glycerol] using a ground-glass homogenizer. The samples were heated at 100° C for 5-7 minutes and stored at -20° C. Supernatants from the solution FO wash and H_2O washes were also diluted in SDS-sample buffer and heated at 100° C as described. All procedures prior to the addition of SDS-sample buffer were performed at 0-2° C. Proteolysis during some extractions was limited by the inclusion of 0.2 mM phenylmethylsulfonyl fluoride in homogenization and wash solutions. No difference in protein patterns was observed with or without inclusion of phenylmethylsulfonyl fluoride, therefore, it was not routinely used.

Gel Electrophoresis

Protein samples were subjected to SDS-polyacrylamide gel electrophoresis (SDS-PAGE) based on the methods of Lamelli (1970). Linear polyacrylamide (28%T/2.7%C) gradient gels of 6.93-20.44% were cast with a thickness of 1.5 or 0.75 mm and photopolymerized with riboflavin. Protein samples were microfuged for 5 minutes prior to placement in gel wells to remove any insoluble material. Proteins were electrophoresed generally at 30 mAmps, constant current, per gel for approximately 4 hours at 4° C until the tracking dye had migrated from the gel.

Electrophoresis was continued for an additional 45-60 minutes to optimize protein separation. Protein standards (Bio-Rad, high and low) were run concurrently for determination of molecular mass. Upon completion of electrophoresis, gels were fixed in an aqueous solution of 45% methanol, 10% glacial acetic acid for at least six hours, stained with 0.05% Coomassie blue R-250 in 25% isopropanol and 10% acetic acid for at least six hours, and detained with 5% methanol and 10% acetic acid until the background became clear. Molecular masses were determined according to the methods of Lambin (1978).

Limited Proteolysis

Limited proteolysis was performed essentially according to the methods of Cleveland et al. (1977). Extracted vitelline envelope and egg protein samples were separated by SDS-PAGE as described above, stained with Coomassie blue for 5 minutes, and destained for 30 minutes. Appropriate protein bands were excised from the gel, placed in equilibration buffer (0.125 M Tris-Cl, pH 6.8, 0.1% SDS, 1 mM EDTA) for 30 minutes, and loaded onto a discontinuous gel. The discontinuous gel consisted of a 2.5 cm-long, 3.5% stacking gel overlying a 11.5 cm-long 9-16% linear gradient separating gel. The gel bands were overlayed with equilibration buffer containing 20% glycerol. Specific proteases (0.01-10 ug per lane) in equilibration buffer containing 10% glycerol were then overlayed in a volume of

10 ul. Proteases used for digestions were *Staphlococcus aureus* V8 protease (Type XVII), trypsin (Type XI), and chymotrypsin (Type VI), all purchased from Sigma. The proteins were electrophoresed at 50 volts, constant voltage, until the tracking dye had migrated to about 1 cm above the separating gel. The current was turned off for one hour to allow protein digestion to occur. The current was then reapplied at 50 volts, constant voltage, overnight and electrophoresis stopped when the bottom of the tracking dye had migrated from the gel. Gels were fixed, stained with Coomassie blue and destained as described.

PAS Staining of Gels

Protein samples were subjected to SDS-PAGE as described. The gels were stained with periodic acid-Schiff's reagent to demonstrate carbohydrate moieties by the procedure of Dubray and Bezard (1982). Briefly, the gels were fixed overnight in 25% 2-propanol and 10% acetic acid at 23° C followed by treatment with an aqueous 7.5% acetic acid solution for 30 minutes at 23° C. The gels were then incubated in aqueous 0.2% periodic acid for one hour at 4° C, transferred into Schiff's reagent (Fisher Sci.) without rinsing for one hour at 4° C, and destained in 7.5% acetic acid at 23° C.

Dry Mass and Amino Acid Analysis

The vitelline envelope dry mass was determined by manual isolation of vitelline envelopes. Eggs were punctured, grasped with watchmaker forceps, and washed with 1 M NaCl at 4° C using a mouth-operated pipet. Isolated vitelline envelopes were washed again in several changes of H_2O, dried under vacuum for at least 12 hours, and the samples weighed. Amino acid analyses were performed on both purified, non SDS-sample buffer extracted vitelline envelope pellets, prepared in the standard manner up through the final H_2O wash and on the insoluble residue remaining after protein extraction in SDS-sample buffer. Excess water was removed from the purified vitelline envelope pellet, 0.5 ml of 6 N HCl added, and the sample transferred to a reaction vessel. The insoluble residue remaining after SDS-sample buffer extraction was washed with three changes of acetone, transferred into a reaction vessel, and the acetone dried off. Five hundred ul of 6 N HCl was added to the residue. The reaction vessels were sealed under vacuum after flushing with nitrogen gas. Acid hydrolysis was carried out for 24 hours at 110° C and amino acid determination performed with a Hitachi Amino Acid Analyzer.

Results

Light Microscopy

The vitelline envelope appears as a thick band between the oocyte and its overlying follicle cells (Fig. 59) during development. It attains a final thickness of approximately 4-6 um. A description of the vitelline

Fig. 59. Light micrograph of vitelline envelope from a midvitellogenic oocyte (O). Note the striated appearance (arrows) caused by pore canals within the vitelline envelope. JB-4 resin, H&E. x 470.

Fig. 60. Light micrograph of follicles stained with PAS. Note the heavy staining of the vitelline envelope (arrows) of the cortical alveoli-stage oocyte whereas only the outermost layer of the vitelline envelope (arrowheads) stains strongly in the late vitellogenic stage oocyte (O). Cortical alveoli are also stained in both oocytes. x 300.

Fig. 61. Phase and fluorescence photomicrograph pairs of control and experimental treatments of follicles stained with WGA. a,b) Control section treated with 1 M N-acetylglucosamine. Note the complete staining of the vitelline envelope (arrowheads) in cortical alveoli-stage oocytes while the vitellogenic oocyte lacks staining of the inner layer (arrows). Ignore the staining of the cortical alveoli as this is totally nonspecific. (O) Oocyte. x 370. c,d) Experimental section of vitellogenic oocytes treated with WGA. Complete staining of the vitelline envelopes (arrows) is obvious. (O) Oocyte. x 510. e,f) Control sections treated with 1 M N-acetylglucosamine. Note again that the outermost vitelline envelope layer (arrowheads) is stained nonspecifically whereas lectin binding to the inner layer is specifically blocked by this sugar. Cortical alveoli continue to stain nonspecifically. (O) Oocyte. x 330.

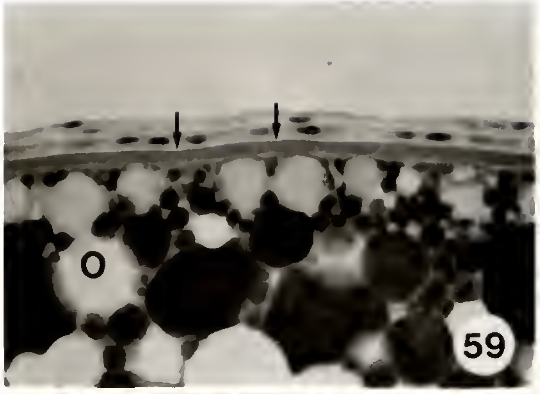
O
59

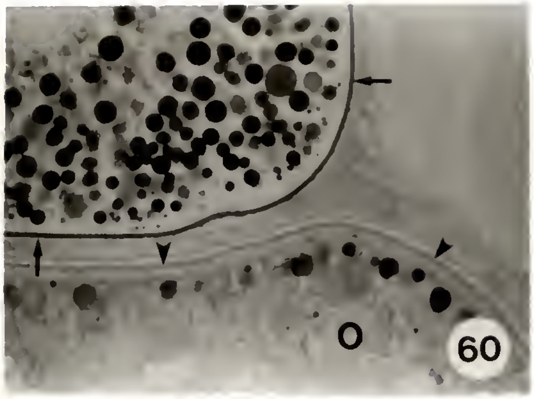
O
60

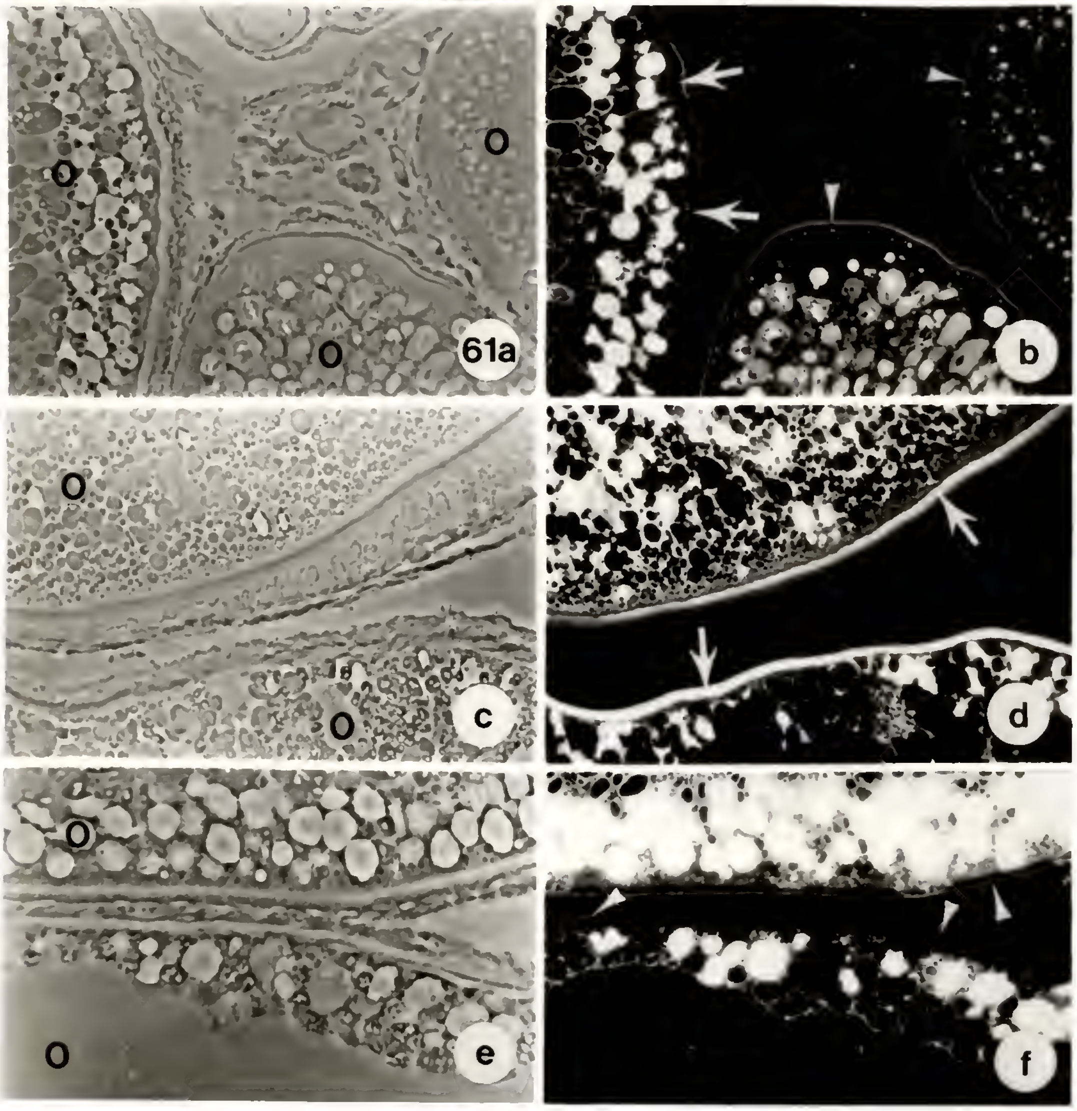
O
O
O
61a
b
O
O
c
d
O
O
e
f

envelope in its earlier stages is provided in Chapter III. The vitelline envelope of the developing oocyte generally has a striated appearance (Fig. 59) due to the presence of pore canals. This striated pattern is absent in the mature egg, a consequence of microvillar process retraction. The vitelline envelope is light refractive under phase and interference microscopy. Histochemical staining of ovary sections with the PAS reagents reveals the carbohydrate nature of the vitelline envelope layers. The vitelline envelope first becomes apparent in cortical alveoli-stage oocytes with the appearance of a PAS positive band (Fig. 60) between the oocyte and its overlying follicle cells in accord with earlier observations by Anderson (1967). As oocytes progress through the vitellogenic growth period, the vitelline envelope becomes differentially stained. The outermost layer (Fig. 60) retains the strongest PAS-positive reactivity while the innermost layer is stained less intensely. This differential appearance continues through maturation.

Lectin Staining

Lectin treatment of ovarian follicles indicated sugar specific binding of Con A, RCA, and WGA to the vitelline envelope while other lectins tested did not competitively bind to the vitelline envelope. Concanavalin A binding to the vitelline envelope, once formed, was observed throughout oocyte development [depicted in Chapter III, (Figure 43)]. Ricinus communis agglutinin binding was weak but appeared to stain the entire vitelline envelope. Wheat germ agglutinin gave a non-uniform binding during oocyte development. Wheat germ agglutinin binding to the outermost layer of the vitelline envelope (Fig. 60a, b, e, f) was not inhibited by N-acetylglucosamine or chitotriose (Fig. 60a, b, e, f) and appears to be non-specific. Binding of WGA to the inner layer of the vitelline envelope, on the other hand, was competitively blocked by N-acetylglucosamine or chitotriose (Fig. 61a, b, e, f). Thus, WGA in the presence of competing sugar gave a similar result to that provided by PAS staining. Although WGA staining of the outermost layer is nonspecific, it does allow us to observe the movement of this layer of the vitelline envelope during oocyte development.

Vitelline Envelope Ultrastructure

The light microscopic changes of the vitelline envelope are reflected at the ultrastructural level. Prior to vitelline envelope formation, perinucleolar primary growth oocytes extend microvillar processes toward the investing monolayer of follicle cells (Chapter III, Fig. 36). The initial formation of the vitelline envelope occurs in the earliest cortical alveoli-stage oocytes with the deposition of a homogeneous electron-lucent layer between the microvillar processes (Fig. 62), designated Z1 by Anderson (1967). By mid to late cortical alveoli stage,

Fig. 62. Electron micrograph of vitelline envelope in early cortical alveoli-stage oocyte (O). The vitelline envelope initially appears as a homogeneous, electron lucent material (Z1; arrows) between the microvillar processes. (FC) Follicle cell. x 16,900.

Fig. 63. Electron micrograph of vitelline envelope in later cortical alveoli-stage oocyte (O). The vitelline envelope assumes a trilaminar appearance as Z2 and Z3 appear beneath the Z1 layer. (FC) Follicle cell. x 16,900.

Fig. 64. Electron micrograph of vitelline envelope from a midvitellogenic stage oocyte (O). The vitelline envelope has undergone compaction, particularily of the Z3 layer. The Z2 layer seems to have disappeared. The Z1 layer (arrowheads) remains but is much thinner than in previous stages. Note the horizontal lammellar bands (arrows) within the structure of the envelope. Oocyte and follicle cell (FC) microvillar processes are present within the pore canals of the vitelline envelope. x 16,900.

Fig. 65. Electron micrograph of vitelline envelope of mature egg. Note the retention of the outer Z1 layer (arrowheads) and the fully compacted inner Z3 layer of the envelope. The microvillar processes have disappeared and only remnants of the pore canals (arrows) remain. The horizontal lamellae seen in Figure 64 are still prominent. x 16,300.

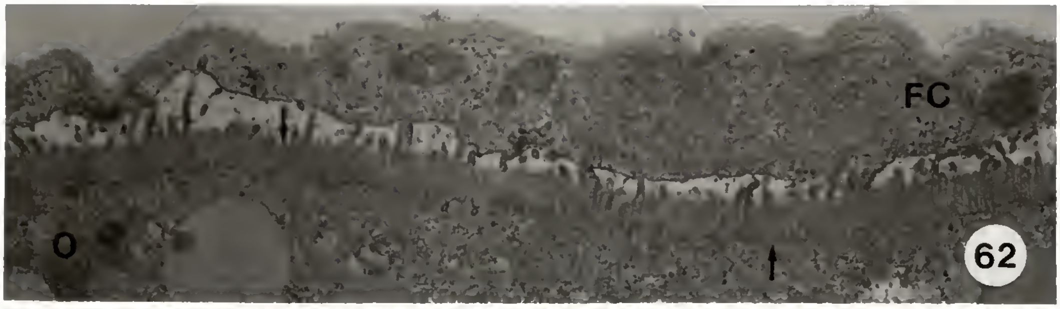
FC
O
62

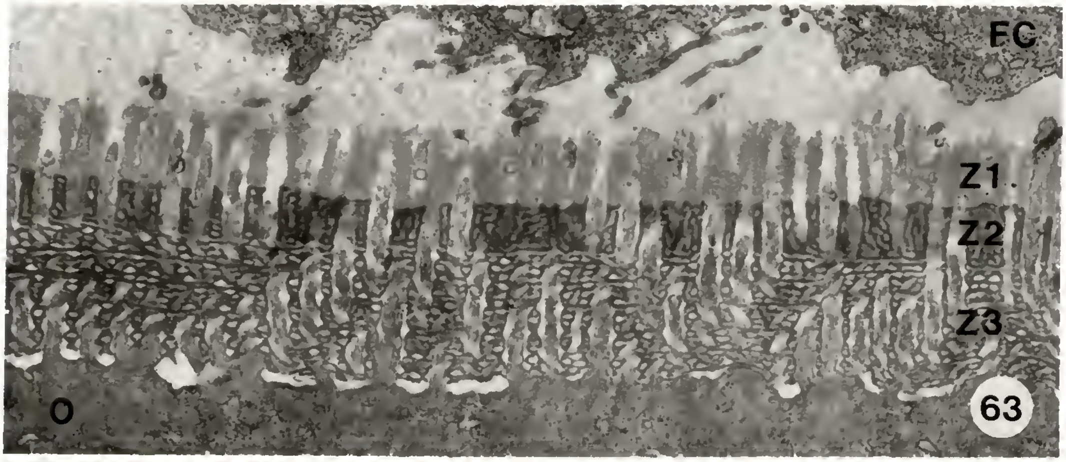
FC
Z1
Z2
Z3
O
63

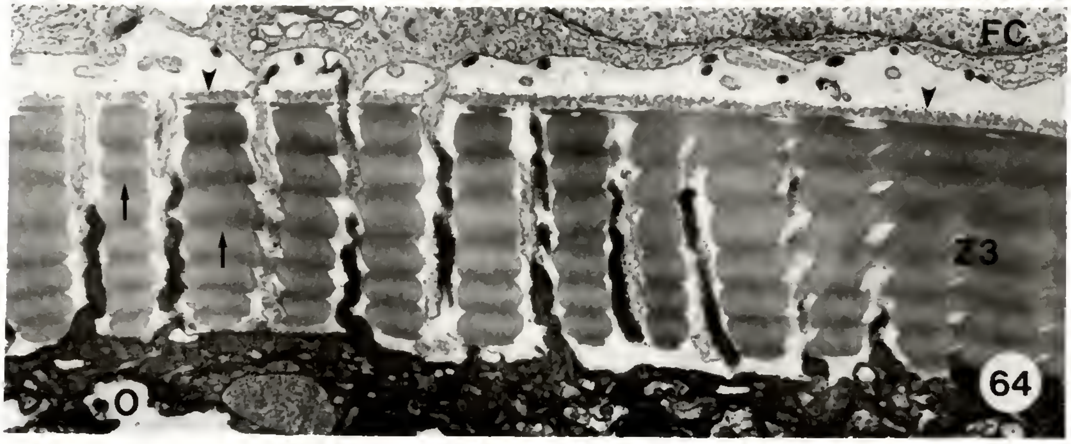
FC
Z3
O
64

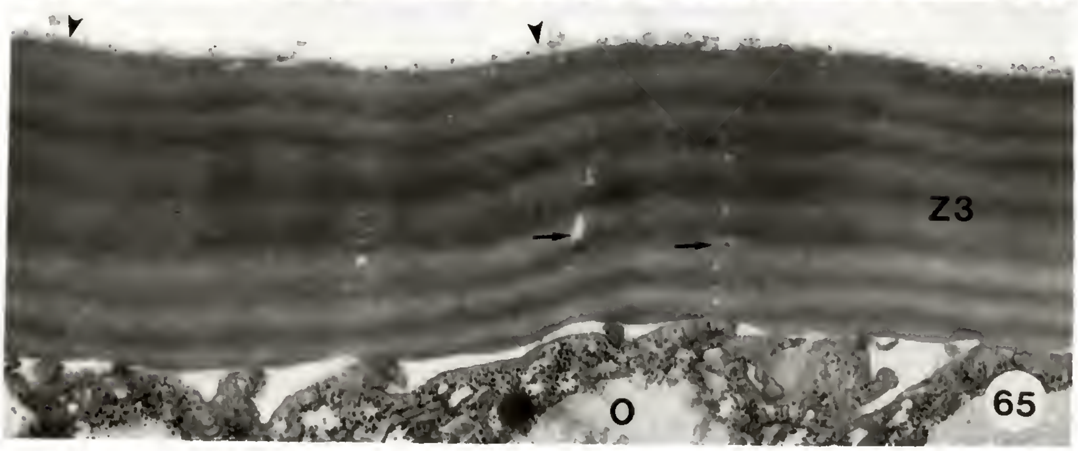
Z3
O
65

the architecturally complex Z2 and Z3 layers form giving a trilaminar appearance to the vitelline envelope (Fig. 63). During vitellogenic growth, the vitelline envelope undergoes compaction of particularly the Z3 layer (Fig. 64). Finally, by the time the oocyte transforms into a mature egg, the microvillar processes and pore canals are lost from the vitelline envelope (Fig. 65). The Z1 layer is retained throughout oocyte development including the mature egg, although it becomes much reduced in thickness as oocyte development progresses (Figs. 62-65). The lamellar nature of the vitelline envelope becomes apparent as the Z3 layer becomes compacted (Fig. 64) and it also is present in the mature egg (Fig. 65).

Purity of the Vitelline Envelope Pellet

Macroscopically, the egg vitelline envelope is transparent and when mechanically compressed is pliable. The mechanical properties of the vitelline envelope, however, change after the egg is activated either by natural fertilization or artificially with the ionophore A23187 (1 ug/ml). With this activation, the chorion as it is now called, becomes rigid and encases the newly formed embryo or activated egg.

The purity of vitelline envelopes isolated from the mature eggs was initially assessed by macroscopic observation (Fig. 66) and subsequently by electron microscopy (Fig. 67). The use of mature eggs for the

Fig. 66. Photomicrograph of manually isolated vitelline envelopes. Note the transparent nature and collapsed bag-like appearance. x 18.

Fig. 67. Electron micrograph of the vitelline envelope pellet obtained by the extraction protocol. These purified vitelline envelopes were not extracted with SDS-sample buffer. Note the absence of cytoplasmic contaminants and the similar structural appearance of the isolated envelopes as compared to that seen in the intact egg (Fig. 65). The Z1 layer (arrows) is retained. x 9,300.

Fig. 68. Higher magnification of the purified, nonextracted egg vitelline envelope. The Z1 layer (arrowheads) is retained. x 50,200.

Fig. 69. High magnification of insoluble residue remaining after extraction of vitelline envelope pellet with SDS-sample buffer. a) Note the fragmented, dense appearance of this insoluble residue. x 50,200. b) Another view of the insoluble residue. Note the filamentous (arrows) and the fibrogranular (*) aspects. x 50,200.

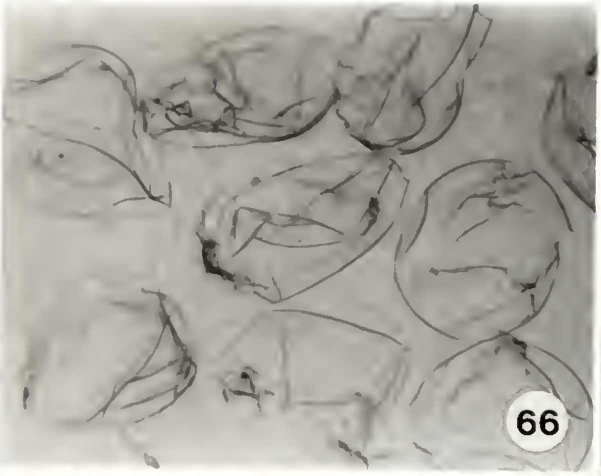
66

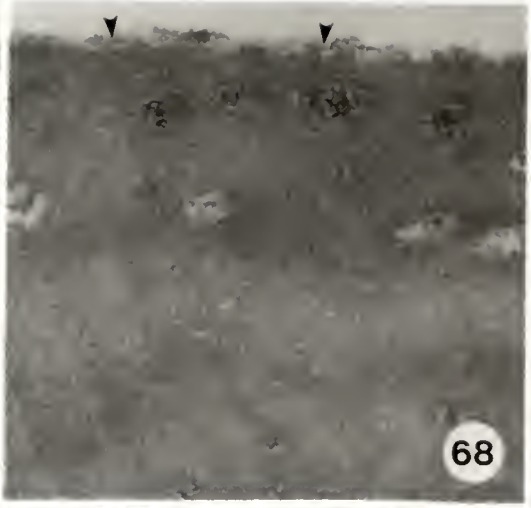
68

67

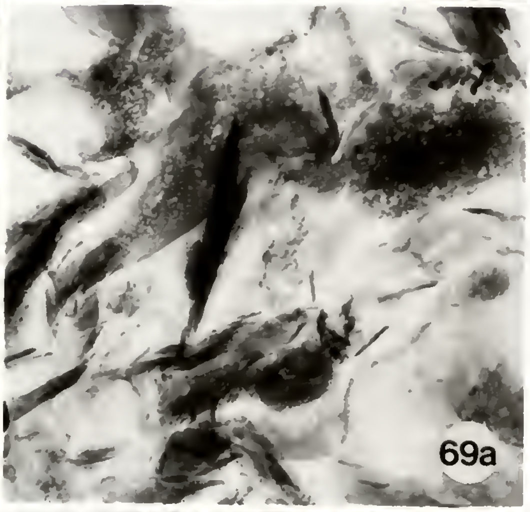
69a

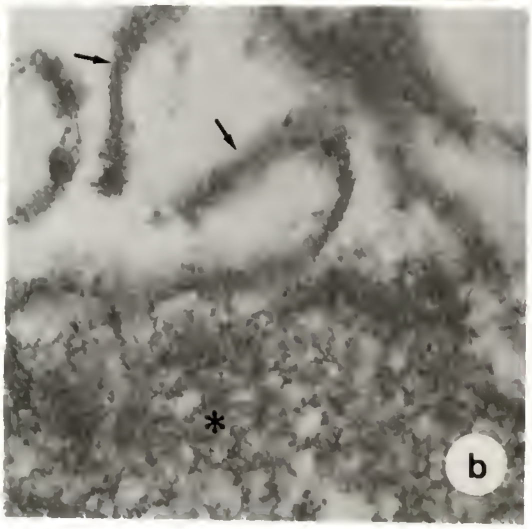

b

isolation of vitelline envelopes prevents contamination with follicle cells and other thecal components. (Protein samples prepared with oocyte vitelline envelopes were similar to protein samples prepared with mature egg vitelline envelopes.) Thus, the mature egg vitelline envelope was used as the starting material for all vitelline envelope isolations. Sonication during the 1 M NaCl washes was essential to completely remove egg cytoplasmic debris from the envelope preparation. The envelopes isolated using sonication in the extraction protocol yields a pellet fraction as shown in Figure 67. The appearance of the vitelline envelopes in this purified fraction (Figs. 67, 68) resembles that of the intact mature egg envelope (Fig. 65).

There is an insoluble residue remaining after SDS-sample buffer extraction. The ultrastructural apppearance of this material is varied but generally has three forms (Figs. 69a, b) There is a fragmented, dense material (Fig. 69a), a thin filamentous component (Fig. 69b), and a fibrogranular form (Fig. 69b) that appears to be incompletely extracted.

Sequential Protein Extraction

In order to assess the degree of biochemical purity of vitelline envelope proteins obtained with the extraction protocol, samples were prepared from pellet fractions after solution FO, H_2O, and 1 M NaCl washes. These samples were then subjected to SDS-PAGE, with the results depicted in Figure 70. Whole egg homogenate was run as a control to demonstrate the major yolk proteins observed and for comparison with purified vitelline envelope proteins. Purification of the vitelline envelope proteins occurs with each successive wash treatment, and especially after the 1 M NaCl wash, as evidenced by the loss of a smaller protein band from the lower vitelline envelope protein band and the loss of many smaller protein bands present in the whole egg homogenate. The sequential extraction demonstrates that two major extractable proteins (Fig. 70, lane 4), having molecular masses of 109 and 98kDa respectively, can be isolated from the vitelline envelope. Scanning densitometric analysis of the purified vitelline envelope protein preparation indicated that the 109 and 98kDa proteins are present in approximately a 1:2 ratio (data not shown). Comparison of the purified vitelline envelope proteins to other egg proteins also indicated that the 98kDa vitelline envelope protein migrated very closely with the major egg yolk protein (Fig. 70).

The protein content of the purified, non SDS-sample buffer extracted, vitelline envelope was determined by amino acid analysis and found to be approximately 4.2 ug protein per envelope (Table 1). The protein content remaining in the insoluble residue constitutes only 1-2% of

Fig. 70. SDS-PAGE of sequentially extracted vitelline envelope pellet proteins stained with Coomassie blue. Lane designations are 1) molecular weight standards; 2) solution FO wash pellet; 3) H_2O wash pellet; 4) 1 M NaCl wash pellet; 5) whole egg homogenate supernatant (compare with Fig. 56). A total of 5 vitelline envelopes were electrophoresed per pellet lane. A 94kDa protein band (arrowheads) can be seen in both FO (lane 2) and H_2O pellets (lane 3), as well as several lower molecular weight whole egg protein bands. Note the loss of the 94kDa band and lower protein bands after washing in 1 M NaCl (lane 4). Lane 4 illustrates the purified vitelline envelope proteins. Molecular masses are indicated on the left margin of the gel.

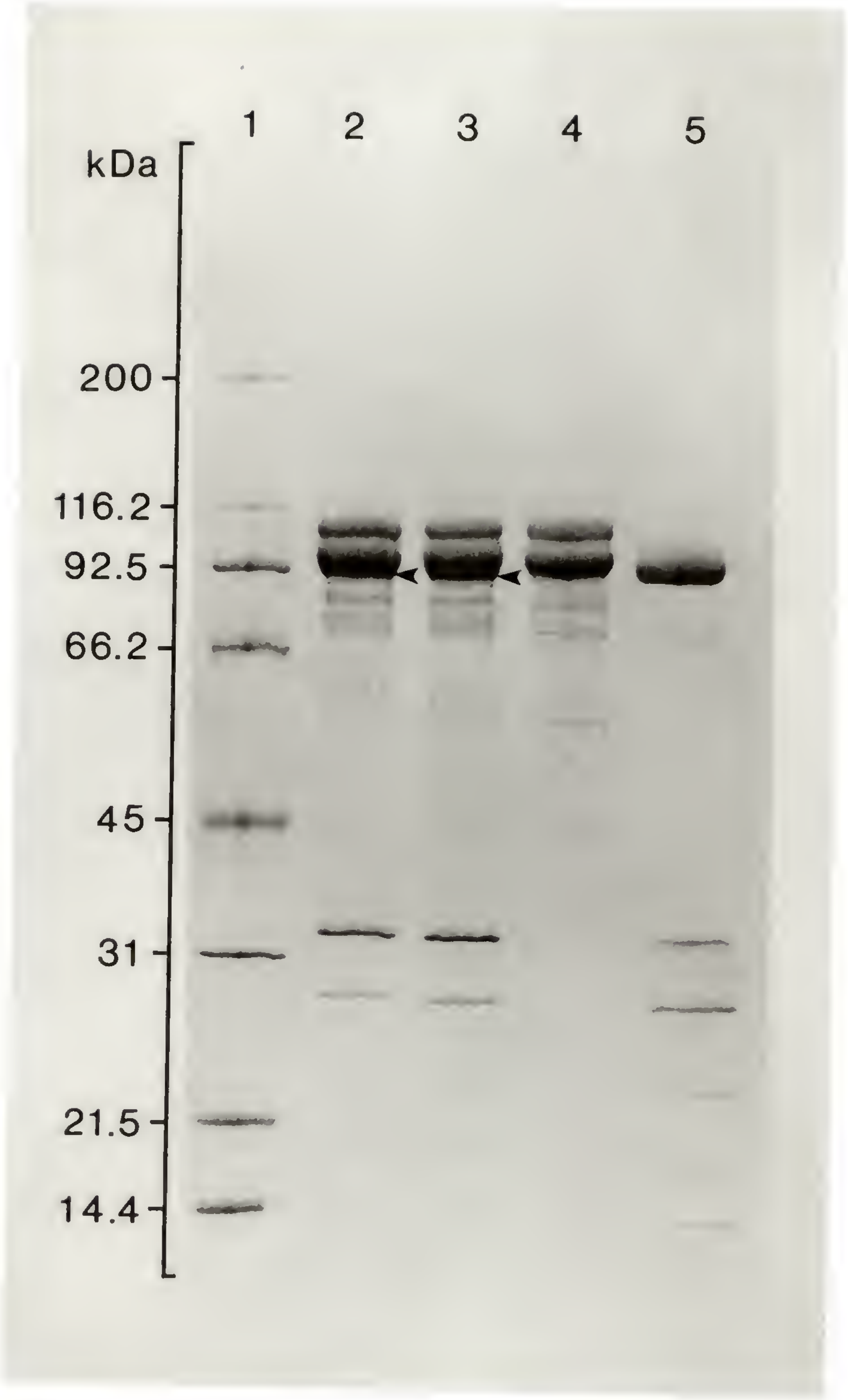
1
2
3
4
5
kDa
200
116.2
92.5
66.2
45
31
21.5
14.4

Table 1. Protein Content of Vitelline Envelopes Determined by Amino Acid Analysis.

Amino Acid	Nanograms[a]	Standard Deviation
Aspartic acid	369	5.3
Threonine	369	6.5
Serine	253	4.8
Glutamic acid	521	45.9
Glycine	519	10.1
Alanine	88	3.9
Valine	211	3.5
Cysteine	219	26.6
Methionine	117	4.8
Isoleucine	210	3.0
Leucine	167	4.2
Tyrosine	163	4.7
Phenylalanine	128	10.7
Lysine	92	1.1
Histidine	106	4.4
Arginine	292	21.3
Proline	369	30.4
Totals	4193	65.3

[a] Values represent mean mass per envelope based on 3 separate vitelline envelope preparations.

this value. The dry mass of the 1 M NaCl-washed vitelline envelope is approximately 5.8 ug per envelope. An attempt to determine the neutral sugar content of the purified, non SDS-sample buffer extracted, vitelline envelope by the anthrone method (Spiro, 1966) using glucose as the standard was unsuccessful. Approximately 290 ug of purified vitelline envelope material was assayed but the absorbance of the samples was below the lower limits of the standard curve.

Limited Proteolytic Digestion

The similar mobilities of the 98kDa vitelline envelope protein band and the major yolk protein band required further study to demonstrate conclusively that the 98kDa vitelline envelope protein was distinct from the major yolk band of approximately 94kDa. Hence, limited proteolytic digestion by the method of Cleveland et al. (1977) was used to generate peptide fragments of the 98kDa vitelline envelope and the major egg yolk protein. Peptide maps using trypsin, chymotrypsin, and *S. aureus* V8 protease indicated unique peptides for both proteins (Fig. 71). Furthermore, the 109kDa envelope protein demonstrated unique peptide fragment patterns when compared to both the 98kDa envelope protein and the major egg-yolk protein.

Carbohydrate Moieties Associated with VE Proteins

The glycoprotein nature of the extracted vitelline envelope proteins was assessed by PAS staining of gels.

Fig. 71. SDS-PAGE of limited proteolytic digestion products from 109 and 98kDa vitelline envelope proteins and major 94kDa yolk-protein bands. Proteins were stained with Coomassie blue. The 94kDa yolk protein control lane is indicated (Lane 1; Egg Con). Trypsin treatments (10 ug/lane) are in lanes 2-5. Chymotrypsin treatments (0.1 ug/lane) are in lanes 6-9. S. aureus V8 protease treatments (0.75 ug/lane) are in lanes 10-13. Lane 14 contains 109 kDa vitelline envelope protein control. Protease control lanes depict protein-staining patterns of the specific proteases themselves. Sample designations are the 94kDa yolk protein (Egg), the 98kDa vitelline envelope protein (VE-98kDa), and the 109kDa vitelline envelope protein (VE-109kDa). Note the individual peptide fragments of the egg contents versus the 98kDa envelope protein with each of the different protease treatments. Note also the different peptide fragments of the 109 versus the 98kDa vitelline envelope proteins. Molecular masses are indicated on the left margin of the gel.

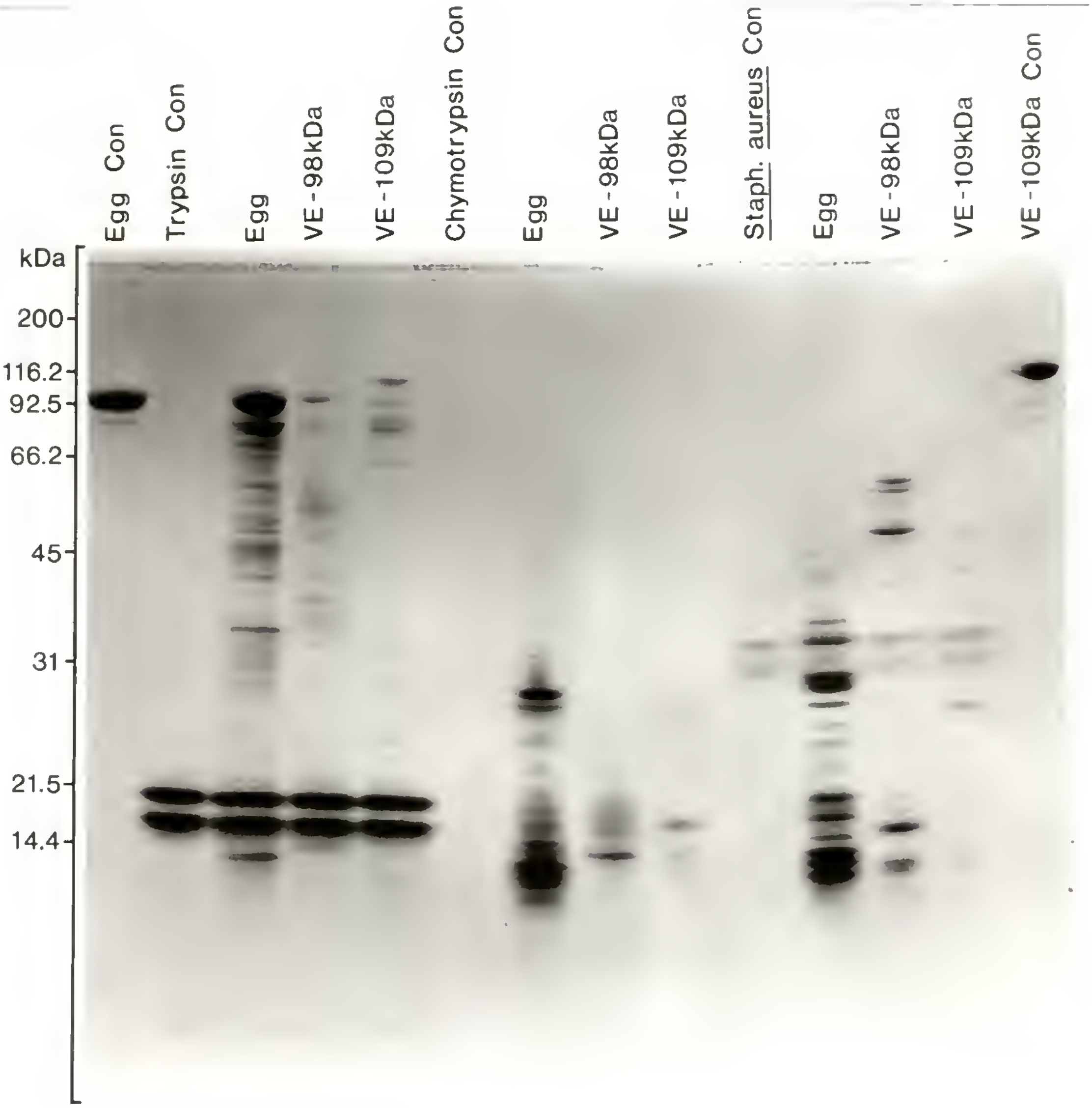
Egg Con
Trypsin Con
Egg
VE-98kDa
VE-109kDa
Chymotrypsin Con
Egg
VE-98kDa
VE-109kDa
Staph. aureus Con
Egg
VE-98kDa
VE-109kDa
VE-109kDa Con
kDa
200
116.2
92.5
66.2
45
31
21.5
14.4

Fig. 72. SDS-PAGE of vitelline envelope proteins and egg proteins stained with Coomassie blue (a) and periodic acid-Schiff's reagent (b). Note that the 98kDa vitelline envelope band stains for carbohydrate whereas the 109kDa envelope protein does not. The major egg yolk protein also stains for PAS. Positive ovalbumin control for the PAS reaction is indicated. Approximately 60 ug protein was run per vitelline envelope lane. Molecular masses are indicated on left margin of gel.

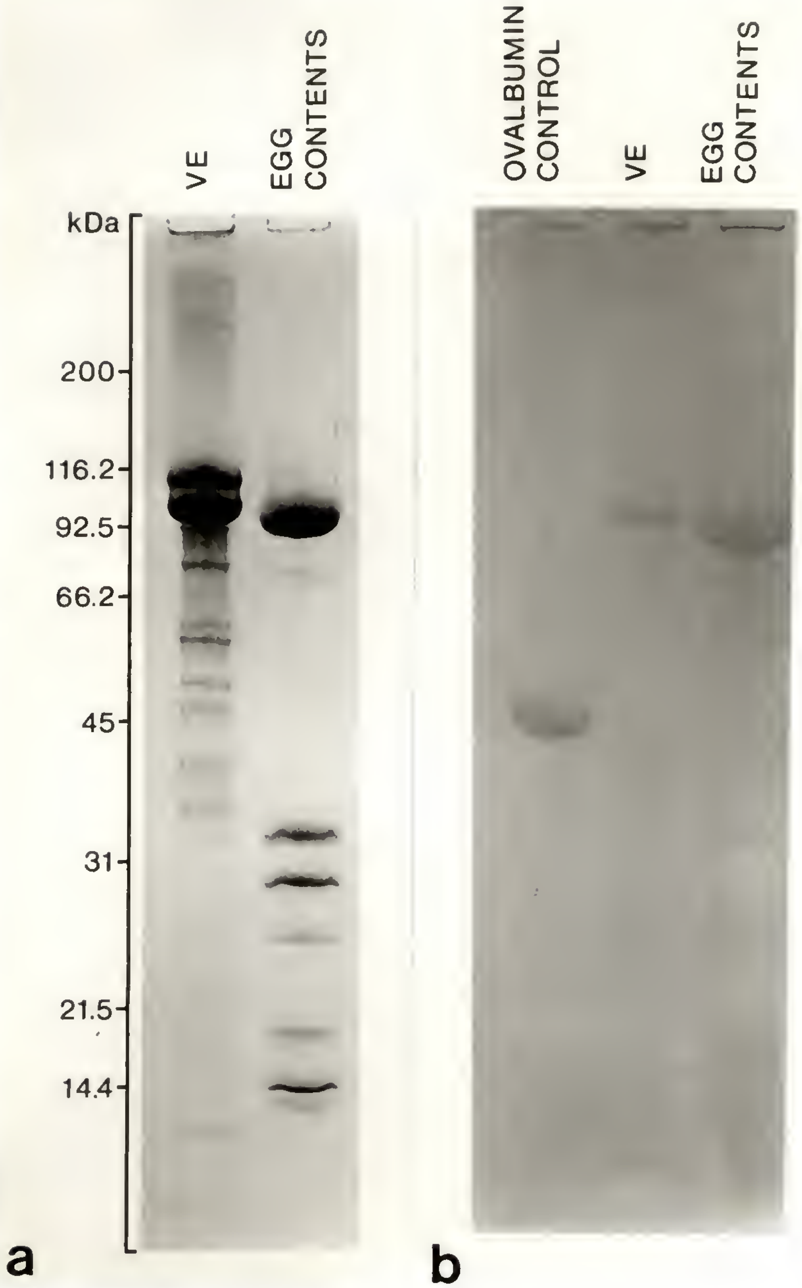
VE
EGG CONTENTS
kDa
200
116.2
92.5
66.2
45
31
21.5
14.4
a
OVALBUMIN CONTROL
VE
EGG CONTENTS
b

The results (Fig. 72) indicated that the 98kDa vitelline envelope protein stains positively for PAS whereas the 109kDa protein does not stain. The major yolk protein band of 98kDa also reacts with PAS.

Discussion

The structural complexity of the pipefish vitelline envelope during its formation is similar to that of several other teleosts (Flugel, 1967a; Busson-Mabillot, 1973; Wourms, 1976; Flegler, 1977). The initial multilayered appearance gives rise to a highly dense, compacted inner layer termed the "zona interna" (Dumont and Brummett, 1985) that comprises most of the envelope structure. A thin outer layer or "zona externa" is also present on the external surface of the vitelline envelope. The dense internal layer of the pipefish vitelline envelope has a lamellar appearance (Fig. 64, 65). These lamellae appear to be a common feature for many teleost egg envelopes (Lonning, 1972; Busson-Mabillot, 1973; Dumont and Brummett, 1980; Kudo, 1982). The internal layer of the vitelline envelope in Fundulus heteroclitus is strongly birefringent under polarized light (Kaighn, 1964). This birefringence most likely relates to the vitelline envelope lamellae observed ultrastructurally.

The carbohydrate nature of many teleost vitelline envelopes has been previously established (Kaighn, 1964; Anderson, 1967; Busson-Mabillot; 1973, Hagenmaier, 1973;

Tesoriero, 1977b). Anderson (1967) indicated that the pipefish vitelline envelope is PAS positive, an observation this study confirms. However, the additional observation of a differential reactivity of the vitelline envelope with PAS during oocyte development is reminescent of that observed for the trout (Hagenmaier, 1972) and medaka (Tesoriero, 1977b). During early vitelline envelope formation in the pipefish, the entire vitelline envelope reacts strongly with PAS. As oocyte development progresses, the strongest PAS reactivity becomes confined to the external margin of the envelope, with the inner layer being less intensely stained (Fig. 60). The initial strong PAS reaction to the vitelline envelope in cortical alveoli-stage oocytes and subsequent localization only to the external margin of the vitelline envelope in later stage oocytes correlates ultrastructurally with the position of the Z1 band.

The lectin-staining results support the observations made with PAS cytochemistry. Lectin staining indicates a more or less uniform distribution of the terminal sugars glucose, mannose, and galactose in the vitelline envelope within the limits of resolution of this procedure. Staining with WGA, however, gave a differential result as inhibition of WGA binding with N-acetylglucosamine was only associated with the internal layer. In early cortical alveoli-stage oocytes, WGA bound to the vitelline envelope nonspecifically. In later stages, nonspecific binding of WGA became confined to the outermost layer of the vitelline envelope. This nonspecific binding may reflect the presence of sialic acid residues as WGA is also known to bind to such residues (Goldstein and Poretz, 1986). One conclusion drawn from the PAS and lectin staining is that the outermost vitelline envelope layer has a different, and perhaps more chemically sensitive, saccharide content than the inner layer. Furthermore, these observations suggest that the Z1 layer is the morphological component of the vitelline envelope possessing the strongest PAS reactivity and WGA nonspecific binding.

The Z1 layer has been described as being lost in the mature egg (Anderson, 1967), however, I have found this not to be the case. The micrographs describing the mature egg in Anderson (1967) actually depict an oocyte, as evidenced by the follicular investments and microvillar processes within the vitelline envelope. As illustrated in Figure 65 of this study, the Z1 layer is retained in the ovulated egg, although greatly reduced in thickness. The Z1 layer also appears to be retained even after purification of vitelline envelopes (Figs. 67, 68). Both, the internal and external layers of the vitelline envelope of Fundulus heteroclitus have proved to be highly resistent to enzymatic proteases (Kaighn, 1964). Furthermore, the external layer of the medaka vitelline envelope is also left intact after digestion of the internal layer with the hatching enzyme, chorionase, and its integrity is destroyed only by the mechanical thrashing of the hatching embryo (Yamamto and Yamagami, 1975). Thus, the outermost covering of the teleost vitelline envelope appears to be a complex carbohydrate that may normally serve to protect the developing embryo from external degradation by xenogenous (bacterial, fungal) enzymes.

The protein nature of the teleost vitelline envelope has been established previously by histochemical means (Anderson, 1967; Busson-Mabillot, 1973; Hagenmaier, 1973) and by amino acid analysis (Young and Smith, 1956; Kaighn, 1964; Kobayaski, 1982). With the exception of two other reports (Cotelli et al., 1986; Hamazaki et al., 1987b), the identification of specific proteins associated with the teleost oocyte and egg vitelline envelope has been lacking. The present studies demonstrate that there are two major, and several minor, extractable proteins resolved by SDS-PAGE in the pipefish egg vitelline envelope and that the major proteins have molecular masses of 109 and 98kDa. The similar electrophoretic mobility of the 98kDa protein and the major egg-yolk protein initially raised questions as to whether these proteins were related or, in fact, distinct. The peptide-fragment patterns produced by limited proteolysis experiments demonstrated that the 98kDa vitelline envelope protein is distinct from the major egg yolk protein of approximately 94kDa. Furthermore, the peptide fragment analyses indicate that the 109kDa is distinct from the 98kDa protein. These analyses thus confirm that the 109 and 98kDa proteins isolated are, in fact, vitelline envelope proteins and not yolk contaminants. This conclusion is also supported by electron microscopic analysis revealing no cytoplasmic contaminants in the purified vitelline envelope pellet.

The 98kDa protein is a glycoprotein based upon its PAS postive staining whereas the 109kDa protein was PAS negative and does not appear to be appreciably glycosylated using this detection method. This differential PAS staining, taken together with limited proteolysis data, suggests that the 109 and 98kDa vitelline envelope proteins are unique proteins and that the 98kDa protein is not a proteolytic product of the 109kDa protein.

The extracted vitelline envelope proteins constitute approximately 72% of the vitelline envelope dry mass. This compares with the vitelline envelope protein content of 84.6% for Xenopus laevis (Wolf et al., 1976), 90% for sea urchins (Glabe and Vacquier, 1977), 71% for pig (Dunbar et al., 1980), and 80% for the mouse (Bleil and Wasserman, (1980). The neutral sugar analysis yielded a negative result. The sensitivity of the anthrone assay (Spiro, 1966) is approximately 20 ug and given the vitelline envelope sample size of approximately 290 ug, neutral sugars would appear to comprise less than about 7% of the vitelline envelope. However, at this time the contribution of neutral sugars to the vitelline envelope remains uncertain.

In conclusion, the pipefish vitelline envelope contains at least two major extractable proteins of 109 and 98kDa, the 98kDa protein being a glycoprotein. These proteins are unique to the vitelline envelope as demonstrated by electron microscopy, SDS-PAGE, and limited proteolysis. The outermost Z1 layer contains a strongly PAS positive component distinct from the inner layer. Terminal glucose, mannose, galactose and N-acetylglucosamine are carbohydrate components found in the vitelline envelope. These studies demonstrate that the pipefish vitelline envelope is complex both morphologically and biochemically. The origin, localization within the vitelline envelope and developmental expression of the 109 and 98kDa proteins during oocyte development remain to be determined.

CHAPTER V
LOCALIZATION AND SYNTHESIS OF VITELLINE ENVELOPE PROTEINS IN THE PIPEFISH FOLLICLE

Introduction

The vitelline envelope (VE), an extracellular coat surrounding the developing oocyte and mature egg, is layed down during oocyte development. Morphologically, the appearance of the vitelline envelope for various teleosts has been well documented (Anderson, 1967; Flugel, 1967a, b; Busson-Mabillot, 1973; Wourms, 1976; Tesoriero, 1977a), but the expression of protein constituents comprising this structure during oocyte development is less clear. The prevailing notion in the literature is that the teleost vitelline envelope is a synthetic product of the oocyte. This idea is based primarily upon morphological observations (Anderson, 1967; Wourms, 1976; Tesoriero, 1977a) and by studies demonstrating ^{3}H-proline incorporation into the vitelline envelope (Tesoriero, 1978). However, definitive experiments to establish the oocyte as the source of vitelline envelope proteins in teleosts have not yet appeared (Dumont and Brummett, 1985). Studies in other vertebrates demonstrate that the zona pellucida (or vitelline envelope) is synthesized by the oocyte (Bleil and Wasserman, 1980a, b; Bousquet et al., 1981; Pinto et al., 1985) or a combination of oocyte and granulosa (follicle) cells (Wolgemuth et al., 1984). Among invertebrates, the vitelline envelope has been reported to be produced by the oocyte (Rosati et al., 1982; Santella et al., 1983)

Contrary to the notion of oocyte origin are recent reports suggesting that the liver contributes synthetically to the composition of the vitelline envelope in the teleost, Oryzias latipes (Hamazaki et al., 1985, 1987a, b). These reports are based upon immunological studies using polyclonal antibodies generated against enzymatically digested embryonic chorions prepared with chorionase (Yamagami, 1981) and have raised new questions regarding the earlier morphological interpretations that the teleost vitelline envelope is synthesized by the oocyte.

The purpose of this chapter is to describe the production of monoclonal antibodies against the pipefish vitelline envelope proteins identified in Chapter IV. This approach was undertaken to determine the cellular origin of the major pipefish vitelline envelope proteins in further detail. The antibody probes have been used to follow the expression of the 109 and 98kDa proteins during oocyte development and evidence is presented which indicates that at least the 98kDa protein is synthesized within the ovarian follicle.

Materials and Methods

Monoclonal Antibody Production

Immunizations were performed by the method of Knudsen (1985) using pieces of nitrocellulose to which the 109 and 98kDa VE proteins had been electroblotted. Approximately 30-35 ug protein were used for each immunization. The nitrocellulose pieces were injected into the subcutaneous dorsal and abdominal regions of two Balb/c mice using a 16 gauge needle and stylet. The needle tip was dipped into Freund's complete adjuvant (Gibco) prior to injection. The mice were reimmunized with subcutaneous injections after one week, rested for 4 weeks, and boosted with subcutaneous and intraperitoneal injections 3 days prior to fusion. The intraperitoneal injection consisted of nitrocellulose containing protein that had been dissolved in 60 ul dimethylsulfoxide. Mouse hybridoma cell lines were prepared according to the general methods of Kohler and Milstein (1975) specifically by the monolayer method of McKearn (1980) as per Linser et al. (1984) using SP2/0 myeloma cells (Shulman et al., 1978).

Hybridoma supernatants were tested for immunoreactivity by three different screening assays. The initial screen was performed by indirect immunofluorescence on purified vitelline envelope fragments that were adhered to the bottom of plastic microtiter wells. (Vitelline envelopes were found advantageously to adhere to plastic.)

Fifty ul of hybridoma-conditioned supernatant were added to microtiter wells containing 50 ul phosphate-buffered saline (PBS; Chapter IV) and VE fragments. Assays were incubated for one hour at 23° C, washed three times with PBS, and incubated with fluorescein-conjugated goat antimouse polyvalent antibody (Boehringer Mannheim; 1:50 dilution) for one hour. The microtiter wells were washed three times and screened for fluorescence using an inverted microscope equipped for epifluorescence. The secondary screen was performed on paraffin embedded tissue sections as described below. The tertiary screen was performed using immunoblots as described below.

Positive colonies were cloned twice and retested for continued antibody production. Positive clones were placed on ice for 30 minutes in 10% dimethylsulfoxide, 20% fetal bovine serum and 70% Dulbecco's minimal essential medium, and frozen slowly in a styrofoam container overnight at -70° C. Vials of cells were transferred to liquid nitrogen for storage. Monoclonal antibody isotype was determined using a commercial screening kit (Zymed Laboratories Inc.) following the manufacturer's recommendations. Negative and positive controls were performed in parallel.

Immunocytochemistry

Freshly collected ovaries were fixed with 4% paraformaldehyde in 0.1 M sodium phosphate buffer, pH 7.4, for 2 hours at 23° C. The tissues were washed for 2 hours in several changes of 0.1 M sodium phosphate, pH 7.4, dehydrated in a graded ethanol series followed by xylene, and embedded in paraffin. Five-um sections were cut, deparaffinized, and rehydrated in PBS for 30 minutes. Sections were incubated with mouse hybridoma supernatant (1:25-1:50 dilution) in PBS for one hour at 23° C. Slides were rinsed 3 times for 5 minutes each in PBS and incubated in fluorescein-conjugated goat antimouse polyvalent antibody (Boehringer Mannheim: 1:50 dilution) for one hour at 23° C. Slides were rinsed 3 times for 5 minutes each and mounted as described in Chapter IV. Antibody localization on tissue sections was identified by indirect immunofluorescence with a Leitz Dialux 20 epifluorescence microscope. Phase and fluorescence images were photographed with Kodak Tri-X 400 ASA or Kodak Ektachrome 400 ASA. Control sections were treated with either no primary antibody, SP2/0-conditioned media, or an irrelevant IgM monoclonal antibody, 5A11, specific for glial cells (Linser and Perkins, 1987).

Immunoblots

Protein samples of purified vitelline envelopes, egg homogenates and supernatant washes from the vitelline envelope extraction protocol were prepared as described in Chapter IV. Protein samples were electrophoresed on 6.93-20.44% linear gradient gels as described in Chapter IV. Upon completion of electrophoresis, proteins were electroblotted onto nitrocellulose membrane (Bio-Rad; 0.45 um) as described by Towbin et al. (1979) with the addition of 0.1% SDS (Bers and Garfin, 1985). Electroblotting was carried out at 4° C for 8 hours at approximately 280 mAmps constant current. The nitrocellulose blot was removed, rinsed in H_2O and allowed to dry. The electroblotted gel was fixed, stained with Coomassie blue, and destained to assess transfer efficiency.

Immunoblot staining was performed by initially blocking the nitrocellulose against nonspecific binding for 1 hour with 1% gelatin or 5% milk protein (Carnation) in a Tris-buffered saline (150 mM NaCl, 20 mM Tris-Cl, pH 7.4). This step and all subsequent incubations were carried out at 23° C. The blocking buffer was drained and the blot incubated with agitation for 2 hours in mouse monoclonal hybridoma supernatant (1:10-1:20 dilution) in Tris-buffered saline (TBS; 0.25% gelatin, 0.05% NP-40, 2mM EDTA, 150mM NaCl, and 20mM Tris-Cl, pH 7.4) containing 2.5% normal goat serum. Blots were then rinsed 3 times for 10 minutes each in TBS containing 5% dried milk (Carnation) but lacking primary antibody, and finally rinsed once in TBS without milk. Blots were then incubated in horseradish peroxidase-conjugated goat antimouse polyvalent antibody (Boehringer Mannheim; 1:400 dilution) in TBS containing 5% milk protein and 2.5% normal goat serum with agitation for 2 hours. Blots were rinsed 3 times for a total of 20 minutes in TBS lacking milk protein. Visualization was accomplished using diaminobenzidine (DAB) as the enzyme substrate. This solution was freshly prepared as 20mM Tris-Cl, pH 7.4, 0.05% DAB, and 0.005% H_2O_2. Blots were rinsed in H_2O to stop the reaction.

Follicle Cell and Oocyte Dissociation

The most efficient method for isolating denuded oocytes and follicle cell/theca complexes was by manual dissection using watchmaker forceps. Ovaries were collected into solution FO and cut open longitudinally. The ovarian wall was dissected free and the ovaries cut transversely into several segments approximately 0.5-1.0 cm in length. These segments were transferred to Ca^{2+},Mg^{2+}-free solution FO and gently agitated. After approximately 30-40 minutes incubation, individual oocytes were manually dissected free of their follicular investments. The denuded oocytes and isolated follicle cells, with or without investing theca, were transferred back into complete solution FO. The follicular layers separated as cell lawns from the oocyte together or separately. The cell dissociation could easily be followed under the dissecting microscope. Verification of the denudation process was assessed by fluorescence microscopy using the method of Greeley et al. (1987). Briefly, isolated denuded oocytes and follicle cell lawns were stained with ethidium bromide (150 ug/ml in 85% L-15) at 23° C for 60 minutes, washed three times in solution FO lacking the dye, and observed with an epifluorescence microscope equipped with a rhodamine filter cube. Images were photographed with Kodak (400 ASA) Tri-X or Ektachrome film.

Protein Synthesis

Intact follicles, denuded oocytes, and follicle cell-theca complexes were isolated as described above. Pieces of fresh liver were also collected for these experiments. Intact follicles (0.3-0.8 mm diameter) and denuded oocytes (0.5-0.7 mm diameter) were separated into appropriate groups according to size. The follicle cell-theca complexes were pooled from all of the denuded oocyte groups within an experiment. Three replicates of the experiment were performed. The various culture groups were placed into 100-200 ul solution FO containing 200 uCi/ml of ^{35}S-methionine (Trans ^{35}S-Label, ICN; specific activity=1191 Ci/mmole) and placed on ice for approximately 75-90 minutes. The cultures were warmed to room temperature and incubated with label present for 2-3 additional hours. The cells were then washed briefly, transferred into 85% L-15 media containing 2 mM cold methionine, and incubated for 24 hours at 23° C. At the end of the culture period, cells were transferred into Eppendorf tubes, the media removed, and lysis buffer (O'Farrell, 1977) containing 0.2% SDS was added. Intact follicles, denuded oocytes, and liver samples were homogenized in the lysis buffer and stored at -70° C. The follicle cell-theca samples were subjected to three freeze-thaw cycles and stored at -70° C.

Isoelectric Focussing and Two-Dimensional Gels

Isoelelectric focussing (IEF) of samples was performed exactly according to the methods of O'Farrell (1977) using 2 mm internal diameter tubes. Purified vitelline envelope proteins were prepared in lysis buffer with and without the addition of 0.2% SDS. The addition of SDS enhanced protein extraction from the vitelline envelope. Isoelectric points were determined from samples treated with lysis buffer lacking SDS. Proteins were isoelectrically focussed for 4800 volt-hours prior to fine focussing at 800 volts for 60 minutes. The pH gradient of each IEF run was determined by placing serial 0.5 cm segments of the tube gel into 2 ml of degassed H_2O, waiting approximately 2-3 hours, and then measuring the pH. Isoelectric focussing tube gels were equilibrated in SDS-sample buffer for 60 minutes and frozen at -70° C for storage. The second dimension SDS-PAGE was performed using a 4.8-20.44% gradient gel as described in Chapter IV. Isoelectric focussing tube gels were thawed slowly and equilibrated an additional 60 minutes prior to loading onto the two-dimensional (2D) slab gel. The 2D gel was electrophoresed overnight at 90 volts, constant voltage, until the tracking dye migrated from the gel. The current was then changed to 60 mAmps, constant current, and electrophoresis continued for an additional 60 minutes. Upon completion of electrophoresis, gels were fixed and stained with Coomassie blue to visualize proteins. Alternatively, the proteins were immediately electroblotted onto nitrocellulose as described. Upon completion of electroblotting, the blots were rinsed with H_2O and dried overnight. Autoradiography was then performed on the dry blots by exposure to X-ray film (Kodak X-AR 5) for various times followed by development of the autoradiogram with GBX (Kodak) developer (219 ml/liter). The western blots were immunostained as described previously. Immunoblots and autoradiograms were analyzed by inspection to determine if corresponding protein patterns were present.

Immunoelectron Microscopy

Pieces of ovary were fixed in a variety of fixatives including 1, 2, 3, and 4% paraformaldehyde, 4% glutaraldehyde-2% paraformaldehyde (Karnovsky, 1965), 2% glutaraldehyde-2% paraformaldehyde, all in 0.1 M sodium phosphate buffer, pH 7.2, for 2 hours at 23° C. Other fixatives included 4% paraformaldehyde-0.2% glutaraldehyde (Eldred et al., 1983), a lysine-HCl fixative (McLean and Nakane, 1974), buffered glutaraldehyde-picric acid (Newman et al., 1983) and 50 mM lysine, 1% glutaraldehyde, 4% paraformaldehyde (Erdos et al., 1986). Tissues were embedded in Historesin (LKB), LR White or Epon 812. Silver and silver-gold sections were cut and mounted on nickel grids. Sections were then treated by the following general protocol. All solutions were filtered through a 0.22 um membrane prior to use and incubations were performed at 23° C on drops of the various reagents. Secions were etched by several methods including 10% H_2O_2 or saturated sodium metaperiodate (Bendayan and Zollinger, 1983), 1% NaOH in 50% ethanol (Kuhlmann and Peschke, 1982), and combinations of the above. Etched sections were rinsed in H_2O and washed 3 times with H_2O or PBS (Chapter IV) for 30 minutes. The grids were incubated on 1% bovine serum albumin in PBS for approximately 20 minutes and transferred to primary antibody supernatant containing 5% normal goat serum. Concentrations of primary antibody ranged from a 1:20 dilution to a 20-fold concentrate of hybridoma conditioned supernatant. Control sections were treated with no primary antibody or SP2/0-conditioned medium. Sections were incubated for 1-5 hours on these drops and subsequently washed for 30 minutes in PBS. Grids were then incubated with goat antimouse secondary antibody conjugated to colloidal gold (Janssen; 1:20-1:40 dilution in PBS) for 2 hours. Grids were washed an additional 20 minutes in PBS, rinsed with H_2O, and blotted dry. Sections were stained with uranyl acetate followed by lead citrate (Reynolds, 1963) if necessary. The best results were obtained using the 2% glutaraldehyde-2% paraformaldehyde fixative and 5 minute etching with 1% sodium hydroxide in 50% ethanol.

Results

Fusion Results

A total of 296 hybridoma colonies were screened for immunoreactivity. Twenty-seven colonies were positive with the vitelline envelope fragment assay, 25 colonies were positive by immunoblot analysis, and 19 colonies were positive by immunocytochemistry. A total of 6 separate hybridomas were fully cloned and subjected to further analyses. One hybridoma, designated 5D6 (an IgM), was selected for detailed analysis because of its immunoreactive characteristics.

Immunoblots

The immunoreactivity and specificity of the 5D6 monoclonal antibody was tested on western blots of extracted vitelline envelope fractions and egg homogenates from various stages of the extraction protocol (Chapter IV). Immunoblot analysis demonstrated that the 5D6 monoclonal antibody was highly specific for pipefish vitelline envelope proteins and lacked immunoreactivity to egg-yolk proteins (Fig. 73). The 5D6 antibody was reactive against both the 109 and 98kDa proteins as well as some minor vitelline envelope components. Furthermore, immunoblot analysis of peptide fragments generated by limited proteolysis indicated that there are common

Fig. 73. Specificity of the 5D6 antibody by Coomassie blue (a) and immunoblot (b) analysis of samples from the extraction protocol subjected to SDS-PAGE. Supernatant fractions from solution FO (FO SUP), H_2O (H_2O SUP) and pellet protein samples after H_2O (H_2O PELL) and 1 M NaCl (1 M NaCl PELL) washes are indicated. Both the Coomassie blue and immunoblot gel lanes contain equivalent protein samples for the respective lanes. The immunoblot was stained with the 5D6 antibody and visualized with DAB. Molecular masses are indicated on the left margin of the gels.

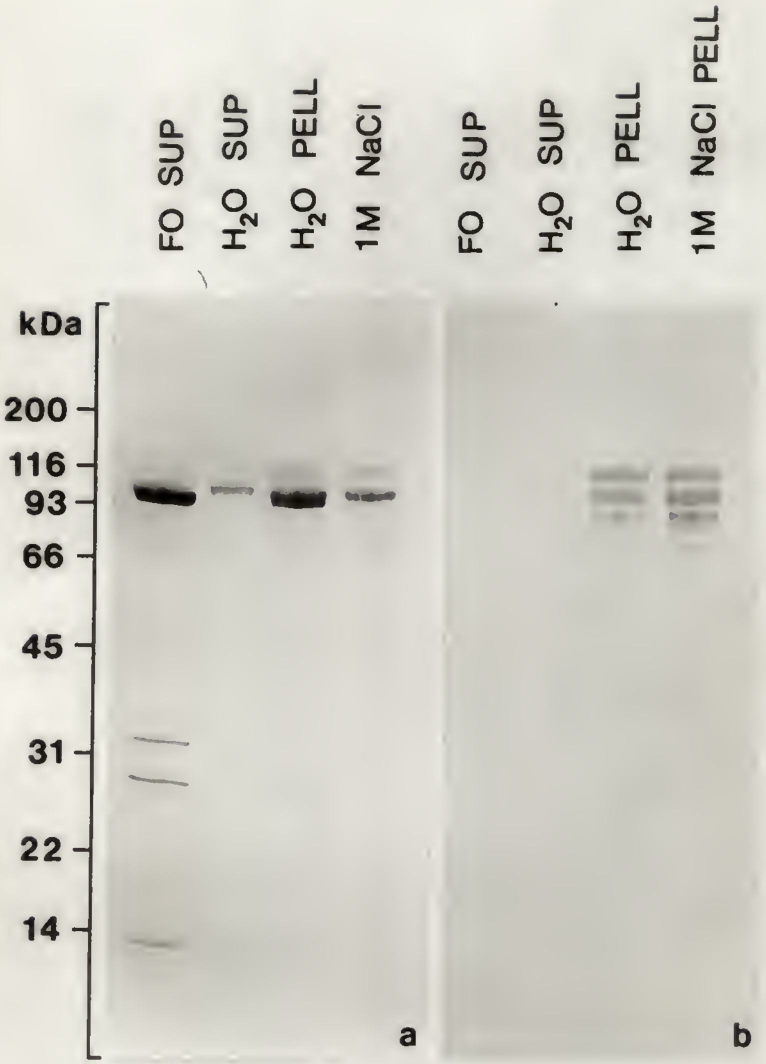
FO SUP
H2O SUP
H2O PELL
1M NaCl
FO SUP
H2O SUP
H2O PELL
1M NaCl PELL
kDa
200
116
93
66
45
31
22
14
a
b

Fig. 74. Specificity of 5D6 antibody for other pipefish protein samples subjected to SDS-PAGE. Lanes 1-5 represent Coomassie blue-stained samples of molecular weight standards (lane 1), purified pipefish vitelline envelope proteins (lane 2), female plasma (lane 3), male plasma (lane 4), and female liver (lane 5). Lanes 2^1-5^1 represent immunoblot staining with the 5D6 antibody to the corresponding protein samples as indicated on the Coomassie blue-stained lanes. Note also the female-specific vitellogenin band (arrowhead) in lane 3. Molecular masses are indicated on the left side of the gel.

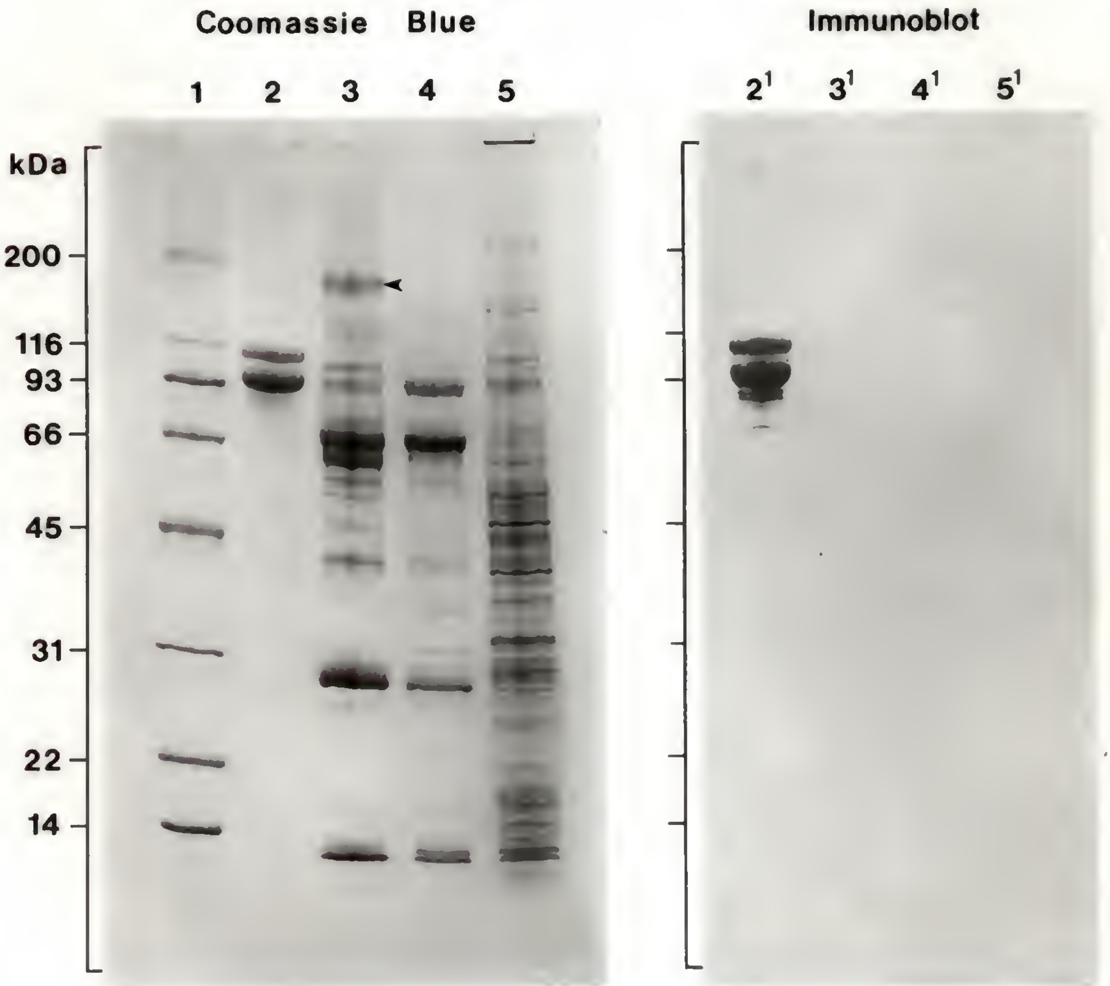
Coomassie Blue
Immunoblot
1
2
3
4
5
2¹
3¹
4¹
5¹
kDa
200
116
93
66
45
31
22
14

immunoreactive peptide fragments for both the 109 and 98kDa proteins (data not shown). The overall peptide fragment patterns, however, are different for these two proteins. The 5D6 antibody demonstrated no immunoreactivity to female plasma, male plasma, or female liver homogenate (Fig. 74).

Immunocytochemistry

The 5D6 antibody was tested for reactivity and specificity by indirect immunofluorescence on paraffin sections of ovarian tissue. This antibody was highly specific for the vitelline envelope of developing oocytes (Figs. 75, 76) as well as mature eggs (Fig. 77). The earliest detection of the 5D6 antigen appears to occur in later cortical alveoli-stage oocytes (Fig. 75) but is not apparent in the earliest cortical alveoli stage or perinucleolar stage oocytes (Fig. 75). The 5D6 antibody appears to react with the entire vitelline envelope at the resolution of the light microscope (Figs. 76, 77). Immunoreactivity was lacking within the oocyte cytoplasm, adjacent follicle cells or other ovarian structures. Control sections treated with the irrelevant 5A11 antibody (Fig. 78), SP2/0 conditioned supernatant, or no primary antibody lacked fluorescence. Immunoreactivity with the 5D6 antibody was absent in adult female liver (Fig. 79).

Phase (a) and fluorescence (b) photomicrograph pairs of developing follicles and liver immunostained with the 5D6 or 5A11 antibodies. Fluorescein-conjugated goat antimouse antibody was used to visualize localizations.

Fig. 75. Early follicle progression illustrating the developmental appearance of the 5D6 antigen. Immunoreactivity (arrow) is initially observed in later cortical alveoli-stage oocyte (O) and continues to be present in later vitellogenic oocytes (arrowheads) as well. Note the specificity of the 5D6 antibody to the vitelline envelope. x 140.

Fig. 76. Higher magnification of immunoreactivity observed in vitellogenic stage oocytes (O). A striated pattern indicates the staining of the vitelline envelope (arrows) but not the microvillar processes within the pore canals. x 540.

Fig. 77. Mature egg (E) illustrating immunoreactivity of the 5D6 antibody (arrows) to the vitelline envelope. Note also the small perinucleolar oocytes (O) that do not stain with the 5D6 antibody. x 350.

Fig. 78. Control section immunostained with the glial cell-specific, 5A11 monoclonal antibody, demonstrating the lack of nonspecific antibody reactivity. (O) Oocyte. x 350.

Fig. 79. Female liver (LIV) immunostained with the 5D6 antibody demonstrating lack of immunoreactivity. x 140.

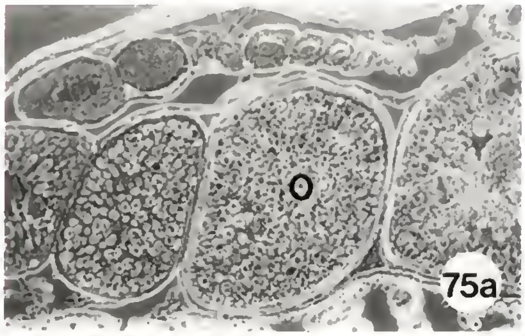
75a

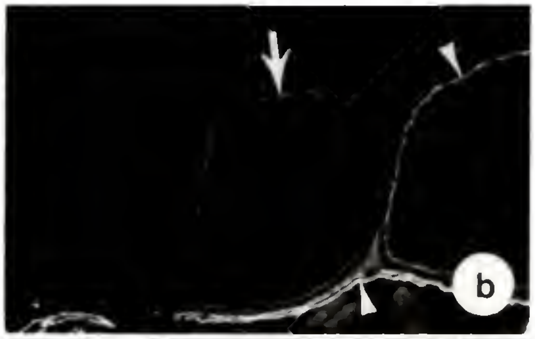
b

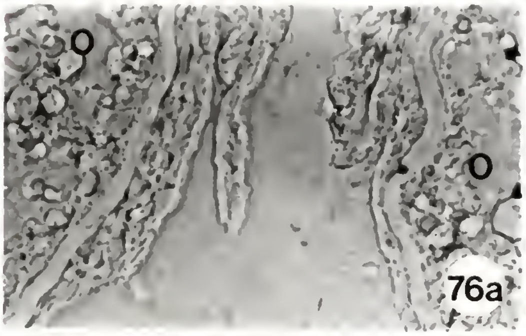
76a

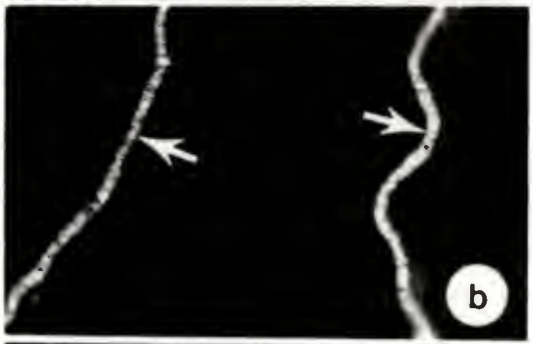
b

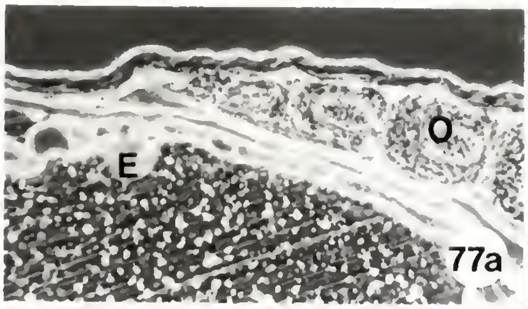
77a

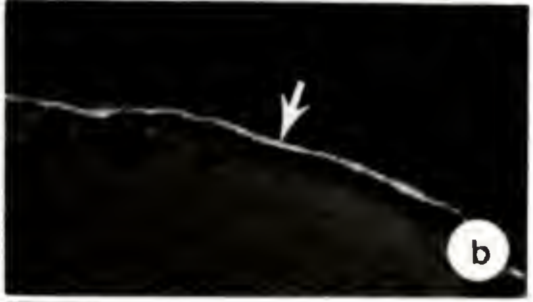
b

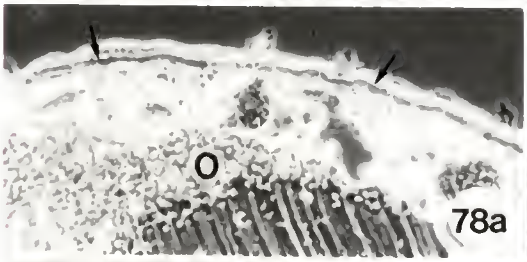
78a

b

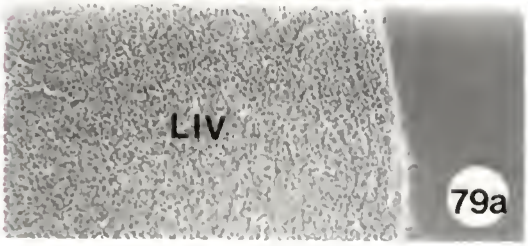
79a

b

Fig. 80. Immunogold labeling of developing vitelline envelope of a vitellogenic oocyte. Note the specificity of the 5D6 antibody to the inner Z3 layer. Note also the lack of reactivity to outer Z1 and Z2 layers (arrows) and microvillar processes within the pore canals. Oocyte (O) and follicle cell (FC) lack immunoreactivity. x 22,150.

Fig. 81. Immunogold labeling of late vitellogenic stage oocyte. Reactivity of the 5D6 antibody is confined to the Z3 layer and is lacking in the outermost Z1 layer (arrows). Note the lack of immunoreactivity to the microvillar processes (arrowheads) within the pore canals. (O) Oocyte. x 12,640.

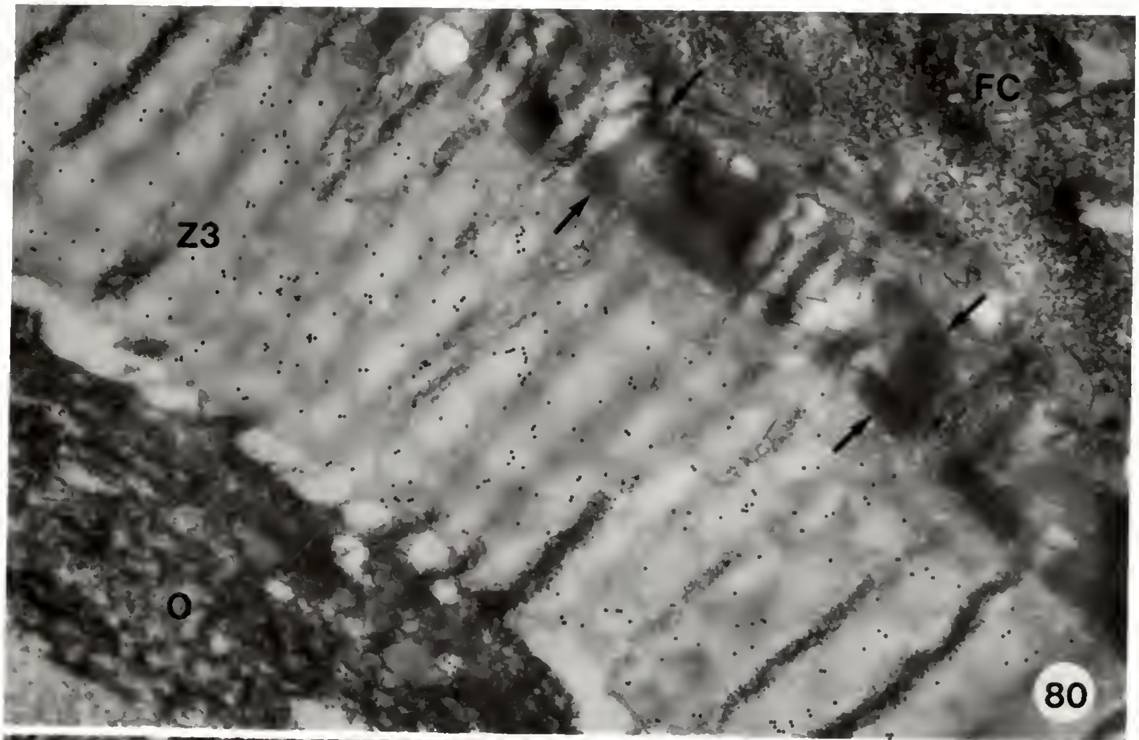
FC
Z3
O
80

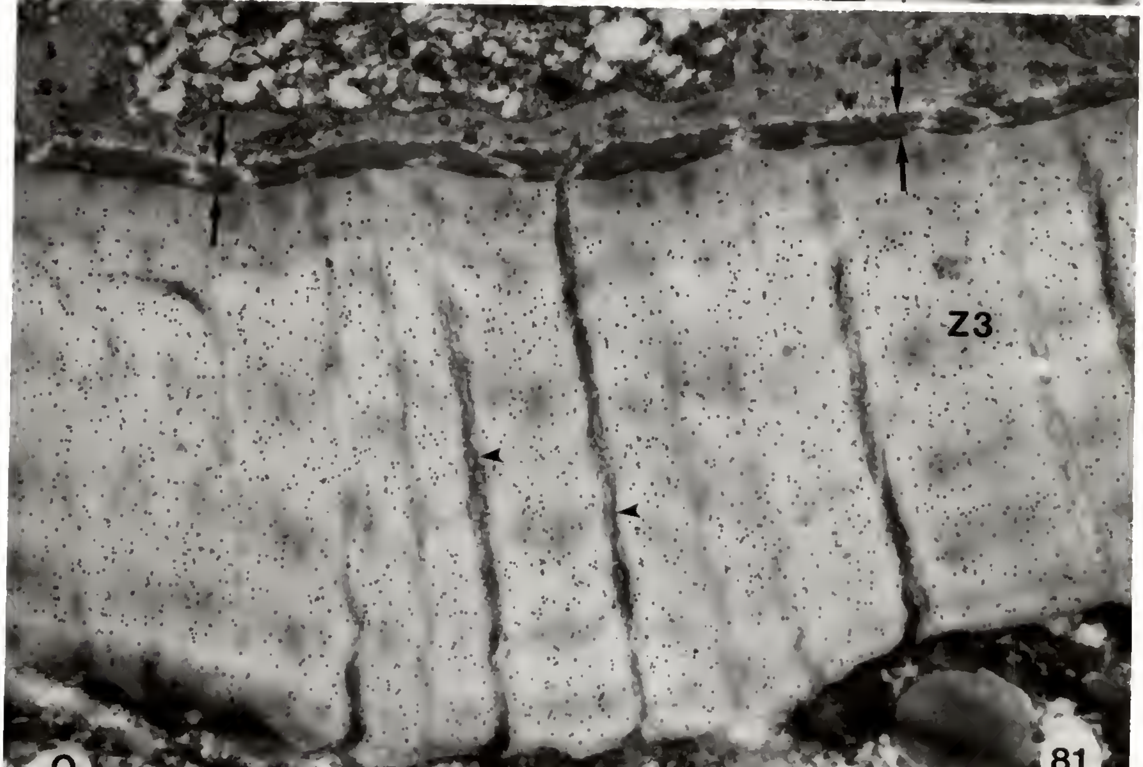
Z3
O
81

Fig. 82. Control immunogold labeling of vitellogenic stage oocyte in which SP2/0-conditioned media was substituted for the 5D6 monoclonal antibody. The lack of nonspecific staining is apparent. Only a few random gold particles nonspecifically adhere (arrowheads). x 13,600.

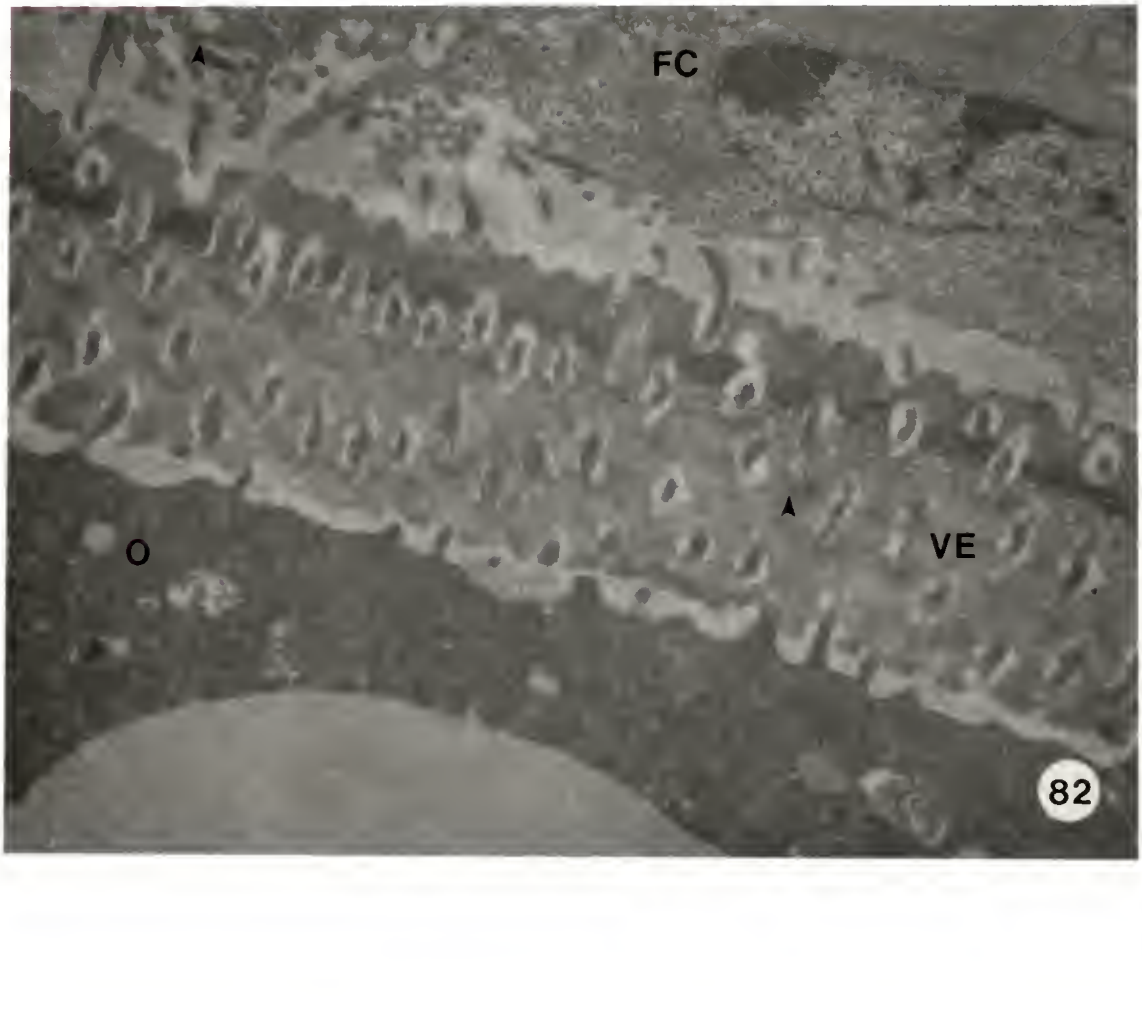
FC
O
VE
82

Immunoelectron Microscopy

The objectives for producing antibody probes to the 109 and 98kDa proteins were to understand the cellular origin of these proteins and their relationship to the structure of the vitelline envelope. Unfortunately, the cellular origin of these proteins could not be resolved at the light microscopic level. Therefore, immunoelectron microscopy studies were initiated in an attempt to localize the vitelline envelope proteins within ovarian follicles in finer detail. Immunostaining of thin sections with the 5D6 antibody revealed that the 5D6 antigen is localized to the inner Z3 layer of the vitelline envelope in developing oocytes (Figs. 80, 81). The outermost layer of the vitelline envelope, both in early (Fig. 80) and late (Fig. 81) vitellogenic oocytes did not react with the 5D6 antibody. Control sections (Fig. 82) indicated little nonspecific gold particle adsorption and confirmed the 5D6 antibody specificity. Intracellular localization of the 5D6 antigen was not definitive enough to identify cellular origin in either the oocyte or follicle cells.

Two-Dimensional Gel Electrophoresis

Two-dimensional SDS-PAGE of extracted vitelline envelope proteins indicated that the 109 and 98kDa proteins, as resolved by one-dimensional methods, are families of differentially charged molecules (Fig. 83). The 109kDa family consists of several polypeptides with

Fig. 83. Two-dimensional SDS-PAGE analysis of pipefish egg vitelline envelope proteins stained with Coomassie blue. Note the basic group of proteins comprising the 109kDa band (arrowhead) and the acidic group of proteins comprising the 98kDa family (arrow). Note also that the 98kDa family consists of a heterogeneous protein doublet. Lane A is a one-dimensional run of extracted vitelline envelope proteins. Basic (pH 7.2) and acidic (pH 5.0) ends of the IEF gel are labeled. Molecular masses are indicated on the left margin of the gel.

Fig. 84. Two-dimensional SDS-PAGE immunoblot analysis of the pipefish egg vitelline envelope proteins reacted with the 5D6 antibody. Lane A is a one-dimensional run of extracted vitelline envelope proteins. Immunolocalization was visualized with DAB. Note the immunoreactivity of the 5D6 antibody to the vitelline envelope proteins observed by Coomassie blue staining. (Arrowhead) 109kDa protein family. (Arrow) 98kDa protein family. Basic (pH 7.9) and acidic (pH 4.8) ends of IEF gel are labeled. Molecular masses are indicated on the left margin of the gel.

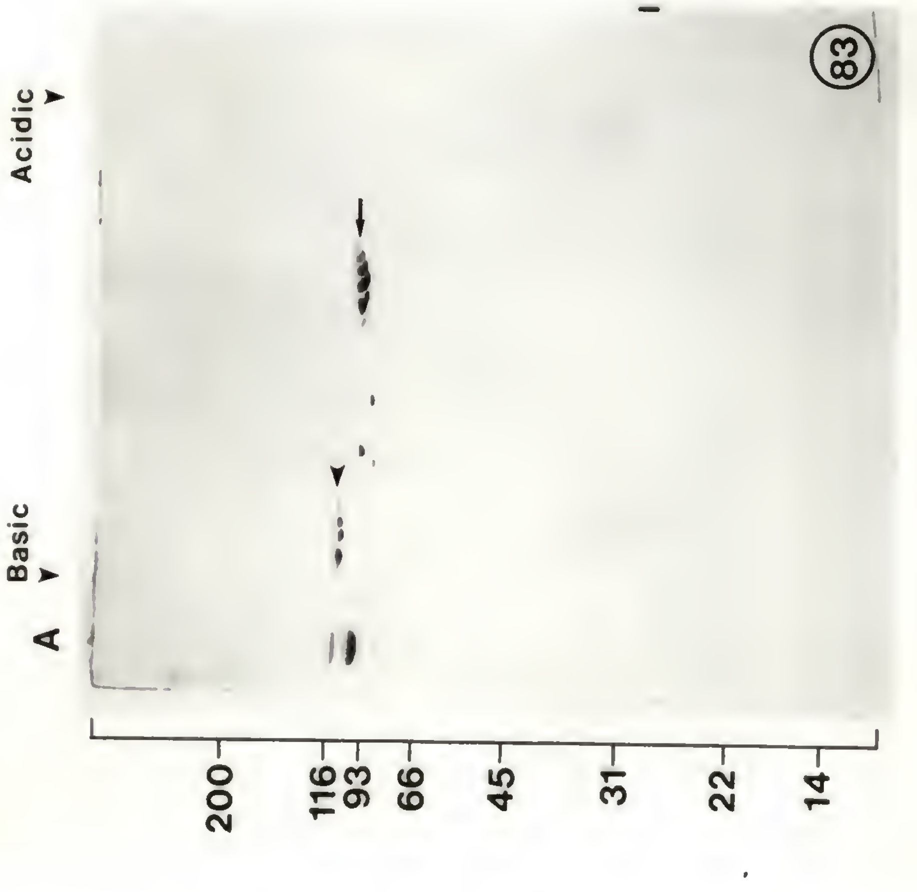

83

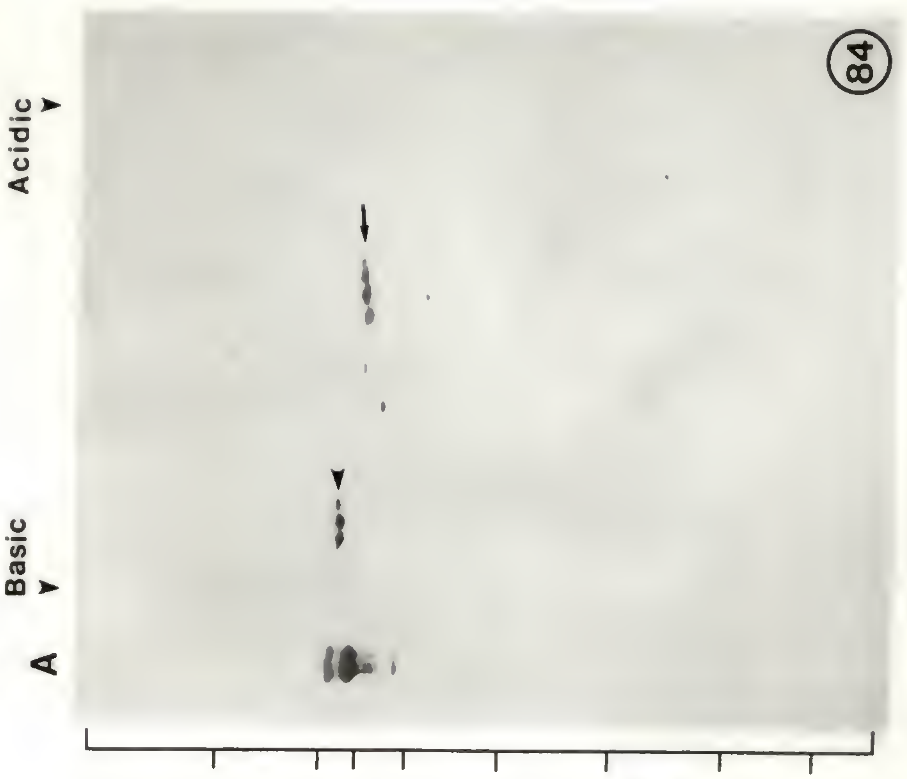

84

isoelectric points of approximately 7.2-7.5. The 98kDa group is a heterogeneous family of protein doublets having slight charge modifications, with approximate isolectric points ranging near 6.7. Immunoblot analysis of the 2D SDS-PAGE separation of vitelline envelope proteins demonstrated immunoreactivity of the 5D6 antibody to the charged species of both the 109 and 98kDa polypeptide families (Fig. 84).

Radiolabeled Protein Synthesis

The origin of the vitelline envelope proteins was not demonstrated by immunocytochemical means. Consequently, *in vitro* protein synthesis experiments using intact follicles and isolated cell populations were performed in a further attempt to define the cellular origin of the vitelline envelope proteins. The autoradiographic pattern of proteins synthesized by an intact follicle preparation is indicated in Figures 85 and 88. The immunoblot pattern of the same preparation is illustrated in Figure 86. Analysis of the autoradiogram and immunoblot demonstrate colocalization of autoradiographic spots and immunoreactive products (Figs. 85, 86) only for the major 98kDa protein family. Radiolabeled protein synthesis of the 98kDa proteins was detected in follicles ranging from 0.3-0.8 mm diameter (data not shown) indicating that synthesis of these proteins occurs throughout much of oocyte development. Immunoreactivity of the 109kDa protein family

Fig. 85. Autoradiogram of proteins synthesized by intact follicles (0.7 mm diameter). Follicles were labeled with ^{35}S-methionine as described. Note the radiolabeled proteins (arrows) of the 98kDa vitelline envelope protein family. Note also the origin of the IEF gel where a labeled band (arrowhead) is present in the 109kDa protein position. A total of 100 ug protein was subjected to 2D SDS-PAGE, the proteins electroblotted onto nitrocellulose, and autoradiography performed on the western blot. Total incorporation into protein was 152,200 cpm per follicle with 297,295 total cpm being loaded onto the IEF gel. Basic (pH 7.2) and acidic (pH 5.0) ends of the IEF gel are labeled. Molecular masses of the protein standards are indicated on the left margin of gel.

Fig. 86. Immunoblot analysis with 5D6 antibody of same western blot illustrated on Figure 85. Note the position of the 98kDa protein family (arrows). When the autoradiogram (Fig. 85) is overlayed on this immunoblot, the radiolabeled proteins indicated (Fig. 85, arrows) are precisely localized above the 98kDa vitelline envelope protein family. The slight immunoreactivity of the 109kDa proteins is indicated (arrowhead) near the origin of the IEF gel. Basic (pH 7.2) and acidic (pH 5.0) ends of the IEF gel and molecular masses of protein standards are indicated.

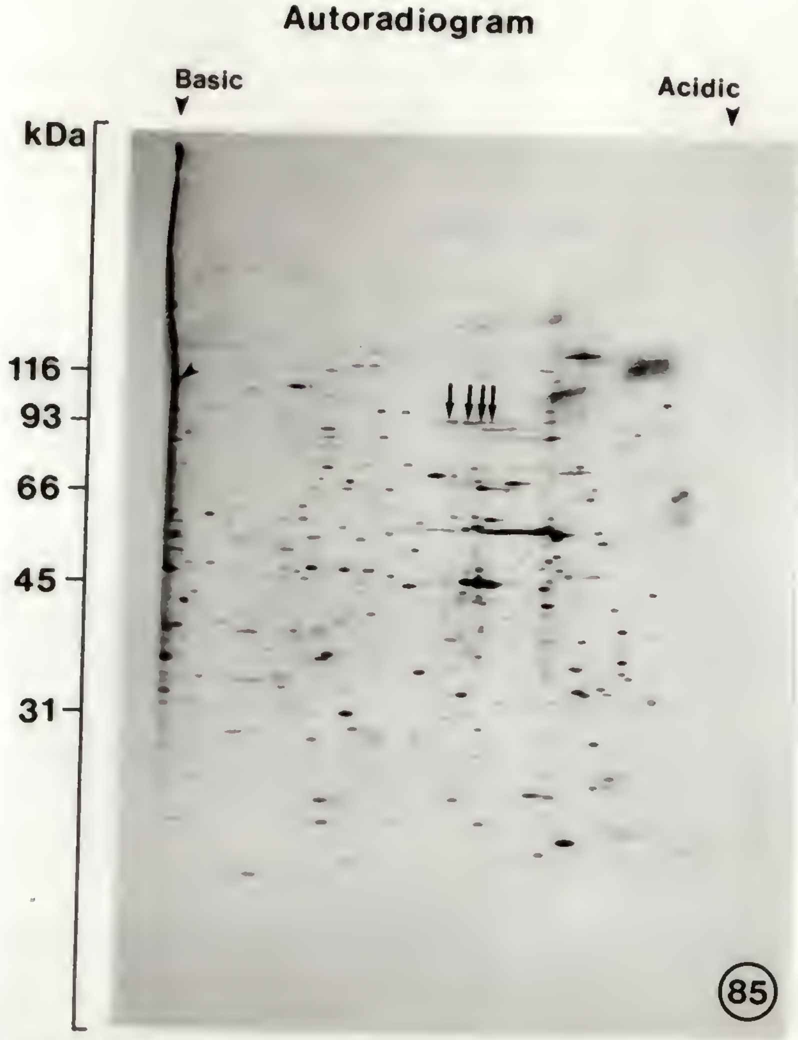
Autoradiogram
Basic
Acidic
kDa
116
93
66
45
31

85

Immunoblot
A
Basic
Acidic

86

was mostly confined to the origin of the IEF tube gel (Fig. 86). Although an autoradiographic spot can be identified at the origin, the results are not conclusive enough to indicate synthesis of the 109kDa protein family.

The protein synthetic patterns of denuded oocytes and follicle cell/theca complexes were also examined. Verification of cell dissociation was first assessed by fluorescence microscopy (Figs. 87a-f). Pure populations of denuded oocytes and follicle cell/theca complexes obtained by the dissociation procedures were radiolabeled for nascent protein synthesis. The protein synthetic pattern of a denuded oocyte preparation is illustrated in Figure 89. The denuded oocyte preparation does not appear to contain any radiolabeled proteins that comigrate with the vitelline envelope proteins identified within the intact follicle preparation (Fig. 88). The protein synthetic pattern of isolated follicle cell/theca complexes is illustrated in Figure 90. The follicle cell/theca complexes do appear to contain radiolabeled proteins (Fig. 90) in a very similar position as the 98kDa family synthesized within the intact follicle (Fig. 88). There is not, however, a precise pattern match and immunoreactive products were not readily detected by immunoblot analysis. Liver samples lack radiolabeled proteins in the appropriate position by 2D SDS-PAGE analysis and demonstrate no immunoreactivity by immunoblot analysis.

Fig. 87. Phase and fluorescence micrograph pairs of various cell-dissociation preparations. a, b) Intact follicle demonstrating complete fluorescent staining of investing cell layers by ethidium bromide. x 33. c, d) Denuded oocyte preparation showing a lack of fluorescence, indicating the removal of investing cell layers. x 32. e, f) Follicle cell lawn obtained by manual dissection of the complex from an oocyte. Note the baglike fluorescence outlined by the follicle cell lawn. x 33.

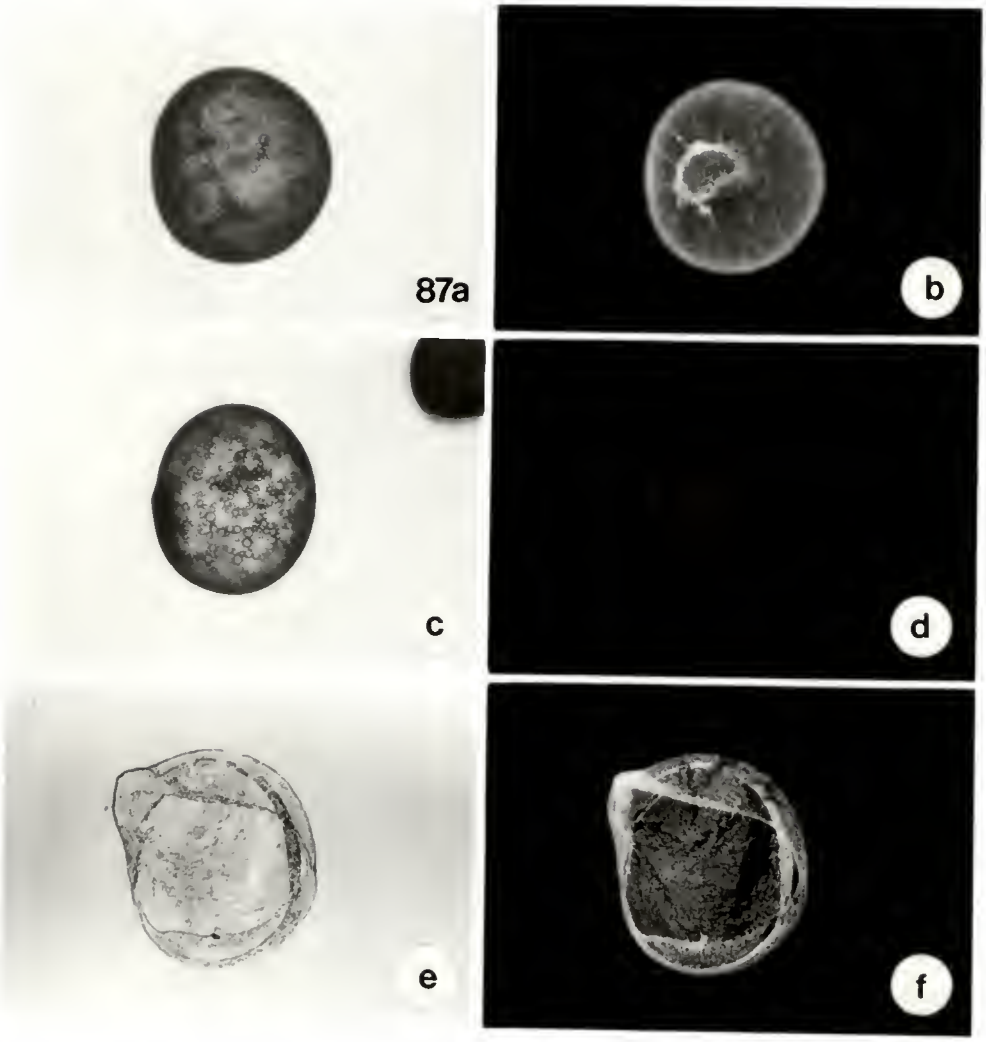
87a
b
c
d
e
f

Fig. 88. Higher resolution autoradiogram of radiolabeled proteins from intact follicles as shown in Figure 85. The 98kDa vitelline envelope protein spots are indicated (arrows). Reference proteins used for analysis of autoradiograms are indicated as spot 1, spot 2, spot 3, and spot A (actin; Bravo and Celis, 1984). Molecular masses of standards are indicated.

Fig. 89. Autoradiogram of radiolabeled proteins synthesized by 0.5 mm-denuded oocytes. Note the lack of autoradiographic spots in the region (circle) where the vitelline envelope proteins were identified in the intact follicles (Fig. 88). A total of 100 ug protein was subjected to 2D SDS-PAGE. Total protein incorporation was 66,000 cpm per oocyte, and 264,365 cpm was loaded onto the IEF gel. Basic (pH 7.2) and acidic (pH 5.0) ends of IEF gel are indicated. Reference spots 1, 2, 3, A, and molecular masses of protein standards are indicated.

Fig. 90. Autoradiogram of radiolabeled proteins synthesized by isolated follicle cell/theca complexes and labeled as described in Materials and Methods. Note the cluster of proteins (between arrowheads) in a position very similar to that observed for the 98kDa proteins in the intact follicle preparation (Fig. 88). Approximately 35 follicle cell/theca complexes were subjected to 2D SDS-PAGE. Total protein incorporation was approximately 78,900 cpm per complex, with a total of 2,760,660 cpm loaded on the IEF gel. Basic (pH 7.2) and acidic (pH 5.0) ends of IEF gel are indicated. Reference spots 1, 2, 3, A, and molecular masses of protein standards are indicated.

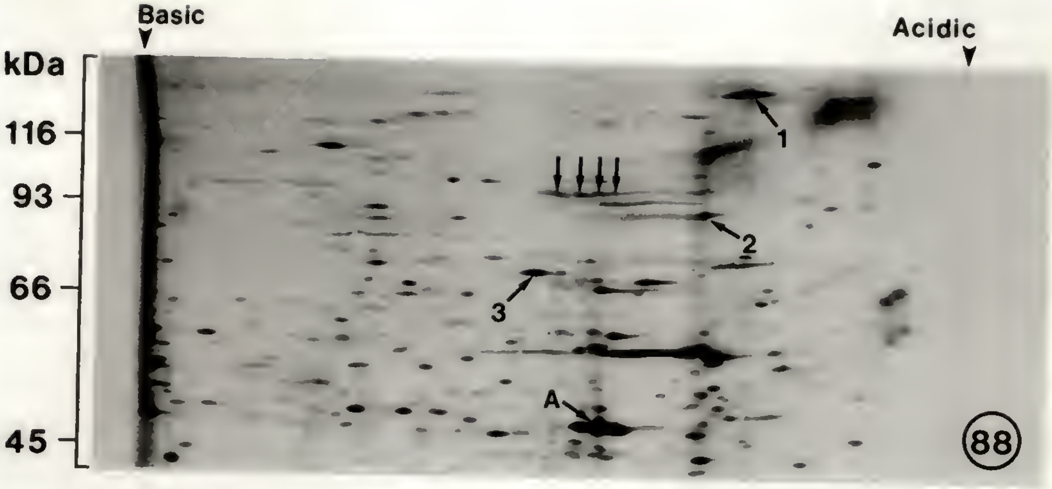
Basic
Acidic
kDa
116
93
66
45
1
2
3
A

(88)

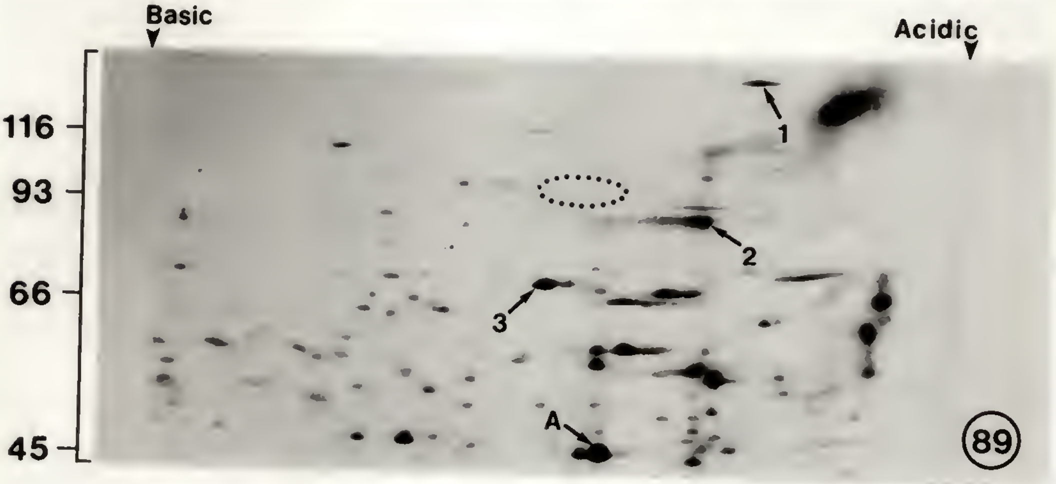
Basic
Acidic
116
93
66
45
1
2
3
A

(89)

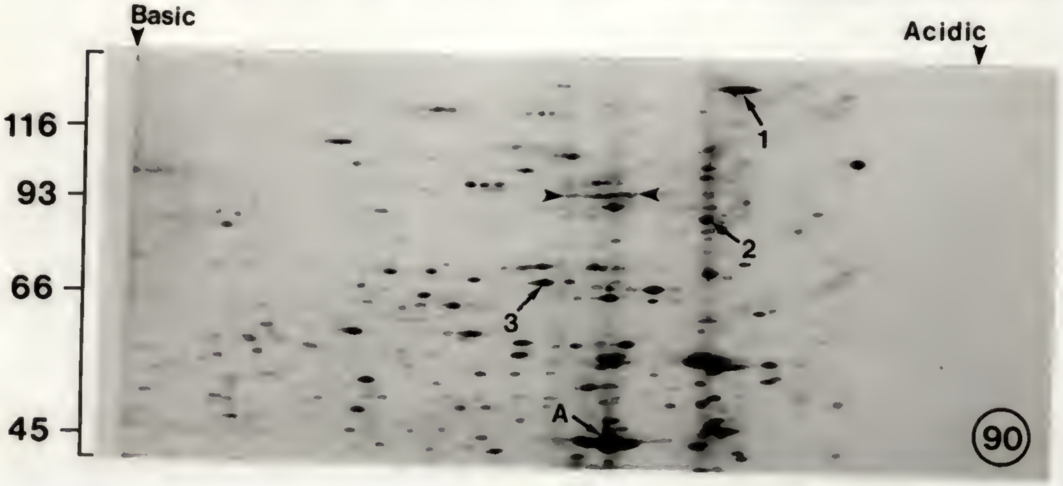
Basic
Acidic
116
93
66
45
1
2
3
A

(90)

Fig. 91. Phase (a) and fluorescence (b) photomicrograph of a *Fundulus heteroclitus* oocyte stained with the 5D6 antibody. The antibody is specific to the vitelline envelope (arrow). x 150.

Fig. 92. Phase (a) and fluorescence (b) photomicrograph of control section of *F. heteroclitus* follicle immunostained with the 5A11 monoclonal antibody. Nonspecific reactivity of this antibody to the vitelline envelope is lacking. x 370.

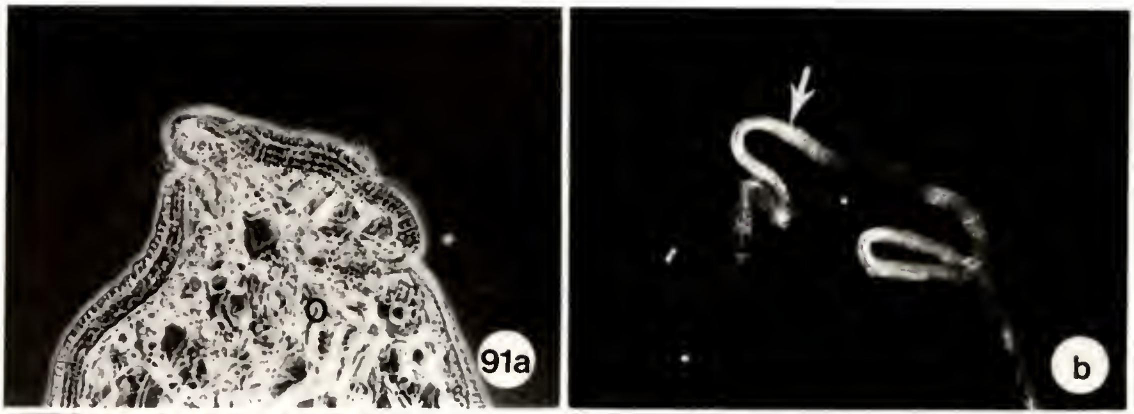
o
91a
b

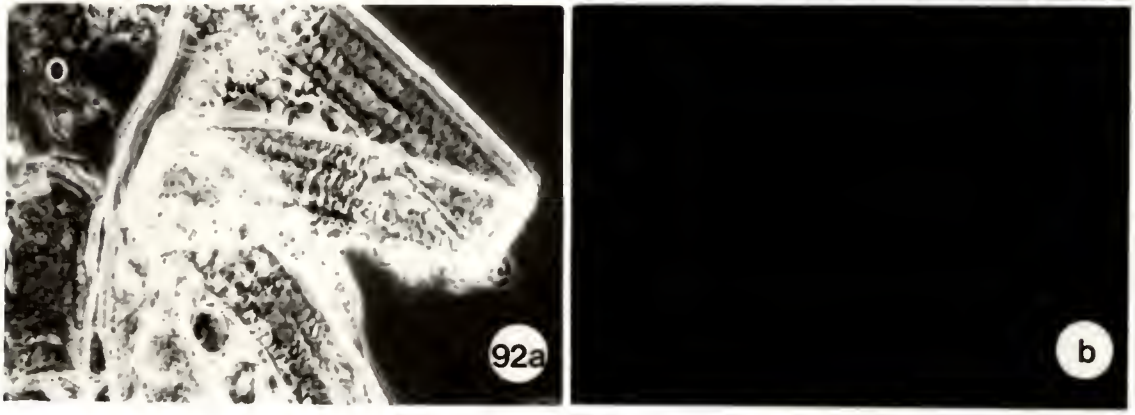
o
92a
b

Cross-Reactivity

The 5D6 antibody is immunocytochemically cross-reactive to the vitelline envelope of *Fundulus heteroclitus* oocytes (Figs. 91, 92). Furthermore, the 5D6 antibody cross-reacts to vitelline envelope proteins in an enriched *F. heteroclitus* vitelline envelope fraction by dot blot analysis (data not shown). The 5D6 antibody was also tested against the oocyte vitelline envelope of the frog *Xenopus laevis*, but no immunocytochemical cross-reactivity was observed.

Discussion

In this chapter the production of an IgM monoclonal antibody, 5D6, against pipefish vitelline envelope proteins is described. The 5D6 antibody is highly specific for the 109 and 98kDa vitelline envelope proteins by immunoblot analyses (Figs. 73, 74) and for the developing oocyte and egg vitelline envelope by immunocytochemistry (Figs. 75-78). Immunocytochemical studies have localized the 5D6 antigen within the structure of the vitelline envelope. Radiolabeling studies also demonstrate that at least the 98kDa glycoprotein family is synthesized within the ovarian follicle. This represents the first report to document synthesis of vitelline envelope proteins within a teleost follicle. These data lend experimental support to the hypothesis that teleost vitelline envelope proteins are synthesized locally by the oocyte (Anderson, 1967; Wourms, 1977; Tesoriero, 1978a) or associated follicle cells (Chaudhry, 1956).

The results presented in this chapter are contrary, however, to recent reports indicating a hepatic involvement in vitelline envelope formation in the medaka, O. latipes (Hamazaki et al., 1987a, b). In this species, the liver synthesizes a 49kDa spawning female-specific plasma protein (Hamazaki et al., 1987a) that has a similar amino acid composition and electrophoretic mobility to a 49kDa vitelline envelope protein. Polyclonal antibodies against medaka embryonic chorion protein digests cross-react to the spawning female-specific plasma protein by immunodiffusion (Hamazaki et al., 1987b) and to the female liver and vitelline envelope by immunocytochemistry (Hamazaki et al., 1985). Thus, in medaka, the available evidence suggests a hepatic contribution to the vitelline envelope, although Hamazaki et al. (1987b) speculate that the hepatically produced plasma protein may be taken up by the oocyte, processed and subsequently resecreted.

Immunofluorescence microscopy indicates that the 5D6 antigen is first detected in later cortical alveoli-stage oocytes and is retained with further oocyte development. The appearance of the 5D6 antigen correlates approximately with the initial ultrastructural appearance of the Z3 layer (Chapter III, Fig. 41). Further analysis with immunoelectron microscopy localized the 5D6 antigen only to the innermost Z3 layer of the vitelline envelope. Localization of the 5D6 antigen specifically to the Z3 layer is also supported by the absence of immunofluorescence and immunogold staining to the Z1 layer in the earliest cortical alveoli-stage oocytes. Therefore, one conclusion drawn from these studies is that the 109 and 98kDa proteins are the major consituents of the inner Z3 layer of the pipefish vitelline envelope. This conclusion further indicates that the inner Z3 layer is biochemically distinct from the outer Z1 layer.

The results of the protein synthesis experiments presented in this chapter clearly demonstrate that at least the 98kDa glycoprotein family is synthesized within the pipefish ovarian follicle. The denuded oocytes do not appear to express these proteins under the current experimental conditions. The isolated follicle cell/theca complexes synthesize a group of proteins that migrate electrophoretically very similarly to the 98kDa family. Based upon these results, the follicle cells should be considered as a possible source of the 98kDa proteins. However, it is premature to ascribe any specific cell as being the synthetic source of the vitelline envelope proteins. The inability of either the denuded oocytes or follicle cell/theca complexes to clearly synthesize the vitelline envelope proteins could be a consequence of the cell dissociation procedures used. This appears to be unlikely, however, because complex protein patterns were obtained for both denuded oocyte and follicle cell/ theca complex preparations. Alternatively, the cell association between the oocyte and follicle cells may be necessary for the expression of certain cell-specific proteins. Examples of cell contact-mediated regulation of protein synthesis between oocyte and follicle cells have been previously documented both qualitatively (Osborn and Moor, 1982; Moor, 1983) and quantitatively (Wallace et al., 1981; Wasserman et al., 1986). One final explanation for the lack of radiolabeled proteins in the denuded oocyte preparation would be that the oocyte could synthesize the proteins, followed by rapid secretion into the culture medium where the proteins would not be detected.

The relationship of the pipefish egg vitelline envelope proteins to the medaka vitelline envelope proteins is not known. The cross-reactivity of the 5D6 antibody to the _F. heteroclitus_ vitelline envelopes, however, warrants further comparative studies. The 5D6 antibody shows no immunoreactivity to the pipefish liver or female plasma proteins (Fig. 74), and thus is different from the medaka. Considering that synthesis of the 98kDa proteins occurs within the intact pipefish follicle, hepatic involvement in the synthesis of these vitelline envelope components is unlikely. Consequently, there is now experimental evidence for two different teleosts that provides conflicting data as to the cellular origin of the vitelline envelope in teleosts. It is possible that there are, indeed, different mechanisms for vitelline envelope formation among different species of fish. This appears to be the case among mammals because recent reports suggest that the rabbit zona pellucida is synthesized by not only the oocyte but also the follicle cells (Wolgemuth et al., 1984), contrary to the findings in the mouse where the zona pellucida proteins are synthesized exclusively by the oocyte (Bleil and Wasserman, 1980b).

The relationship of the 98kDa family to the 109kDa family is not completely understood. These two proteins are different in many respects including electrophoretic mobility, PAS staining, peptide cleavage patterns, heterogeneity of the protein families, and isoelectric points. The charge differences of the 98kDa glycoprotein family are probably the result of differential posttranslational glycosylation of the proteins as carbohydrate heterogeneity is known to affect isoelectric mobility (Dunbar, 1987). The heterogeneity of the 109kDa family may be due to phosphorylation or sulphation which also affects protein charge (Dunbar, 1987). The 109 and 98kDa proteins, however, do share some common epitope that is recognized by the 5D6 antibody (Fig. 73), although the overall peptide fragment patterns between the two proteins are still different. Whether a precursor-product relationship exists between these two proteins remains uncertain as there is insufficient data to evaluate this possibility at this time .

There are many unresolved questions remaining concerning the pipefish vitelline envelope and teleost vitelline envelopes in general. These studies have established that the pipefish 109 and 98kDa proteins are constituents of the inner Z3 layer of the vitelline envelope. Furthermore, at least the 98kDa protein family is synthesized within the ovarian follicle. Identification of the cell(s) responsible for synthesis of the vitelline envelope proteins within the ovarian follicle of the pipefish will require further experimentation. The modifications, if any, which the vitelline envelope proteins undergo extracellularly during compaction and expansion of the vitelline envelope also remain to be discerned. Nevertheless, a molecular probe has been generated that should prove to be valuable for understanding the assembly of the vitelline envelope and the synthetic initiation of the 109 and 98kDa proteins during oocyte development. The expression of these proteins and elaboration of the vitelline envelope as a developmentally regulated event during pipefish oocyte development awaits further investigation.

CHAPTER VI
SUMMARY AND FUTURE DIRECTIONS

These studies have documented the morphological features of the pipefish ovary, the cytological changes oogonia and oocytes undergo during their formative and development stages, and some biochemical properties of the egg vitelline envelope. These analyses have addressed several levels of ovarian organization including the organ level (Chapter II), the cellular level (Chapter III) and the molecular level (Chapters IV, V) in S. scovelli. The results presented lay the necessary framework for additional study of this atypical vertebrate ovary and establish the usefulness of the pipefish as a model system for studying specific questions concerning oogenesis and oocyte development.

The organization of the ovary was elaborated in Chapter II and demonstrates the practicality of studying oocyte development in this species. Specifically, the spatial organization of follicle development provides a better understanding of how folliculogensis occurs. Follicle formation occurs in a specific region of the ovary, the germinal ridge. Primordial follicles form within and bud off of this germinal ridge to become definitive follicles. Consequently, the cellular associations that exist during folliculogenesis are readily accessible for observation and experimental manipulation. The temporal events of early oocyte growth are also spatially related within the ovary. Another distinguishing feature of oocyte development in the pipefish is the apparent polarization of later stage oocytes in relation to ovarian anatomy. The acquisition of egg polarity is poorly understood (Gerhart et al., 1986), yet this polarity is basis of axis formation in the embryo for many organisms (Raven, 1961). Inquiry as to how polarity is attained during oocyte development in the pipefish warrants further investigation. The anatomical relationships observed in the pipefish ovary may provide some insight into this important developmental question.

The cytology of developing oogonia and oocytes in relation to the ovarian anatomy were documented in Chapter III. The results presented indicate that many basic processes occurring during oocyte development, such as the elaboration of cortical alveoli, vitellogenesis, and oocyte maturation are similar to other teleost species. These studies also indicate that certain processes, including oogonial proliferation and the initiation of vitellogenesis, may be advantageously studied in the pipefish. The results of Chapter III identify morphological features of oogonia and early meiotic oocytes and establish the germinal ridge as the proliferative germinal segment of the ovary. Preliminary experiments indicate that ^{3}H-thymidine incorporation into germ cells can occur up to 10 days after being placed in culture. The relationship of these in vitro observations to in vivo phenomena with respect to controlling mechanisms remain to be discerned. Investigation of the controlling mechanisms of oogonial proliferation may potentially prove to be one of the most experimentally unique aspects of the pipefish ovary. The ability to isolate and culture the germinal ridge should thus allow further dissection of the controlling mechanisms of oogonial proliferation. The present studies have set the stage for these experiments by understanding both the cellular relationships that exist in the germinal ridge and how the process of folliculogensis occurs.

The possible role of multivesicular bodies, present in the perinucleolar through early vitellogenic oocytes, in vitellogenesis is another potentially good area for future study. Data presented in Chapter III using the yolk-specific, highly electron-dense inclusion to follow early yolk-sphere formation suggests a possible relationship between forming yolk spheres and multivesicular-like structures. The data presented do not prove this relationship, but the preliminary results are consistent with the notion of lysosomal involvement in vitellogenesis (Pasteels, 1973; Wallace, 1985). Further study of early yolk formation using the yolk-specific marker, perhaps combined with immunological and radiolabeling studies, may help to understand how vitellogenesis, a major event in oocyte development, is initiated.

The process of lipogenesis may also be a worthwhile area for future investigation. The lipid in pipefish oocytes possesses its own vital staining, which may prove useful in the isolation of this material for further analysis.

The biochemical properties of the vitelline envelope were the final, specific problem during oocyte development examined in some detail. The vitelline envelope initially appears in the cortical alveoli-stage oocytes. The studies in Chapters IV and V identified two major protein families present within the vitelline envelope, one of 109kDa and the other, a glycoprotein, of 98kDa. These protein families are major constituents of the inner Z3 layer as demonstrated by immunoelectron microscopy and do not appear to be present within the outer Z1 layer. The outer Z1 layer is biochemically and morphologically distinct from the Z3 layer based on carbohydrate- and WGA-staining properties. At least the 98kDa protein family is synthesized within the ovarian follicle, as demonstrated by radiolabeled amino acid incorporation. Additional data presented do not indicate any involvement of the liver in providing precursor material for the formation of the vitelline envelope in the pipefish. Additional experimentation and use of the monoclonal antibody probes generated against the pipefish vitelline envelope proteins should identify more precisely the cellular origin of the pipefish vitelline evelope. Furthermore, the relationship between the 109 and 98kDa protein families requires additional analysis to understand how these proteins are organized in the contruction of this important extracellular matrix.

The mechanism of vitelline envelope formation in the pipefish appears to be different from that observed in the medaka (Hamazaki et al., 1987a, b) where the liver has been implicated as participating in vitelline envelope formation. The disparate results between the pipefish and medaka suggest that different mechanisms of vitelline envelope formation may exist for different teleost species. While the results from my research project would be consistent with the concept of oocyte origin of the vitelline envelope (Anderson, 1967; Tesoriero, 1978; Dumont and Brummett, 1985), follicle-cell involvement cannot be excluded at this time. Therefore, taken together, the pipefish results and the results obtained for medaka (Hamazaki et al., 1987a, b) raise additional questions regarding the cellular origin of teleost vitelline envelopes in general. Whether there are indeed multiple mechanisms in teleosts for synthesis and elaboration of the vitelline envelope remains to be explored.

Germ cells are one of the most remarkable cell types because of their universal capacity for self perpetuation, thereby being immortal. These amazing cells have the unique ability to undergo several states of differentiation. Germ cells have the capacity to alter their phenotype, both in terms of their biochemical synthetic capacity as well as their morphological characteristics, depending upon the differentiation state that the cell possesses. In the female, the circular cycle of differentiation may begin with an oogonium which transforms into an oocyte, ultimately giving rise to a mature egg. The mature egg, upon fertilization, divides into embryonic blastomeres, a population of which segregates to become primordial germ cells that will populate the developing gonad. Here the primordial germ cells become oogonia (or spermatogonia) to start the cycle all over again. The interest in germ cells probably lies in part in working with an immortal cell line, which is different in a sense, from immortal cell lines such as tumor cell lines. The developmental program of the female germ cell cycle remains intact, with this program being turned on and off at the appropriate time. Undoubtedly, there are multiple internal and external mechanisms for controlling these processes.

Much of the programming or setting the stage for successful embryonic development occurs during oocyte development. Thus, it is imperative to understand the developmental events occurring during oocyte development in order to fully appreciate the processes that occur during embryogenesis. The study of oogenesis and oocyte development remains very much linked to the fascinating question: How does a single cell give rise to the multiple cell and tissue types seen in the adult organism while still retaining its own cellular autonomy? The observations and experiments presented here provide a solid foundation for future research of especially the earliest periods of oogenesis and oocyte development in the pipefish, _S. scovelli._ The study of egg formation in this teleost will hopefully provide further insight into this complicated question.

REFERENCES

Abraham, M., V. Hilge, S. Lison, H. Tibika, and A. Rahamim (1982) The envelope cells of the oocytes and the pathway of intravenously injected HRP in the teleostean ovary. Gen. Comp. Endocrinol. 46:390-391.

Abraham, M., V. Hilge, S. Lison, and H. Tibika (1984) The cellular envelope of the oocytes in teleosts. Cell Tissue Res. 235:403-410.

Albertini, D.F. (1984) Novel morphological approaches for the study of oocyte maturation. Biol. Reprod. 30:13-28.

Allison, A.C., and M.R. Young (1969) Vital staining and fluorescence microscopy of lysosomes. In J.T. Dingle and H.B. Fell (eds): Lysosomes in Biology and Pathology. Vol. 2. Amsterdam: North Holland Publishing Co., pp. 600-628.

Al-Mukhtar, K.A.K., and A. Webb (1971) An ultrastructural study of primordial germ cells, oogonia and early oocytes in Xenopus laevis. J. Embryol. Exp. Morphol. 26:195-217.

Anderson, E. (1967) The formation of the primary envelope during oocyte differentiation in teleosts. J. Cell Biol. 35:193-212.

Anderson, E. (1968) Cortical alveoli formation and vitellogenesis during oocyte differentiation in the pipefish, Syngnathus fuscus, and the killifish, Fundulus heteroclitus. J. Morphol. 125:23-60.

Azevedo, C. (1974) Evolution des envelopes ovocytaires, au cours de l'ovogenese, chez un teleosteen vivipare, Xiphophorus helleri. J. Microscop. 21:43-54.

Back, J.F., J.M. Bain, D.V. Vadehra, and R.W. Burley (1982) Proteins of the outer layer of the vitelline membrane of the hen's eggs. Biochim. Biophys. Acta 705:12-19.

Barr, W.A. (1963) The endocrine control of sexual cycle in the plaice, Pleuronectes platessa. I. Cyclical changes in the normal ovary. Gen. Comp. Endocrinol. 3:197-204.

Bayer, R.D. (1980) Size, seasonality, and sex ratios of the bay pipefish (*Syngnathus leptorhynchus*) in Oregon. Northwest Science 54:161-167.

Begovac, P.C., and R.A. Wallace (1986) Vitelline envelope proteins in the pipefish. J. Cell Biol. 103(5):369a.

Begovac, P.C., and R.A. Wallace (1987) Ovary of the pipefish, *Syngnathus scovelli*. J. Morphol. 193:117-133.

Bendayan, M., and M. Zollinger (1983) Ultrastructural localization of antigenic sites on osmium-fixed tissues applying the protein-A gold technique. J. Histochem. Cytochem. 31:101-109.

Berglund, A., G. Rosenqvist, and I. Svensson (1986) Mate choice, fecundity and sexual dimorphism in two pipefish species (Syngnathidae). Behav. Ecol. Sociobiol. 19:301-307.

Bers, G., and D. Garfin (1985) Protein and nucleic acid blotting and immunobiochemical detection. Biotech. 3:276-288.

Biggers, J.D., and A.W. Schuetz (eds) (1972) Oogenesis. Baltimore: University Park Press, pp. 1-543.

Bleil, J.D., and P.M. Wasserman (1980a) Structure and function of the zona pellucida: Identification and characterization of the proteins of the mouse oocyte's zona pellucida. Develop. Biol. 76:185-203.

Bleil, J.D., and P.M. Wasserman (1980b) Synthesis of zona pellucida proteins by denuded and follicle-enclosed mouse oocytes during *in vitro* culture. Proc. Natl. Acad. Sci. USA. 77:1029-1033.

Bohlke, J.E., and C.C.G. Chaplin (1970) Fishes of the Bahamas and adjacent tropical waters. Wynnewood, PA: Livingston Publishing Co., pp. 176-197.

Bousquet, D., M.C. Leveille, K.D. Roberts, A. Chapdelaine, and G. Bleau (1981) The cellular localization of the zona pellucida antigen in the human and hamster. J. Exp. Zool. 215:215-218.

Braekevelt, C.R., and D.B. McMillan (1967) Cyclic changes in the ovary of the brook stickleback *Eucalia inconstans* (Kirtland). J. Morphol. 123:373-396.

Bravo, R., and J.E. Celis (1984) Catalog of HeLa cell proteins. In J.E. Celis and R. Bravo (eds): Two-Dimensional Gel Electrophoresis of Proteins. Methods and Applications. Orlando: Academic Press, Inc., pp. 445-476.

Briggs, P.T. (1975) Shore-zone fishes of the vicinity of Fire Island inlet, Great South Bay, New York. N. Y. Fish Game J. 22:1-12.

Browder, L.W. (ed) (1985) Developmental Biology. Volume 1, A Comprehensive Synthesis. Oogenesis. New York: Plenum Publishing Co., pp. 1-617.

Brown, J.D. (1972) A comparative life history of four species of pipefishes (Family Syngnathidae) in Florida. Ph.D. Dissertation, University of Florida.

Brummett, A.R., J.N. Dumont, and J.R. Larkin (1982) The ovary of Fundulus heteroclitus. J. Morphol. 173:1-16.

Brusle, S. (1980) Fine structure of early previtellogenic oocytes in Mugil (Liza) auratus Risso, 1810 (Teleostei, Mugilidae). Cell Tiss. Res. 207:123-140.

Brusle, S., and J. Brusle (1978) An ultrastructural study of early germ cells in Mugil (Liza) auratus Risso, 1810 (Teleostei: Mugilidae). Ann. Biol. Anim. Bioch. Biophys. 18:871-875.

Bullough, W.S. (1942) Gametogenesis and some endocrine factors affecting it in the adult minnow (Phoxinus laevis L.). J. Endocrinol. 3:211-219.

Busson-Mabillot, S. (1973) Evolution des envelopes de l'ovocyte et de l'oeuf chez un poisson teleostean. J. Microscop. 18:23-44.

Busson-Mabillot, S. (1984) Endosomes transfer yolk proteins to lysosomes in the vitellogenic oocyte of the trout. Biol. Cell. 51:53-66.

Chaudhry, H.S. (1956) The origin and structure of the zona pellucida in the ovarian eggs of teleosts. Z. Zellforsch. 43:478-485.

Cleveland, D., S.G. Fisher, M.W. Kirshnir, and U.K. Laemmli (1977) Peptide mapping by limited proteolysis in sodium dodecyl sulfate and analysis by gel electrophoresis. J. Biol. Chem. 252:1102-1106.

Coggins, L.W. (1973) An ultrastructural and radiographic study of early oogenesis in the toad Xenopus laevis. J. Cell. Sci. 12:71-93.

Coggins, L.W., and J.G. Gall. (1972) The timing of meiosis and DNA synthesis during early oogenesis in the toad Xenopus laevis. J. Cell Biol. 52:569-576.

Cotelli, F., F. Andronico, R. Bassi, M. Brivio, C. Ceccagno, S. Denis-Donini, M.L. La Rosa, and C.L. Lamia Donin (1986) Studies on the composition, structure and differentiation of the fish egg chorion. Cell Biol. Internat. Rep. 10:471.

Cunningham, J.T. (1898) On the histology of the ovary and of the ovarian ova in certain marine fishes. Quart. J. Microscop. Sci. 40:101-163.

Dadzie, S., and M. Hyder (1976) Compensatory hypertrophy of the remaining ovary and the effects of methallibure in the unilaterally ovariectomized Tilapia aurea. Gen. Comp. Endocrinol. 29:433-440.

Dawson, C.E. (1970) A Mississippi population of the opossum pipefish, Oostethus lineatus (Syngnathidae) Copeia 1970(4):772-771.

Dawson, C.E. (1972) Nektonic pipefishes (Syngnathidae) from the Gulf of Mexico off Mississippi. Copeia 1972(4):844-848.

Dawson, C.E. (1977) Synopsis of Syngnathine pipefishes usually referred to the genus Chthyocampus with description of new genera and species. Bull. Mar. Sci. 27:595-650.

Dawson, C.E. (1981) Notes on 4 pipefishes Syngnathidae from the Persian Gulf. Copeia 1981(1):87-95.

Dawson, C.E. (1984) Bulbonaricus Pisces Syngnathidae. A senior synonym of Enchelyocampus with description of Bulbonaricus brucei new species from eastern Africa. Copeia 1984(3):565-571.

Dawson, C.E., and J.E. Randall (1975) Notes on Indo Pacific pipefishes Syngnathidae with description of 2 new species. Proc. Biol. Soc. Wash. 88:263-280.

Dodd, J.M. (1977) The structure of the ovary of nonmammalian vertebrates. In S. Zuckerman and B. Weir (eds): The Ovary. 2nd ed. Vol. I, General Aspects. New York: Academic Press, pp. 219-263.

Dubray, G., and G. Bezard (1982) A highly sensitive periodic acid-silver stain for 1,2-diol groups of glycoproteins and polysaccharides in polyacrylamide gels. Anal. Biochem. 119:325-329.

Dumont, J.N. (1978) Oogenesis in Xenopus laevis (Daudin) VI. The route of injected tracer transport in the follicle and developing oocyte. J. Exp. Zool. 204:193-208.

Dumont, J.N., and A.R. Brummet (1980) The vitelline envelope, chorion, and micropyle of Fundulus heteroclitus eggs. Gamete Res. 3:25-44.

Dumont, J.N., and A.R. Brummett (1985) Egg envelopes in vertebrates. In L. W. Browder (ed): Developmental Biology. Vol. I, Oogenesis. New York: Plenum Press, pp. 235-288.

Dunbar, B.S. (1987) Two Dimensional Electrophoresis and Immunological Techniques. New York: Plenum Press, pp. 77-102.

Dunbar, B.S., N.J. Wardrip, and J.L. Hedrick (1980) Isolation, physiochemical properties, and macromolecular composition of zona pellucida from porcine oocytes. Biochem. 19:356-365.

Eddy, E.M. (1975) Germ plasm and the differentiation of the germ cell line. Internat. Rev. Cytol. 43:229-280.

Eldred, W.D., C. Zucker, H.J. Karten, and S. Yazulla (1983) Comparison of fixation and penetration enhancement techniques for use in ultrastructural immunocytochemistry. J. Histochem. Cytochem. 31:285-292.

Ellinwood, W.E., T.M. Nett, and G.D. Niswender (1978) Ovarian vasculature. In R.E. Jones (ed): The Vertebrate Ovary: Comparative Biology and Evolution. New York: Plenum Press, pp. 583-614.

Erdos, G.W., C.M. West, J.F. Finelli, and R.W. Davis (1986) Enhancement of morphology and determination of the carbohydrate epitopes using EM immunocytochemistry. J. Cell Biol. 103:516a.

Fargnoli, J., and G.L. Waring (1982) Identification of vitelline membrane proteins in Drosophila melanogaster. Develop. Biol. 92:306-314.

Flegler, C. (1977) Electron microscopic studies on the development of the chorion of the viviparous teleost Dermogenys pusillus (Hemirhamphidae) Cell Tiss. Res. 179:255-270.

Flugel, H. (1967a) Elektronenmikroskopische Untersuchungen an den Hullen der Oozyten und Eier des Flussbarsches Perca fluviatilis. Z. Zellforsch. 77:244-256.

Flugel, H. (1967b) Licht- und elektronenmikroskopische Uuntersuchungen an Oozyten und Eiern einiger Knochenfische. Z. Zellforsch. 83:82-116.

Fritzsche, R.A. (1980) Revision of the eastern Pacific Syngnathidae (Pisces: Syngnathiformes), including both recent and fossil forms. Proc. Calif. Acad. Sci. 42:181-227.

Fritzsche, R.A. (1984) Gasterosteiformes: Development and relationships. In H.G Moser, W.J. Richards, D.M. Cohen, M.P. Fahay, A.W. Kendall, Jr., and S.L. Richardson (eds): Ontogeny and Systematics of Fishes. Lawrence, KS: Allen Press Inc., pp. 400-405.

Gerhart, J., M. Danilchik, J. Roberts, B. Browning, and J.-P. Vincent (1986) Primary and secondary polarity of the amphibian oocyte and egg. In J.G. Gall (ed): Gametogenesis and the Early Embryo. New York: Alan R. Liss, Inc., pp.305-319.

Gilmore, R.G. (1977) Notes on the opossum pipefish, Oostethus lineatus, from the Indian River lagoon and vicinity, Florida. Copeia 1977(4):781-783.

Glabe, C.G., and V.D. Vacquier (1977) Isolation and characterization of the vitelline layer of sea urchin eggs. J. Cell Biol. 75:410-421.

Goetz, F.W. (1983) Hormonal control of oocyte final maturation and ovulation in fishes. In W.S. Hoar, D.J. Randall, and E.M. Donaldson (eds.): Fish Physiology. Volume IX, Reproduction, Part B. New York: Academic Press, pp. 117-170.

Goldstein, I.J., and R.D. Poretz (1986) Isolation, physicochemical characterization, and carbohydrate-binding specificity of lectins. In I.E. Liener, N. Sharon, and I.J. Goldstein (eds): The Lectins. Properties, Functions and Applications in Biology and Medicine. Orlando: Academic Press, pp. 33-214.

Greeley, M.S., P.C. Begovac, and R.A. Wallace (1987) Removal of enveloping follicle cells can trigger resumption of meiotic maturation in *Fundulus heteroclitus* oocytes. J. Exp. Zool. *244*:177-180.

Greeley, M.S., D.R. Calder, M. Taylor, H. Hols, and R.A. Wallace (1986a) Oocyte maturation in the mummichog (*Fundulus heteroclitus*): Effects of steroids on germinal vesicle breakdown of intact follicles *in vitro*. Gen. Comp. Endocrinol. *62*:281-289.

Greeley, M.S., D.R. Calder, and R.A. Wallace (1986b) Changes in teleost yolk proteins during oocyte maturation: Correlation of yolk proteolysis with oocyte hydration. Comp. Biochem. Physiol. *84B*:1-9.

Gudger, E.W. (1905) The breeding habits and the segmentation of the egg of the pipefish, *Siphostoma floridae*. Proc. U. S. Natl. Mus. *29*:447-500.

Guraya, S.S. (1979) Recent advances in the morphology, cytochemistry and function of Balbiani's vitelline body in animal oocytes. Internat. Rev. Cytol. *59*:249-321.

Gutzeit, H.O., and K. Sander (1985) Polarity in the insect egg. In C.B. Metz and A. Monroy (eds): Biology of Fertilization. Vol. 1, Model Systems and Oogenesis. Orlando: Academic Press, pp. 347-377.

Hagenmaier, H.E. (1973) The hatching process in fish embryos. III. The structure, polysaccharide and protein cytochemistry of the chorion of the trout egg *Salmo gairdneri* (Rich). Acta Histochem. *47*:61-69.

Hamazaki, T., I. Iuchi, and K. Yamagami (1985) A spawning female-specific substance reactive to anti-chorion (egg-envelope) glycoprotein antibody in the teleost, *Oryzias latipes*. J. Exp. Zool. *235*:269-279.

Hamazaki, T.S., I. Iuchi, and K. Yamagami (1987a) Production of a "spawning female-specific substance" in hepatic cells and its accumulation in the ascites of the estrogen-treated adult fish, *Oryzias latipes*. J. Exp. Zool. *242*:325-332.

Hamazaki, T.S., I. Iuchi, and K. Yamagami (1987b) Isolation and partial characterization of a "spawning female-specific substance" in the teleost, *Oryzias latipes*. J. Exp. Zool. *242*:343-349.

Haresign, T.W., and S.E. Shumway (1981) Permeability of the marsupium of the pipefish Syngnathus fuscus to [^{14}C]-alpha amino isobutyric acid. Comp. Biochem. Physiol. 69A:603-604.

Heasman, J., J. Quarmby, and C.C. Wylie (1984) The mitochondrial cloud of Xenopus oocytes: The source of germinal material. Develop. Biol. 105:458-469.

Hedrick, J.L., and N.J. Wardrip (1987) On the macromolecular composition of the zona pellucida from porcine oocytes. Develop. Biol. 121:478-488.

Herald, E.S. (1942) Three new pipefishes from the Atlantic coast of North and South America with a key to the Atlantic American species. Stanford Icthyol. Bull. 4:125-134.

Herald, E.S. (1959) From pipefish to seahorse--A study of phylogenetic relationships. Proc. Calif. Acad. Sci. 29:465-473.

Herald, E.S., and C.E. Dawson (1972) A new subspecies of the gulf pipefish, Syngnathus scovelli makaxi (Pisces: Syngnathidae). Copeia 1972(4):781-784.

Herald, E.S., and J.E. Randall (1972) 5 new Indo Pacific pipefishes. Proc. Calif. Acad. Sci. 39:121-140.

Hurley, D.A., and K.C. Fisher (1966) The structure and development of the external membrane in young eggs of the brook trout, Salvelinus fontinalis (Mitchill). Can. J. Zool. 44:173-190.

Jeppesen, T. (1975) Surface epithelium of the fetal guinea-pig ovary: A light and electron microscope study. Anat. Rec. 183:499-516.

Johnson, L.V., M.L. Walsh, and L.B. Chen (1980) Localization of mitochondria in living cells with rhodamine 123. Proc. Natl. Acad. Sci. USA 77:990-994.

Jones, R.E. (ed) (1978) The Vertebrate Ovary. Comparative Biology and Evolution. New York: Plenum Press, pp. 1-853.

Joseph, E.B. (1957) A study of the systematics and life history of the gulf pipefish, Syngnathus scovelli (Evermann and Kendall). Ph. D. Dissertation, Florida State University.

Kaighn, M.E. (1964) A biochemical study of the hatching process in Fundulus heteroclitus. Develop. Biol. 9:56-80.

Karnovsky, M.J. (1965) A formaldehyde-glutaraldehyde fixative of high osmolarity for use in electron microscopy. J. Cell Biol. 27:137a-138a.

Knudsen, K. (1985) Proteins transferred to nitrocellulose for use as immunogens. Anal. Biochem. 147:285-288.

Kobayashi, W. (1982) The fine structure and amino acid composition of the chum salmon egg. J. Fac. Sci. Hokkaido Univ. Ser. VI, Zool. 23(1):1-14.

Kohler, G., and C. Milstein (1975) Continuous cultures of fused cells secreting antibody of predefined specificity. Nature 256:495-497.

Kudo, S. (1982) Ultrastructure and ultracytochemistry of the fertilization envelope formation in the carp egg. Develop. Growth Differ. 24:327-339.

Kuhlmann, W.D., and P. Peschke (1982) Advances in ultrastructural postembedment localization of antigens in Epon sections with peroxidase labelled antibodies. Histochem. 75:151-161.

Laale, H.W. (1980) The perivitelline space and egg envelopes of bony fishes: A review. Copeia 1980(2):210-226.

Laemmli, U.K. (1970) Cleavage of structural proteins during assembly of the head of bacteriophage T4. Nature 277:680-685.

Lambin, P. (1978) Reliability of molecular weight determination of proteins by polyacrylamide gradient gel electrophoresis in the presence of sodium dodecyl sulfate. Anal. Biochem. 85:114-125.

Lehri, G.K. (1968) Cyclical changes in the ovary of the catfish Clarias batrachus (Linn.). Acta Anat. (Basel) 69:105-124.

Linser, P.J., M.S. Perkins, F.W. Fitch, and A.A. Moscona (1984) Comparative characterization of monoclonal antibodies to carbonic anhydrase. Biochem. Biophys. Res. Comm. 125:690-697.

Linser, P.J., and M.S. Perkins (1987) Regulatory aspects of the in vitro development of retinal Müller glial cells. Cell Differ. 20:189-196.

Lonning, S. (1972) Comparative electron microscopic studies of teleostean eggs with special reference to the chorion. Sarsia 49:41-54.

Luna, L.G. (1968) In L.G. Luna (ed): Manual of Histologic Staining Methods of the Armed Forces Institute of Pathology, 3rd ed. New York: McGraw-Hill, pp. 32-46,72-99,153-173.

Masui, Y. (1985) Meiotic arrest in animal oocytes. In C.B. Metz and A. Monroy (eds): Biology of Fertilization. Vol. 1. Orlando: Academic Press, pp. 189-219.

Matthews, S.A. (1938) The seasonal cycle in the gonads of Fundulus. Biol. Bull. 75:66-74.

McCoy, J.P.,Jr. (1986) Contemporary laboratory applications of lectins. Biotech. 4:252-262.

McKearn, T.J. (1980) Fusion of cells in an adherent monolayer. In R.H. Kennett, T.J. McKearn, and K.B. Mechol (eds): Monoclonal Antibodies: Hybridomas, a New Dimension in Biological Analyses. New York: Plenum Press, pp. 368-369.

McLane, W.M. (1955) The fishes of the St. John's River system. Ph. D. Dissertation, University of Florida.

McLean, I.W., and P.K. Nakane (1974) Periodate-lysine-paraformaldehyde fixative a new fixative for immunoelectron microscopy. J. Histochem. Cytochem. 22:1077-1083.

Mendoza, G. (1943) The reproductive cycle of the viviparous teleost, Neotoca bilineata, a member of the family Goodeidae. IV. The germinal tissue. Biol. Bull. 84:87-97.

Metz, C.B., and A. Monroy (eds) (1985) Biology of Fertilization. Volume 1, Model Systems and Oogenesis. Orlando: Academic Press, Inc., pp. 1-391.

Moor, R.M. (1983) Contact, signalling and cooperation between follicle cells and dictyate oocytes in mammals. In A. McLaren and C.C. Wylie (eds): Current Problems in Germ Cell Differentiation. Cambridge: Cambridge Univ. Press, pp. 307-326.

Moser, H.G. (1967) Seasonal histological changes in the gonads of *Sebastodes paucispinis* Ayres, an ovoviparous teleost (Family Scorpaenidae). J. Morphol. 123:329-354.

Nagahama, Y. (1983) The functional morphology of teleost gonads. In W.S. Hoar, D.J. Randall and E.M. Donaldson (eds): Fish Physiology. Vol. IX, Reproduction, Part A. New York: Academic Press, pp. 223-275.

Nagahama, Y., and S. Adachi (1985) Identification of maturation-inducing steroid in a teleost, the amago salmon (*Oncorhynchus rhodurus*). Develop. Biol. 109:428-435.

Newman, G.R., B. Jasani, and E.D. Williams (1983) A simple post-embedding system for the rapid demonstration of tissue antigens under the electron microscope. Histochem. J. 15:543-555.

Niman, H.L., B.R. Hough-Evans, V.D. Vacquier, R.J. Britten, R.A. Lerner, and E.H. Davidson (1984) Proteins of the sea urchin egg vitelline envelope. Develop. Biol. 102:390-401.

O'Farrell, P.H. (1975) High-resolution two-dimensional electrophoresis of proteins. J. Biol. Chem. 250:4007-4021.

Osborn, J.C., and R.M. Moor (1982) Cell interactions and actin synthesis in mammalian oocytes. J. Exp. Zool. 220:125-129.

Pasteels, J.J. (1973) Yolk and lysosomes. In J.T. Dingle (ed): Lysosomes in Biology and Pathology, Vol. 3. Amsterdam: North Holland Publishing Co., pp. 216-234.

Paxton, J.R. (1975) *Heraldia nocturna*, a new genus and species of pipefish (Family Syngnathidae) from eastern Australia, with comments on *Maroubra perserrata* Whitley. Proc. Calif. Acad. Sci. 40:439-447.

Pederson, G.L. (1977) A simplification of the protein assay method of Lowry *et al.* which is more generally applicable. Anal. Biochem. 83:346-356.

Perez-Clavier, R., and R.G. Harrison (1978) The pattern of lymphatic drainage of the rat testis. J. Anat. 127:93-100.

Pinto, M.R., L. Santella, G. Casazza, F. Rosati, and A. Monroy (1985) The differentiation of the vitelline envelope of Xenopus laevis. Develop. Growth Differ. 27:189-200.

Quast, W.D., and N.R. Howe (1980) The osmotic role of the brood pouch in the pipefish Syngnathus scovelli. Comp. Biochem. Physiol. 67A:675-678.

Raven, C.P. (1961) Oogenesis: The Storage of Developmental Information. New York: Pergamon Press, pp. 1-247.

Reid, G.K. (1954) An ecological study of the Gulf of Mexico fishes, in the vicinity of Cedar Key, Florida. Bull. Mar. Sci. Gulf Carib. 4:1-94.

Remacle, C., P. Delaere, and P. Jacquet (1976) Actions hormonales sur les cellules germinales femelles de Carassius auratus L., en culture organotypique. Renversement sexuel et ovogenese in vitro. Gen. Comp. Endocrinol. 29:212-224.

Reynolds, E.S. (1963) The use of lead citrate at high pH as an electron-opaque stain in electron microscopy. J. Cell Biol. 17:208-212.

Robins, C.R. (1971) The deepwater pipefish, Corythoichthys profundus, in the western Caribbean sea. Copeia 1971(2):319-320.

Rosati, F., F. Cotelli, R.D. Santis, A. Monroy, and M.R. Pinto (1982) Synthesis of fucosyl-containing glycoproteins of the vitelline coat in oocytes of Ciona intestinalis (Ascidia). Proc. Natl. Acad. Sci. USA 79:1908-1911.

Santella, L., A. Monroy, and F. Rosati (1983) Studies on the differentiation of egg envelopes I. The starfish, Astropecten aurantiacus. Develop. Biol. 99:473-481.

Satoh, N. (1974) An ultrastructural study of sex differentiation in the teleost Oryzias latipes. J. Embryol. Exp. Morphol. 32:195-215.

Schooley, J.K. (1980) The structure and function of warm temperate estuarine fish communities. Ph. D. Dissertation, University of Florida.

Selman, K., and R.A. Wallace (1982) Oocyte growth in the sheepshead minnow: Uptake of exogenous proteins by vitellogenic oocytes. Tissue Cell 14:555-571.

Selman, K., and R.A. Wallace (1983) Oogenesis in Fundulus heteroclitus. III. Vitellogenesis. J. Exp. Zool. 226:441-457.

Selman, K., and R.A. Wallace (1986) Gametogenesis in Fundulus heteroclitus. Amer. Zool. 26:173-192.

Selman, K., R.A. Wallace, and V. Barr (1986) Oogenesis in Fundulus heteroclitus IV. Yolk-vesicle formation. J. Exp. Zool. 239:277-288.

Shackley, S.E., and P.E. King (1977) Oogenesis in a marine teleost, Blennius pholis L. Cell Tiss. Res. 181:105-128.

Shulman, M., C.D. Eilde, and G. Kohler (1978) A better cell line for making hybridomas secreting specific antibodies. Nature 276:269-270.

Spiro, R.S. (1966) Analysis of sugars found in glycoproteins. In E.F. Neufeld, and V. Ginsburg (eds): Methods in Enzymology. Vol. VIII, Complex Carbohydrates. New York: Academic Press, pp. 3-26.

Stehr, C.M., and J.W. Hawkes (1979) The comparative ultrastructure of the egg membrane and associated pore structures in the starry flounder, Platichthys stellatus (Pallus), and pink salmon, Oncorhynchus gorbuscha (Walbaum). Cell Tiss. Res. 202:347-356.

Stehr, C.M., and J.M. Hawkes (1983) The development of the hexagonally structured egg envelope of the C-O sole (Pleuronichthys coenosus). J. Morphol. 178:267-284.

Tagatz, M.E. (1968) Fishes of the St. John's River, Florida. Quart. J. Fl. Acad. Sci 30(1):25-50.

Tesoriero, J.V. (1977a) Formation of the chorion (zona pellucida) in the teleost, Oryzias latipes I. Morphology of early oogenesis. J. Ultrastr. Res. 59:282-291.

Tesoriero, J.V. (1977b) Formation of the chorion (zona pellucida) in the teleost, Oryzias latipes II. Polysaccharide cytochemistry of early oogenesis. J. Histochem. Cytochem. 25:1376-1380.

Tesoriero, J.V. (1978) Formation of the chorion (zona pellucida) in the teleost, Oryzias latipes III. Autoradiography of [^{3}H] proline incorporation. J. Ultrastr. Res. 64:315-326.

Tokarz, R.R. (1978) Oogonial proliferation, oogenesis, and folliculogenesis in nonmammalian vertebrates. In R.E. Jones (ed): The Vertebrate Ovary. Comparative Biology and Evolution. New York: Plenum Press, pp. 145-179.

Towbin, H., T. Staehlin, and J. Gordon (1979) Electrophoretic transfer of proteins from polyacrylamide gels to nitrocellulose sheets: Procedures and some applications. Proc. Natl. Acad. Sci. USA 76:4350-4354.

Valnes, K., and P. Brandtzaeg (1985) Retardation of immunofluorescence fading during microscopy. J. Histochem. Cytochem. 33:755-761.

Van Gansen, P., and A. Weber (1972) Determinisme de la polarite de l'oocyte de Xenopus laevis: Etude aux microscopes electroniques a balayage et a transmission. Arch. Biol. (Liege) 83:215-232.

Wall, D.A., and I. Meleka (1985) An unusual lysosome compartment involved in vitellogenin endocytosis by Xenopus oocytes. J. Cell Biol. 101:1651-1664.

Wall, D.A., and S. Patel (1987) Multivesicular bodies play a key role in vitellogenin endocytosis by Xenopus oocytes. Develop. Biol. 119:275-289.

Wallace, R.A. (1985) Vitellogenesis and oocyte growth in nonmammalian vertebrates. In L.W. Browder (ed): Developmental Biology. Vol. 1, Oogenesis. New York: Plenum Press, pp. 127-177.

Wallace, R.A., Z. Misulovin, and L.D. Etkin. (1981) Full grown oocytes from Xenopus laevis resume growth when placed in culture. Proc. Natl. Acad. Sci. USA 78:3078-3082.

Wallace, R.A., and K. Selman (1978) Oogenesis in Fundulus heteroclitus I. Preliminary observations on oocyte maturation in vivo and in vitro. Develop. Biol. 62:354-369.

Wallace, R.A., and K. Selman (1981) Cellular and dynamic aspects of oocyte growth in teleosts. Amer. Zool. 21:325-343.

Wallace, R.A., and K. Selman (1985) Major protein changes during vitellogenesis and maturation of Fundulus oocytes. Develop. Biol. 110:492-498.

Wasserman, P.M., J.D. Bleil, H.M. Florman, J.M. Greve, R.J. Roller, and G.S. Salzmann (1986) The mouse egg's extracellular coat: Synthesis, structure, and function. In J.G. Gall (ed): Gametogenesis and the Early Embryo. New York: Alan R. Liss, Inc., pp. 371-388.

Whatley, E.C. (1969) A study of Syngnathus scovelli in fresh waters of Louisiana and salt waters of Mississippi. Gulf Res. Rep. 2:437-74.

Wilson, E.B. (1928) The Cell in Development and Heredity. New York: The Macmillan Co., pp. 256-393.

Winner, S.M., and M.H. Taylor (1985) Ovarian contractions of Fundulus heteroclitus. Amer. Zool. 25:69a.

Wolf, D.P., T. Nishihara, D.M. West, R.E. Wyrick, and J.L. Hedrick (1976) Isolation, physiochemical properties, and the macromolecular composition of the vitelline and fertilization envelopes from Xenopus laevis eggs. Biochem. 15:3671-3678.

Wolgemuth, D.J., J. Celenza, D.S. Bundman, and B.S. Dunbar (1984) Formation of the rabbit zona pellucida and its relationship to ovarian follicular development. Develop. Biol. 106:1-14.

Wourms, J.P. (1976) Annual fish oogenesis 1. Differentiation of the mature oocyte and formation of the primary envelope. Develop. Biol. 50:338-354.

Yamagami, K. (1981) Mechanisms of hatching in fish: Secretion of hatching enzyme and enzymatic choriolysis. Amer. Zool. 21:459-471.

Yamamoto, K., and H. Onozato (1965) Electron microscope study on the growing oocyte of the goldfish during the first growth phase. Mem. Fac. Fish. Hokkaido Univ. 13:79-139.

Yamamoto, M. and K. Yamagami (1975) Electron microscopic studies on choriolysis by the hatching enzyme (chorionase) of the teleost, Oryzias latipes. Develop. Biol. 43:313-321.

Young, E.G., and D.G. Smith (1956) The amino acids in the ichthulokeratin of salmon eggs. J. Biol. Chem. 219:161-164.

BIOGRAPHICAL SKETCH

Paul C. Begovac was born March 10, 1956, in Marquette, Michigan. He attended elementary school in Michigan and California. He attended high school in Arizona and Michigan. Upon graduation from Moon Valley High School in Phoenix, he attended Northern Arizona University and earned a Bachelor of Science degree in zoology in 1978. He was employed by W.L. Gore & Assoc., Inc. in Flagstaff, Arizona, where he worked in the Medical Division Research & Development Group until 1982. In 1982, he returned to graduate school at the University of Florida and married J. Susan Almlof in 1983. He completed the requirements for the degree of Doctor of Philosophy in basic medical sciences in December 1987 and has accepted a postdoctoral research position at the University of Texas System Cancer Center in Houston, Texas.

I certify that I have read this study and that in my opinion it conforms to acceptable standards of scholarly presentation and is fully adequate, in scope and quality, as a dissertation for the degree of Doctor of Philosophy.

Robin A. Wallace

Robin A. Wallace, Chairman
Professor of Anatomy and
Cell Biology

I certify that I have read this study and that in my opinion it conforms to acceptable standards of scholarly presentation and is fully adequate, in scope and quality, as a dissertation for the degree of Doctor of Philosophy.

Kay E. Selman

Kay E. Selman
Associate Professor of Anatomy
and Cell Biology

I certify that I have read this study and that in my opinion it conforms to acceptable standards of scholarly presentation and is fully adequate, in scope and quality, as a dissertation for the degree of Doctor of Philosophy.

Christopher M. West
Associate Professor of Anatomy
and Cell Biology

I certify that I have read this study and that in my opinion it conforms to acceptable standards of scholarly presentation and is fully adequate, in scope and quality, as a dissertation for the degree of Doctor of Philosophy.

David H. Evans
Professor of Zoology

This dissertation was submitted to the Graduate Faculty of the College of Medicine and to the Graduate School and was accepted as partial fulfillment of the requirements for the degree of Doctor of Philosophy.

April 1988

Dean, College of Medicine

Madelyn Lockhart

Dean, Graduate School

UNIVERSITY OF FLORIDA
3 1262 08554 3097